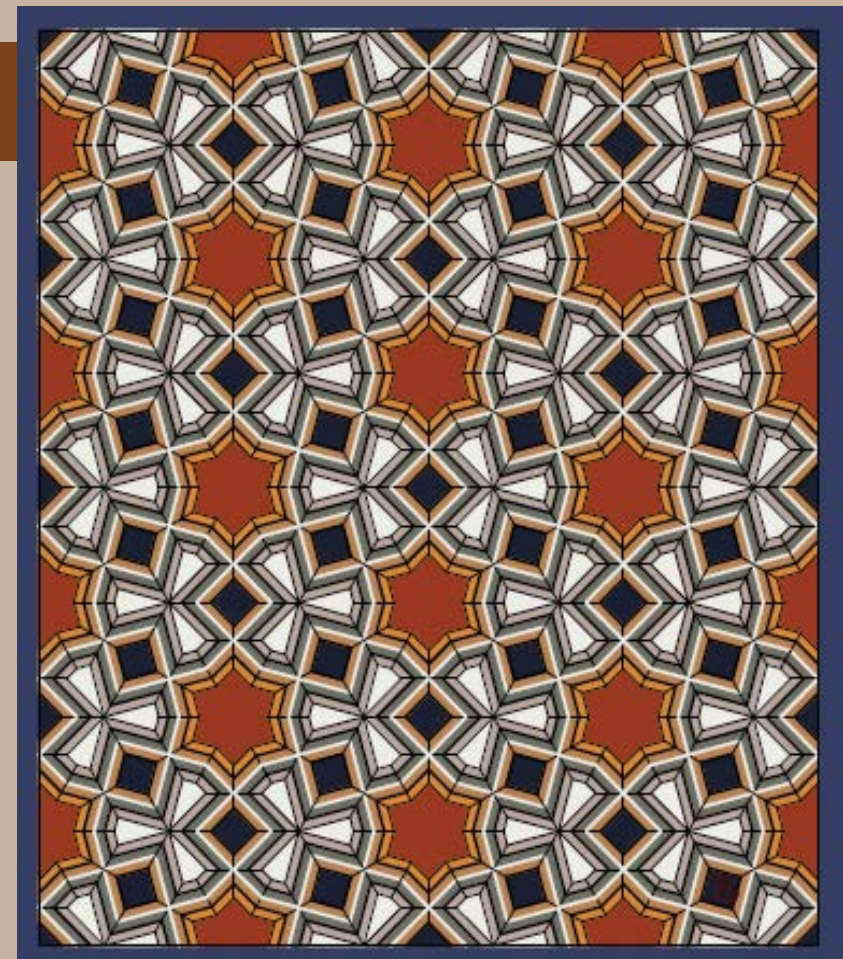


Research Journal of Mathematics and Technology, Volume 13, Number 1, 2024

Research Journal of Mathematics & Technology



Volume 13, Number 1, 2024



**Research Journal of
Mathematics & Technology**

Volume 13, Number 1

ISSN 2163-0380



June 2024

RJMT Editorial Board

Editor-in-Chief

Wei-Chi YANG, Radford University (USA)

Email: wyang@radford.edu

Executive Editor

Yiming CAO, Beijing Normal University (China)

Email: caoym@bnu.edu.cn

Managing Editor

Douglas B. MEADE, University of South Carolina (USA)

Email: meade@math.sc.edu

Guest Editor

Mirosław MAJEWSKI, New York Institute of Technology (United Arab Emirates)

Email: mirek.majewski@gmail.com

Web site: <http://rjmt.mathandtech.org/>

Published by:

Mathematics and Technology, LLC

PO Box 215

Welcome, NC27374-0215, USA



Foreword

We hope that you, as friends and colleagues, along with your families and your loved ones, are all in good health and good spirits.

The Research Journal of Mathematics and Technology (RJMT) is a printed forum for the publication of selected papers from the Electronic Journal of Mathematics and Technology (eJMT: <http://ejmt.mathandtech.org/>). One of eJMT's goals is to publish peer-reviewed papers demonstrating how "technology" can be utilized to make mathematics and its applications fun (F), accessible (A), challenging (C) and theoretical (T).

This special issue contains papers from the 2022 CADGME conference in Jerusalem, the 10th in the series. The conference took place from 12 to 14 September 2022. We thank Professor Csaba Sárvári for serving as a guest editor for this issue. As you read these five papers you will see discussions of different areas of mathematics using various technologies. We hope these innovative ways of exploring mathematics will be beneficial to you and your students. As you do so, we encourage you to write about your experiences for future issues of eJMT. Instructions for preparing and submitting papers to eJMT can be found online at <https://ejmt.mathandtech.org/SubmissionGuidelines.html>.

As this edition of RJMT is being prepared, we are planning the 29th ATCM (Asian Technology Conference in Mathematics: <https://atcm.mathandtech.org/>) to be held in hybrid format from December 8-11, 2024, which is to be in Yogyakarta, Indonesia Thank you all for your continued support of eJMT, RJMT, and ATCM.

Mirosław Majewski
Guest Editor

Wei-Ch Yang
Editor-in-chief

TABLE OF CONTENTS

3D printing and laser cutting of architectural heritage for use in mathematics education

Sergio Alonso, Álvaro Martínez-Sevilla -----1

Problems in Randomization of Online Question Banks (Case Studies)

Ildikó Perjési-Hámori, Dóra M. Szegő -----19

Inversion of Equiangular Spirals

Elias Abboud -----31

Easy (but exact) study of caustics of conics

Zoltán Kovács -----39

A STEAM approach to canal surfaces

Thierry Dana-Picard -----60

3D printing and laser cutting of architectural heritage for use in mathematics education

Sergio Alonso

e-mail: zerjioi@ugr.es

Department of Languages and Computer Systems
University of Granada. Spain

Álvaro Martínez-Sevilla

e-mail: asevilla@ugr.es

Research Institute on Data Science and Computational Intelligence DaSCI
University of Granada. Spain

Abstract

The recent introduction of new technologies such as 3D printing or laser cutting has made it possible to support the visualization and manipulation of mathematical objects with easy-to-produce parts. These parts, as opposed to the handcrafted ones, are manufactured from a digital file containing the design of the part.

In this article we focus on mathematical objects derived from architectural and art elements. They are of special interest, both for their mathematical design and for their link to art, to history, and to the emotions produced by their contemplation in the monumental heritage. This, together with the engineering of their design and the technology of their production, makes them a real STEAM material.

We will expose the manufacture of some elements such as muqarnas ceilings, cross ribbed vaults, iconic renaissance elements, islamic mosaics and some more. We will detail the geometric characteristics of these elements, their design process to obtain a 3D or 2D model and the means of fabrication to obtain an operable piece. Finally we will discuss some examples and indications of their use in didactic workshops for mathematics education.

1. Introduction

The historical architectural heritage contains many examples of objects with geometric nature and great visual appeal. These elements have been used to analyze the significance of monuments and also as a resource in mathematics education [8, 9]. In the latter aspect, the historical values, the cultural and emotional connection that they represent and their geometric elaboration over centuries make them a great resource to organize mathematical visits, workshops and collaborative tasks for students.

However, some of these elements are difficult to understand at a glance, even using images and drawing mathematical layers over them (for example using GeoGebra [16]). However, the display of a physical 3D model and its manipulation takes the student to another world of spatial recognition and improves attention, understanding of the object and increases the interest in it.

Fortunately, in recent years, the rising technologies of **3D printing** and **laser cutting**, have emerged helping us to materialize this kind of models. Both technologies are very suitable for reproducing architectural objects, whose main design rules are of geometrical type (curves, tessellations, Euclidean geometry in 2D or 3D, and so on), which may be complex to understand. Moreover, many models can be decomposed in different pieces forming a kind of puzzle, which once assembled emulates the architectural object and shows all its parts and their relationship. To sum up, they are great for spatial understanding and as visual and conceptual stimulation.

In this article we will focus on some intricate and complex architectural heritage objects. We describe how to model and produce them, in order to use them as an aiding tool to explain mathematical concepts that are applied in architecture and arts.

Particularly, we will focus on muqarnas vaults and ribbed domes, typical of Islamic architecture, and some other renaissance and baroque iconic objects. We will also show how to laser cut some of the best known and geometrically pleasing objects, the mosaics of Andalusian decoration. These wood tiles, once painted and mounted, are an excellent tool to teach about math concepts such as reflections, rotations and translations. Even more, using those tiles we can explain the different configurations of the “wallpaper groups”. Last, but not least, we also show how we have modeled and produced some tools to be used in math education in order to manipulate concepts like proportions and the configuration parameters from horseshoe arches.

2. Muqarnas vaults

Muqarnas vaults are some of the most complex 3D geometrical objects in Andalusian architecture. They are produced by aggregation of simpler structures [4, 11, 12]. Muqarnas are marvelous pieces of architectural decoration, which produce amazement and recreate our visual capacity in their geometric interlocking (Fig. 1).



Figure 1. Muqarnas vault. *Dos Hermanas* hall. La Alhambra (Granada).

To produce a realistic model of a muqarnas vault we part from 4 basic prisms with section sizes based on $\sqrt{2}$ proportions that interlock (Fig. 2). These prisms are called *conza*, *medio cuadrado* (half square), *dumbaque* and *jaira* (Fig. 3). In addition to the basic prisms some other singular prisms such as *estrella* (star), *almendrilla* or other special ones are added. The star shaped prism usually forms the central piece or center of local radial symmetries in the vault.

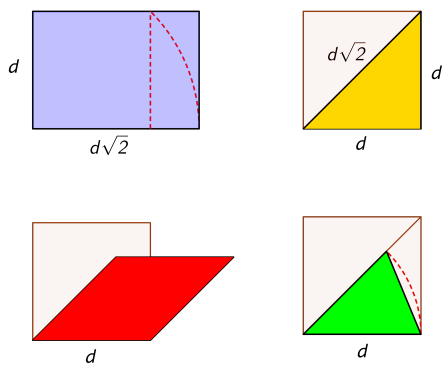


Figure 2. Muqarnas prisms plan.

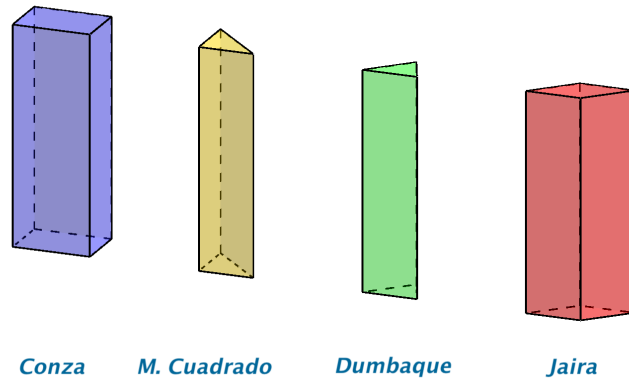


Figure 3. Muqarnas prisms.

All together they cover a tessellation of a rectangular or polygonal area, like those of a vault plan (see Fig. 4). The amount of possible designs to produce this covering of the plane using the 4 prisms is very big. However, all designs must reflect some basic symmetry properties, such as the symmetry of perpendicular central axes in the case of a rectangular plan or radial symmetry in the case of a (regular) polygonal plan. The production of the particular designs we find in monuments is a combination of those symmetry properties and the creativity of the craftsmen.

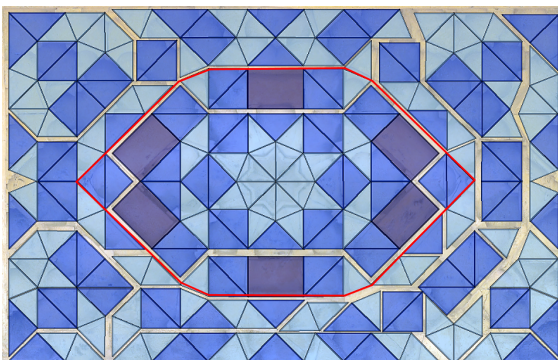
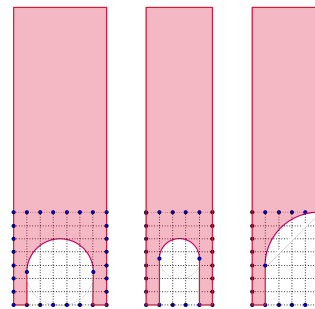


Figure 4 (left). Muqarnas vault plan. Puerta del Lagarto.
Figure 5 (right). Convex cutting of a *conza*.



The basic prisms are cut to produce rounded concave shapes on them. The cuts are precisely defined by ancient treaties, and are based on divisions of 7 and 5 (the quotient of $7/5$ closely approximates $\sqrt{2}$). These cuts leave elongated supports whose size is $1/7$ the width of the base piece (if they are on the longest side) or $1/5$ (if they are on the shortest). These pins are called *patillas* and they form clusters when the pieces join together. In Fig. 5 we show these cuts for a *conza* piece.

This cutting process makes shapes more pleasing to the eye. The muqarnas are arranged starting from a central piece (usually a star) and adding new pieces around the previous ones. The new layers are arranged at lower levels, which causes them to hang down the walls. This arrangement together with the concave cuts finally give the appearance of a dome-like structure with stalactites (Figs. 6 and 7).

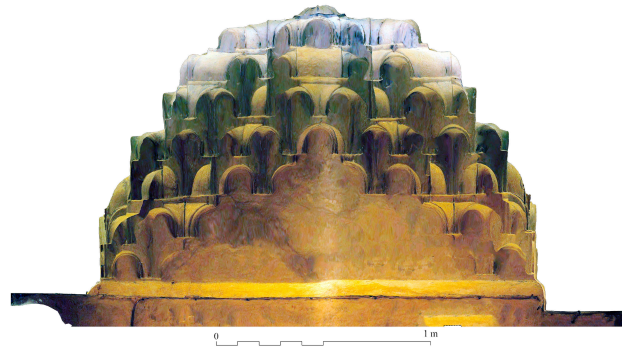


Figure 6 (left). Muqarnas vault. Puerta del Lagarto. Picture from bottom.

Figure 7 (right). *The Lagarto vault* reconstruction with photogrammetric techniques shows the resulting dome-like structure.

Particularly, we have modeled and 3D printed the central part of the oldest and best preserved muqarnas ceilings in Andalusia: the one above the *Puerta del Lagarto* (XII A.D.), in the Cathedral of Seville. This central part comprises 8 different models (Fig. 8) (65 total pieces) that are mounted over a 3 layer foundation (Figs. 9 and 10). The original muqarnas ceiling comprises a total 235 pieces and 7 different layers.

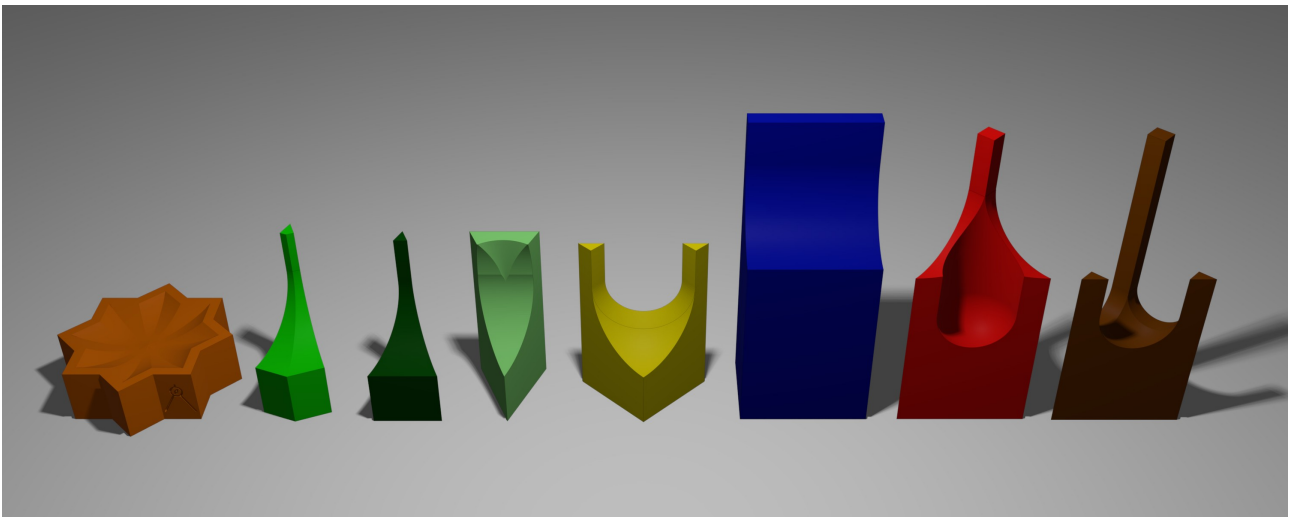


Figure 8. Set of 8 pieces modeled for the central part of the Muqarnas vault at *Puerta del Lagarto*.

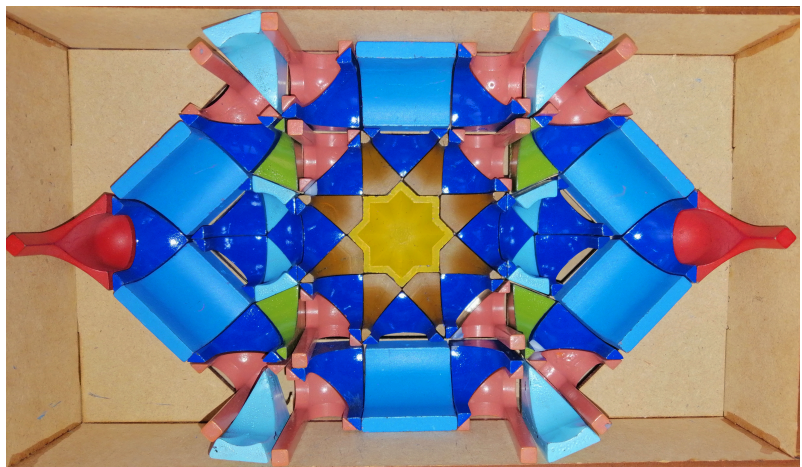
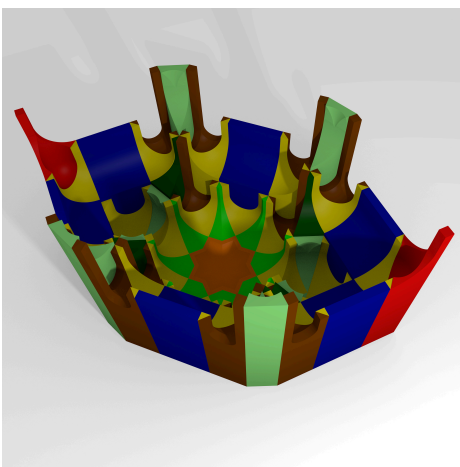


Figure 9 (left). Rendered model of the central part of the Muqarnas vault at *Puerta del Lagarto*.

Figure 10 (right). The 3D printed and mounted central part of the Muqarnas vault.

3. Ribbed domes

A ribbed dome is a dome composed of arches that cross each other, forming the support of the roof. In the Great Mosque of *Córdoba* we can find 3 pioneering ribbed domes whose main purpose is to sustain a central smaller dome (*cupulín*) and allow the entrance of light from the sides [2, 3]. This is an innovative solution in architecture, which until that moment had been solved with simpler types of domes.

All domes have 8 ribs, but differ in the way they cross from one to another. Depending on the placement and interlocking of the arches they provide a greater or lesser space for the *cupulín*. The first to be built, that of the Villaviciosa Chapel, minimizes the number of arch crosses, with only 4 of a lattice + diamond type. The dome of the Maqsura, the most majestic and beautiful, has 8 crosses with 8 equal arches. It forms a stellated polygon of type $[8/2]$ (Schläfli symbol for stellate polygons, where $[p/q]$ means that it is built on a regular polygon with p sides, joining the vertices separated by a distance q), which maximizes the size of the *cupulín* it supports above its arches. The eastern and western lateral domes of the Maqsura, have the maximum number of crosses (12) adopting in their projection the form of a stellated polygon of type $[8/3]$. In this case the extension of the *cupulín* is reduced. In Fig. 11 we show some images of those domes in which the structure of the arch crossings is clearly appreciated.

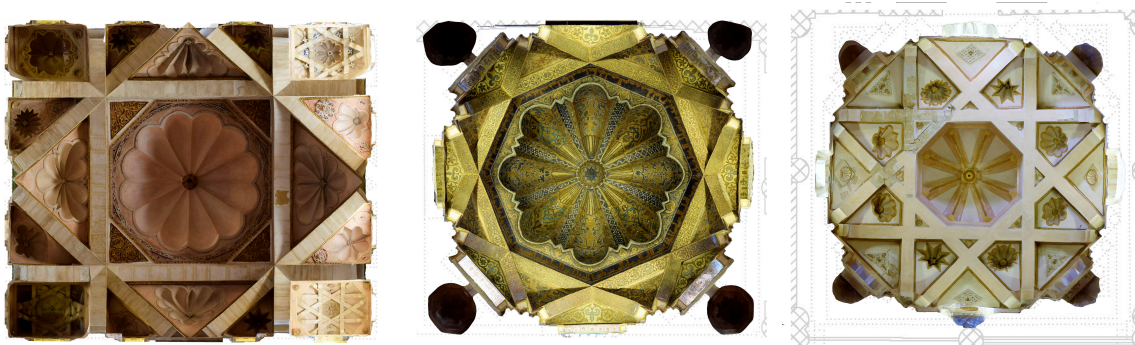


Figure 11. Photogrammetric view of the 3 types of ribbed domes. From left to right: Villaviciosa chapel, Maqsura and lateral Maqsura domes.

In Fig. 12 we show the geometrical structure of the three domes.

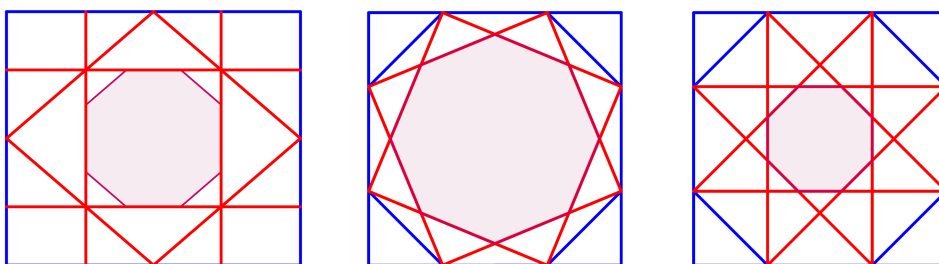


Figure 12. The geometry of the 3 ribbed domes (Villaviciosa chapel, Maqsura and lateral Maqsura domes). All with 8 arches, but with a different number of crossings (4, 8 and 12 respectively).

The different domes at the Mosque of Córdoba present different construction difficulties due to the nature of the arch crossings (Fig. 13). In the Villaviciosa chapel and the Maqsura the ribs cross each other spatially and require complex crossing pieces for their construction, in the shape of 4 or 6 quadrangular prisms joined to the faces of a cube. Those pieces accommodate the ribs that converge in them. The lateral Maqsura domes are geometrically more complicated as they have a greater

number of crosspieces. However, that pieces are the easiest to replicate, since the ribs cross locally in a plane, which avoids the need for clefts or notches. This makes it possible for the stones at the intersection to fit together with simple cutouts, which are easier to produce and fit. It can be seen as an architectural version of the computational principle known as *divide and conquer* [13]. The solution to the problem of the crossings is given by dividing the problem into multiple problems of less complexity each, and then joining the solutions of all of them. This type of solution to construct a dome has been the most widely accepted in history, expanding rapidly to the rest of al-Andalus, to the Christian *mudéjar* (moorish style when Christian kings ruled) architecture, and to the European technical and cultural communication route that was the *Camino de Santiago*, in the north of the Iberian Peninsula, from where it spread to France, Great Britain, Germany, and even to the Middle East.

For these ribbed domes we have designed and printed the basic arcs that conform the domes with a series of grooves and slots that allow to mount a model of the domes in which is easy to understand the advantages and problems that each one of the structures present. In Fig. 15 we show the 3D printed and mounted pieces for each one of the 3 types of domes in the Mosque of *Córdoba*.



Figure 13. Rendering of the 3 types of ribbed domes: lattice + diamond, and stars [8/2] and [8/3].



Figure 14 (left). Photograph of the Maqsura dome in the Mosque of Córdoba.

Figure 15 (right). Manufacturing with 3D printing the 3 distinct ribbed domes. Assembly of 9 pieces per dome.

4. Renaissance and baroque iconic objects

We have also designed and produced other architectural elements as 3 regular polygons inscribed one each other. These polygons are the bronze knockers on a renaissance façade at a Granada palace, *Casa de los Tiros*.

They are a triangle, a square and an octagon of precise measurements (Fig 16). The uniqueness of these three mathematical objects on the façade has to do with their symbolic meaning as basic pieces of geometry and iconic as a representation of medieval hermetic knowledge. It is very significant that other artists of the time, such as Leonardo Da Vinci or Nicoletto Rosex da Modena, implicitly or explicitly used these 3 polygons in a similar relationship with each other. In Figs. 17 and 18 we show the geometric construction of each one of the polygons and their size relations and the 3D model depiction that we have produced to easily show the proportions of each polygon.



Figure 16. 3 bronze knockers in the main façade of a renaissance palace.

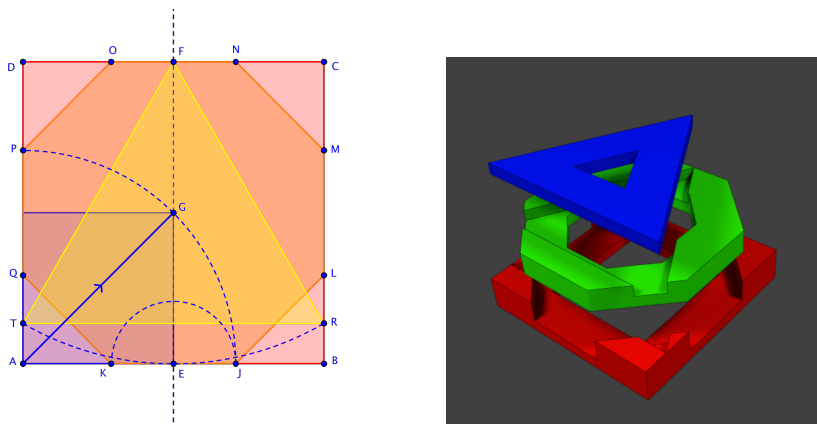


Figure 17 (left). Geometric construction of the inscribed polygons.

Figure 18 (right). Rendering of the 3D model for the polygons.

We have also designed and 3D printed the double star-shaped polygon $[8/3]$ on Fig. 19. They have different radius for each of the stars and a twist of 22.5 degrees with respect to the other (Fig. 20). The tips (and the notches) from every star alternates between them. They can be seen as an oculus with a symbolic meaning in the baroque façade of the Cathedral of Granada. In Fig. 21 we show the produced model to show the construction of such a double star-shaped polygon from the basic star shapes.

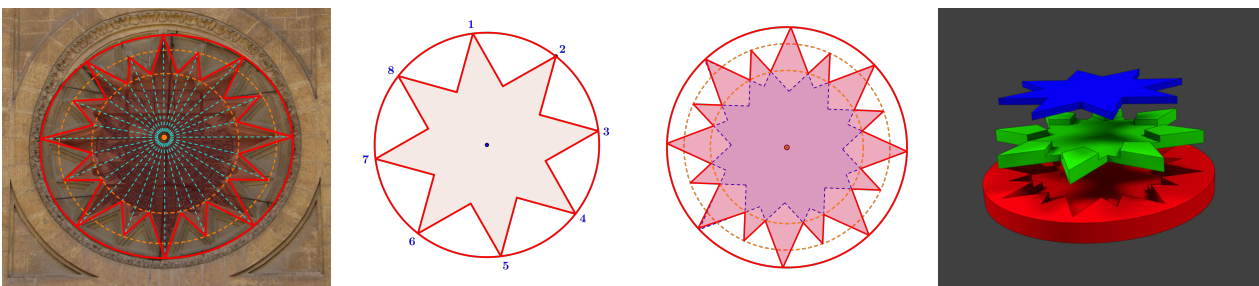


Figure 19 (left). Double star oculus in the Cathedral of Granada.

Figure 20 (middle). Construction of a star polygon $[8/3]$ (middle left) and double rotated star polygon (middle right).

Figure 21 (right). Rendering of the double star polygons over a basis with their relative measures.

5. Laser cut mosaics

The mosaics found in walls, ceilings and floors of the Alhambra and other Nasrid (the last Islamic dynasty that ruled the kingdom of Granada) and *mudéjar* monuments, are one of the summits of 2D geometric decoration. They have motifs that tessellate the plane [1, 5, 6], exhibiting a wide variety of symmetries and rotations. So, they are ideal for explaining their geometric properties whereas solving puzzles with them.

Even more, they can be easily reproduced by laser cutting on a laminated wooden board. Once the pieces have been cut and painted with the different colors, assembling the mosaic is an excellent exercise in geometric fitting and observation of the plane isometries in the mosaic.

We have reproduced 8 different mosaics in wood. All of them are extracted from the same designs in hispanic-muslim decoration. They allow to explain and observe the concepts of translation, rotation, symmetries or glide symmetries and to materialize them in an easy way. For more advanced levels, they also allow us to talk about crystallographic groups in 2D (wallpaper groups), at least the simplest ones given by rotations and symmetries. Also some unique mosaics, containing decagonal and pentagonal stars or intertwined ribbons of Almohad origin.

In figures 22, 23 and 24 we show the wood laser cut mosaics and the corresponding designs of the Nasrid palace of the Alhambra (Granada) on which they are based. For the mathematical determination of the mosaics we follow the common notation of the International Union of Crystallography [5, 6]: $p3$, $p4$, cm ...

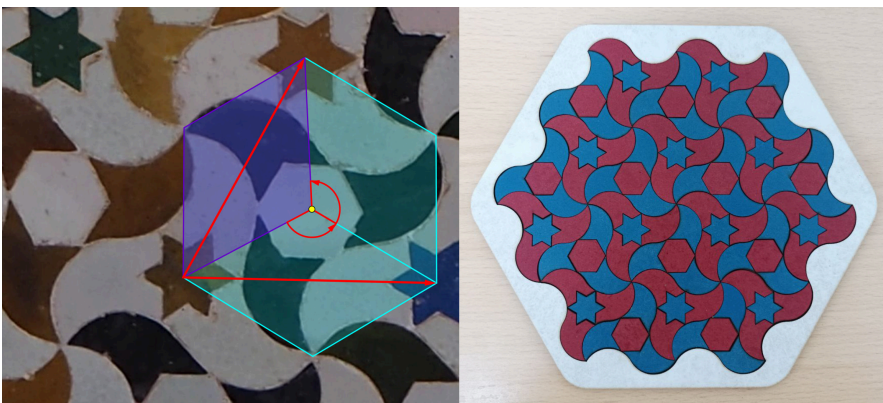


Figure 22. *The little Spanish folded paper bird mosaic*. A $p3$ model with only order 3 rotations (apart from translations).

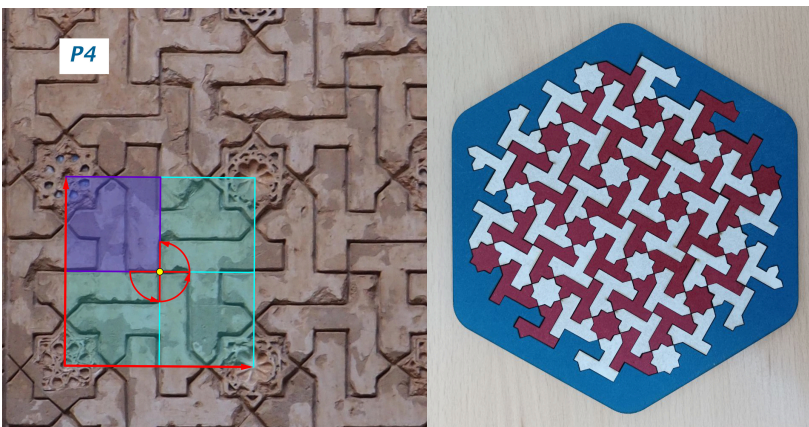


Figure 23. *The mosaic of keys*. A $p4$ model, with only order 4 rotations. It is an Umayyad inspiration which is often found with many possible variants.



Figure 24. *The mosaic of leaves.* A cmm model, which preserves the leaves colors.

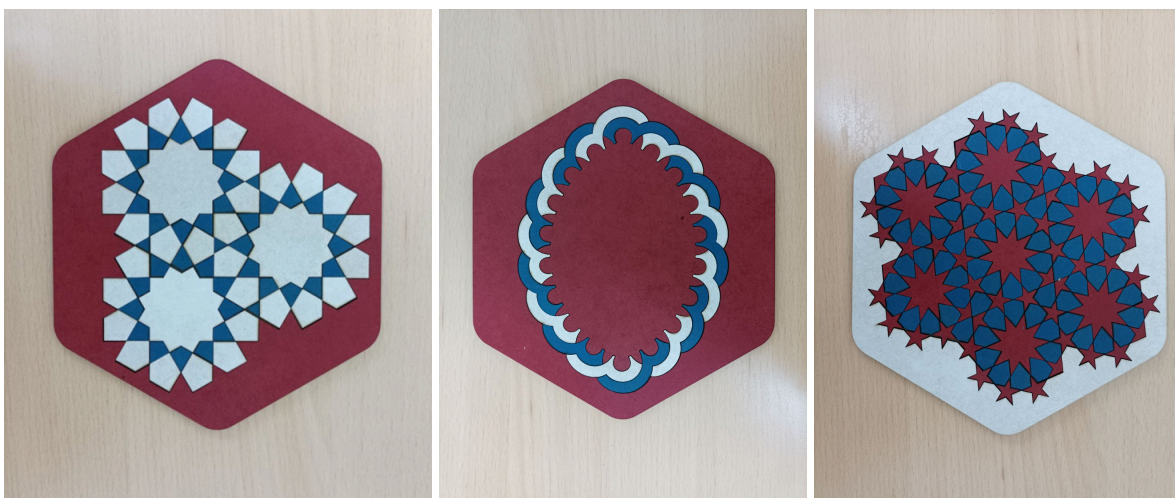


Figure 25. Other mosaics, including radial ones, Almohad straps and a quite singular tessellation with pentagonal stars.

6. Laser cut tools for direct mathematical measures

We have also made some tools in order to easily get measures of mathematical relations significant in monumental art. When we take a measure it is important for students to understand that, sometimes, we are aiming to measure not for exact quantities but for a relation among them. This is true for classical proportions that are found in many architectural monuments or the parameters that conform a horseshoe arch.

6.1. Mathematical ratios measuring kit

We have designed and laser cut a measuring kit that helps determining which ratio is used in a particular monument (door, window, façade...). We can choose from 10 different predefined proportions: 1:1 (square), 5:4, Cordoba proportion, $\sqrt{2}$, 3:2, ϕ (golden ratio), $\sqrt{3}$, 2:1 (double square), $\sqrt{5}$, and δ_s (silver ratio). Once we choose a proportion, we pick up the rectangular frame with that proportion from the kit. Then, we try to make it coincide with the architectural object we want to measure, by moving it in front of our eyes. Obviously, this will not give a very precise measurement, but can help to distinguish among the different proportions that may have been used in each monument. In Fig. 26 we show a picture of the produced and laser cut ratios measuring kit.



Figure 26. Kit of frames for direct measurement of proportions.

6.2. Tool for the measurement of horseshoe arch parameters

In the case of horseshoe arches, relative measurements of their main parameters (superelevation, thread and eccentricity) against the radius of the arch (R) are also important. These parameters are associated with different historical and artistic periods, as well as with the evolution among them. It is therefore important to know them from a mathematical point of view for a history of art classification. We have designed and laser cut a tool that allows to easily (and approximately) measure these parameters in relative terms (Fig. 27).

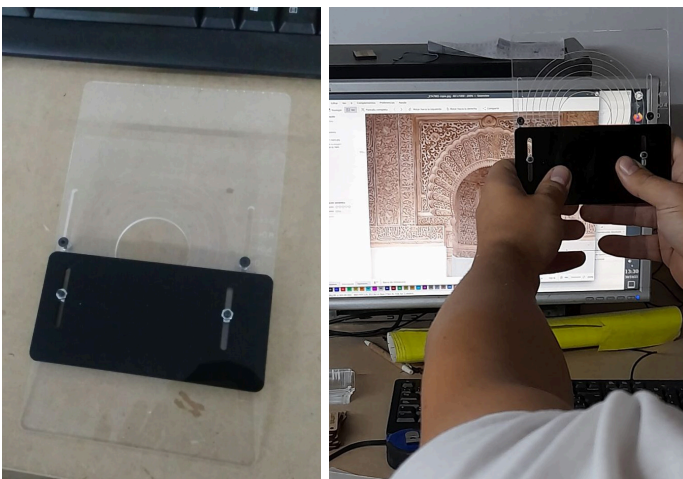


Figure 27. Tool for measurement of horseshoe arches and an example of a measure over an arch.

The presented tools show how simple measuring tools can be designed and produced easily with laser cut technology. We usually use methacrylate and wood to create different layers that are assembled with some bolts and nuts.

7. Design process for models

To design the different models we started from a previous study on the object we were dealing with. To do this, we consulted some specialized literature about the construction processes that were carried out to create the monuments and art pieces that we are going to model. Moreover, we have always tried to visit the monuments in order to get accurate measurements, photographs and even to produce our own photogrammetric models, which are of a great help to create accurate digital models, as many of the real world objects cannot not be easily accessed due to their location (ceilings, walls...) and their protection status. In fact, photogrammetry is a digital technique which is greatly increasing its application in the field of arts and restoration [7, 10].

Once the preliminary study works conclude we are ready to create the models. To do it, we have used several different digital tools that range from mathematical ones as GeoGebra [16] to 2D and 3D modeling applications as Blender [14], FreeCad [15] and Inkscape [17]. Those pieces of software are free software or at least (in the case of GeoGebra) free to use. Moreover those programs have plenty of documentation and tutorial that allows anyone to get introduced in the modeling tasks that are needed for this kind of projects.

For example, in the case of the modeling of the muqarnas vaults pieces we usually part from a simple 2D shape (half square, a rectangle...) which is extruded to form a prism. That prism is then modified using other 3D primitives as are cubes, spheres, cylinders by means of boolean operations as unions, intersections and subtractions. For example in Fig. 28 we present the modeling process of four of the pieces (*atacia*, *conza*, *almendrilla* and *medio cuadrado ciruelo*) in which from the basic prism some spheres, cylinders and cubical prisms are subtracted.

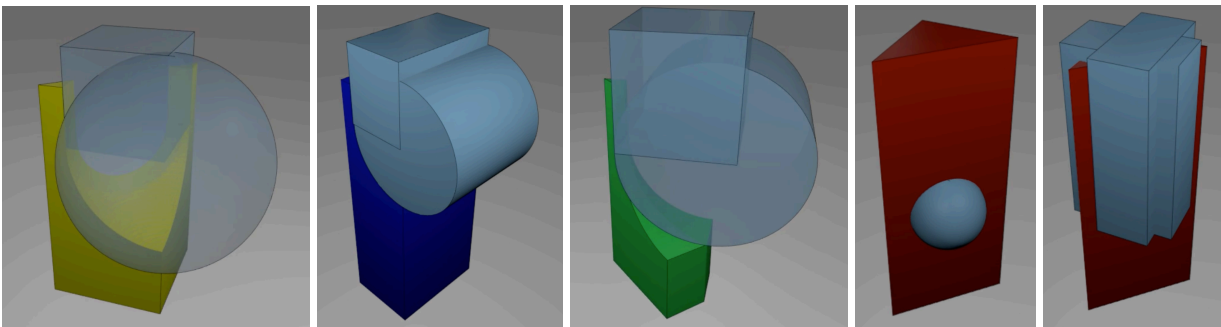


Figure 28. The modeling process for 4 muqarnas: *atacia* (yellow), *conza* (blue), *almendrilla* (green) and *medio cuadrado ciruelo* (red).

In addition to the intrinsic characteristics of each of the modeled pieces we have also included some modifications in order to help mounting the different components of each 3D printed architectural object. For example, in the case of the muqarnas ceilings we also made some holes to insert or screw some cylindrical neodymium magnets that held all pieces together (Fig. 29).

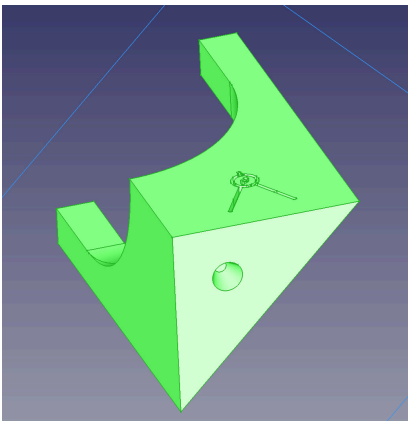


Figure 29. A hole in the bottom of the *atacia* model to screw a cylindrical neodymium magnet.

In order to attach the muqarnas together we have also designed a three level support box in which some cylindrical holes (with some metallic sheets that helps magnets to attach to) help to create the whole muqarnas structure (Fig. 30).

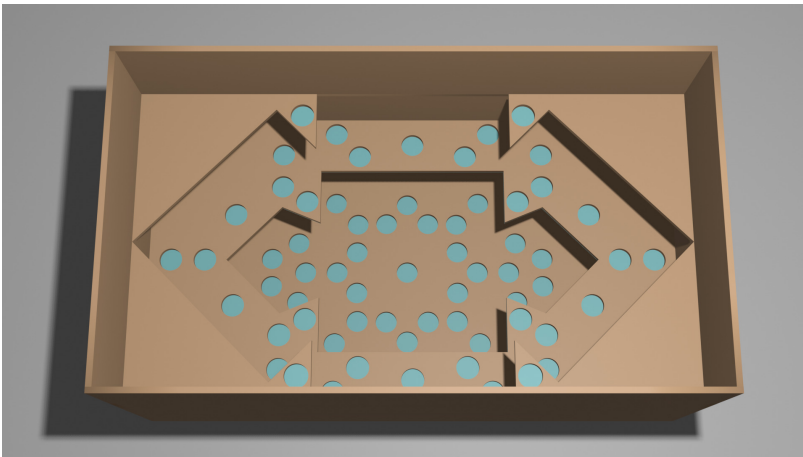


Figure 30. Support box to mount all muqarnas. The cylindrical holes allow neodymium magnets to attach to a metallic sheet (in blue).

In other models, as for example the ones in the ribbed domes, we have not only modeled the arches themselves, but we had to incorporate some cut-outs to allow to assemble the different arches together. Those cut-outs have been designed with enough tolerance to allow the full construction of the domes. In Fig. 31 we show an example of the cut-outs for the ribs of the *Villaviciosa chapel* as they are the most complex that we have produced because in each of the intersections coincide three simultaneous arches.

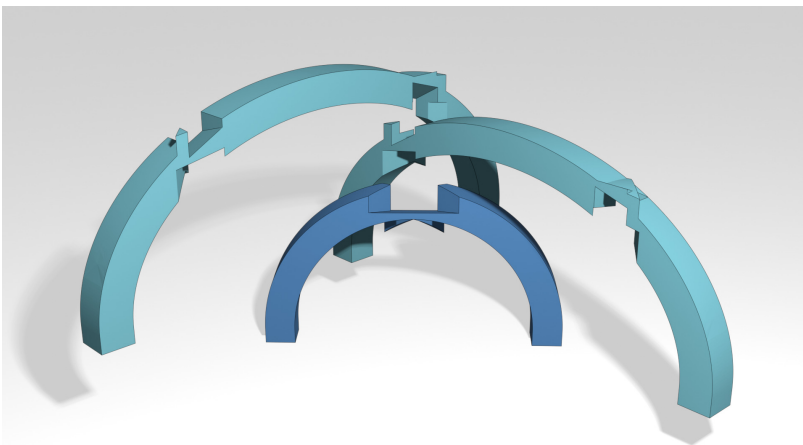


Figure 31. The modeled arches from the *Villaviciosa chapel*.

8. Fabrication technology

Once the models have been designed, we proceeded to manufacture them. We basically have used two different technologies to do it. The first one is 3D printing which in the last years have become very popular. Schools and particulars usually do have this kind of printers at hand. The most popular 3D printers to date are FDM printers. They mainly work by depositing thermoplastic that is heated (in order to melt it) and then extruded through a nozzle. The plastic is deposited as a filament forming 2D layers that one stacked together to produce the printed piece (Fig. 32).

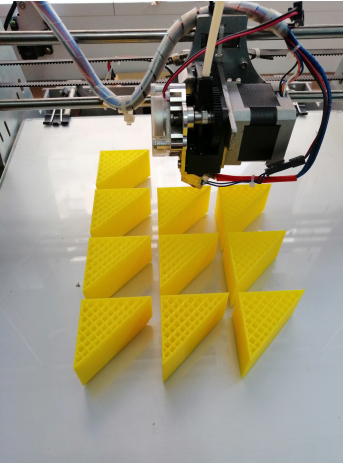


Figure 32. The FDM printer manufacturing some muqarnas models.

In recent years other 3D printing technologies have appeared and have been made accessible for the general public. For example, liquid resin printers (also called stereolithography or SLA) work also in a 2D layer by layer fashion. However, SLA printers work by curing liquid resin by means of a light source (typically in the ultra-violet wavelengths) which hardens into a solid piece of plastic (Fig. 33).

In all our pieces we have used both 3D printing technologies. We can highlight some advantages and disadvantages of each one of them:

- FDM is cheaper as the thermoplastic is usually less expensive than liquid resins.
- FDM results are not so good as SLA ones: the 2D layers are much more evident and the pieces may suffer a higher cleavage both in the printing process and when the piece is manipulated. Moreover, SLA offers higher detail which is indeed quite important when you need to ensemble several pieces together.
- SLA needs of additional steps than just the printing process: pieces have to be cleaned and cured (with ultraviolet light) in order to harden their surface, which is a tedious and dirty process (Fig. 34).
- SLA is, in general, faster than FDM: Many pieces can be printed in one single go. For example if a piece takes 1 hour to print, if we need 8 pieces with SLA we can print the 8 of them in one single 1 hour print, whilst FDM would need 8 hours of printing.



Figure 33 (left). SLA printer with a set of muqarnas models already printed.

Figure 34 (right). Curing process of the printed pieces.

For flat pieces (for example the mosaics and the measuring tools that we have developed) we have used laser cutting. Laser cutting allows precise and fast cuts of different materials. Although there

exists many different kinds of laser cutting machines, allowing different materials (even thick metals) we have used less powerful ones that allow cutting different sheets of wood or MDF or even some plastic sheets like methacrylate. One of the main advantage of laser cutting is its speed, which allows to fast prototyping of the models. It also has the advantage of price, since the materials used (especially MDF) is cheap and durable. In Fig. 35 we show the process of laser cutting some mosaics.

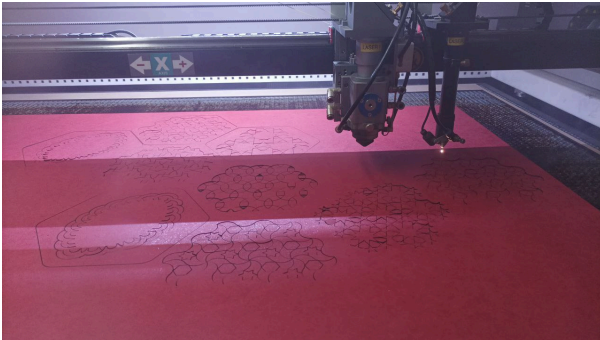


Figure 35. Laser cutting some mosaics.

Finally we must point out that even those fabrication technologies (3D printing and laser cutting) are not perfect and quite often it is necessary to do some post-processing work on the manufactured pieces. For example, in many occasions some of the pieces have to be sanded in order to remove burrs, magnets have to be glued or screwed to the pieces and they have to be painted by hand if we want them in different colors (Fig. 36).



Figure 36. Post-processing works on the pieces: sanding and attaching magnets.

9. Experiences in Mathematics Education with the produced models

With all the fabricated objects we have conducted numerous workshops and demonstrations for students. They have also been part of long training courses for math teachers, technology teachers and other specialists in art history or heritage studies. They also allow to start in the use of 3D resources through digital technologies in the classroom.

Parts are durable, reusable, and resistant to rough handling. In case of breakage, it is easy and cheap to replace them. They can be disassembled and mounted by all participants, allowing everyone to actively participate. To date, more than 100 math walks and 40 workshops have been carried out using these items (Fig. 37).

The groups that have used all these items have been very heterogeneous. For example, the laser cut mosaics have been widely used with different groups of students ranging from 8 to 16 years. With the younger ones a much more ludic approach was taken, mounting the mosaics as if they were puzzles. With older students the concepts of rotations, translations and symmetries were shown over the mosaics whilst they were mounting them.

Secondary students and adults groups were particularly interested in the most complex pieces as the ribbed domes or the muqarnas ceilings (specially in the math walks were they visited the actual monuments). Those pieces allowed the understanding of basic stellated polygons construction and different kinds of symmetries (radial, axial, and so on). Moreover, muqarnas also offered the possibility to explain to the most interested public the mathematical design process of the individual pieces by means of the application of boolean operators as intersection or subtraction of simple 3D objects (cylinders, prisms and so on).

The groups sizes ranged between 15 and 30 attendees. When groups were small in size it has been also feasible to introduce the tools for measuring proportions. They easily allow to understand what a particular ratio means in an artistic object and how those ratios can be found in almost every monument.



Figure 37. Examples showing the use of 3D printed objects in math walks and demonstrations.

The main mathematical topics that are covered in these experiences using the fabricated objects change according to the level of the students. For example, we have talked about 2D and 3D symmetries, reflections, translations, movement groups of a plane, proportions, concavity and convexity, regular and stellated polygons, spaces coverage by prisms, arches and their parameters, arch crossings, curves in 3D space and spatial lattices.

In addition, the manipulation of the manufactured parts allows a clear appreciation of the possibilities of the application of mathematics in fields such as architecture or engineering. Moreover, students have shown a greater interest in these digital technologies.

From those workshops and math walks we have deduced some facts:

- In the workshops we have challenged the students to assemble the 3D objects like a puzzle. This challenge have increased their focus and attention to the mathematical aspects of the pieces (Fig. 38).
- The assessment of the carried out courses and activities has been very satisfactory in all cases.
- Elementary or middle school students never turn down a puzzle challenge. Students demonstrate that they understand the mathematical knowledge involved in the challenge.

- Cooperation between students, which spontaneously tend to form small groups, arises naturally when taking on these challenges. What one student “sees” (deduces and understands) is shared. Therefore, a collaborative team approach is easily established.
- In the **mathematical walks**, the simple act of showing the models has greatly increased the interest of the participants, breaking at some point the barrier that usually exist among the attendants and the guide. Usually the feedback about using these materials during the walks and explanations has been very positive.
- In the **long courses** for teachers and specialists, they have valued the activities with 3D printing and laser cutting and have stated them as a very attractive and transferable alternative to their own projects with their students.



Figure 38. Examples of activities with students and the laser cut and 3D models.

With those experiences we can conclude that objects that can be manipulated are always exciting and allow to directly challenge the spatial vision of the students and their geometric understanding of the objects. The students on those workshops are usually in the 12-16 age range, but we have also satisfactorily tested this experiences with younger students.

10. Conclusions

In this paper we have shown how several architectural objects can be interesting to be modelled and 3D printed in order to obtain objects that can be used to teach the mathematical properties applied in art and monuments. Those models minimize the inherent difficulty of the visualization of the interrelation of their parts. Particularly we have shown the modeling and manufacturing of a section of a muqarnas vault and ribbed domes, typical of Islamic architecture. We have also dealt with objects of different artistic periods as the Renaissance and Baroque ones. Specially the latter, due to the mathematical nature of their artistic works, are very suitable for 3D modeling and printing.

The modeling process involves, apart from the mathematical study, a deep understanding of the spatial construction that includes extrusion, aggregation of surfaces and volumes, superimposition of parts and so on. Moreover, for those models being usable it is also necessary to pay attention to some engineering steps involving cut-outs, addition of magnets and supports, etc.

The mathematical topics that have been addressed are about 2D and 3D symmetries, reflections, translations, movement groups of a plane, proportions, concavity and convexity, regular and stellated polygons, spaces coverage by prisms, arches and their drawings parameters such as eccentricity or superelevation, arch crossings, curves in 3D space, spatial lattices and boolean operations with surfaces.

Some of the advantages offered by the use of 2D and 3D parts are the attractiveness of their manipulation, which leads to a closer personal involvement, as well as the possibility of experimentation. They help to include in the mathematical curriculum topics of geometry, curves or arithmetic calculation with a visual and instrumental approach, more direct and easy to understand and handle. They are also well suited to provide an understanding of 3D spatial arrangements that are otherwise difficult to explain. The relationship between the mathematical object and the manufactured part is established as a very useful pairing, and brings mathematics closer to the field of prototyping and experimentation.

Our kits are mathematical products with links to the world of monumental art, engineering and technology, making them a true STEAM product. Their ability to arouse interest and contextualize in an interdisciplinary framework will help the mathematical understanding and make these technologies a companion in the evolution of mathematics education.

Acknowledgments

The authors would like to thank the referees for their valuable suggestions to improve this paper. We also would like to thank “Fundación Descubre” for providing some of the images for the manuscript.

References

- [1] R. Fathauer, *Tessellations: Mathematics, Art, and Recreation*. A K Peters/CRC Press. 2020. ISBN: 978-0367185961.
- [2] P. Fuentes, *The Islamic Crossed-Arch Vaults in the Mosque of Córdoba*, Nexus Network Journal 21 (2019), 441–463. DOI 10.1007/s00004-018-0403-y.
- [3] P. Fuentes and S. Huerta, *Islamic domes of crossed-arches: Origin, geometry and structural behavior*. Arch' 10. 6th International Conference on Arch Bridges, Fuzhou (China), 2010. 346-353.
- [4] S. Gokmen, A. Basik, Y. Aykin and S. Alacam, *Computational Modeling and Analysis of Seljukid Muqarnas in Kayseri*, Journal on Computing and Cultural Heritage, Vol. 15 (2), (2022), Article No.: 27, DOI 10.1145/3477399.
- [5] B. Grünbaun and Z. Grünbaum, *Symmetry in Moorish and other ornaments*, Comp. and Maths. with Appls. Vol 12B (1986), Nos. 3/4, 641-653.
- [6] B. Grünbaun and G.C. Shepard, *Tilings and Patterns*, Second Edition. Dover Publications. 2016. ISBN: 978-0486469812.
- [7] D. Makris, I. Skaltsas, S. Fotiou, L. Karampinis and M. A. Vlachou, *Digitization of Athens School of Fine Arts Artworks Based on Optical 3-D Scanning and Photogrammetry*. 9th International Conference on Information, Intelligence, Systems and Applications (IISA), 2018, 1-7, DOI 10.1109/IISA.2018.8633603
- [8] A. Martínez-Sevilla, (Coord.) *Paseos Matemáticos por Granada: un estudio entre Arte, Ciencia e Historia*, Ed. Universidad de Granada, Granada, 2017.
- [9] A. Martínez-Sevilla, *Artistic Heritage meets GeoGebra*. GeoGebra Global Gathering, GGG'17, Linz (Austria), 2017.
- [10] R. Matheny, M. Hagseth and T. L. Schendel, *Photogrammetry as an Access Tool: A Case Study of Small Collections From the Evansville Museum of Arts, History & Science*. Collections, 0 (0) (2022). DOI 10.1177/15501906221129340.

- [11] M. Sakkal, *Geometry of Muqarnas In Islamic Architecture*, PhD. Thesis, University of Washington, 1982.
- [12] A. Sáseta Velázquez, *El juego de los mocárabes*, Cuadernos de los amigos de los museos de Osuna, 18, (2016), 135-144. ISSN 1697-1019.
- [13] D. R. Smith, *The design of divide and conquer algorithms*, Science of Computer Programming 5 (1985), 37-58, DOI 10.1016/0167-6423(85)90003-6.

Software Programs

- [14] Blender, a free 3D creation suite. <https://www.blender.org>
- [15] FreeCad, your own 3D parametric modeler. <https://www.freecadweb.org/>
- [16] GeoGebra, *A dynamic mathematics software*. <https://www.geogebra.org>
- [17] Inkscape, a free 2D free design tool. <https://inkscape.org/es/>

Problems in Randomization of Online Question Banks (Case Studies)

Ildikó Perjési-Hámori

e-mail: perjesi.ildiko@mik.pte.hu

University of Pécs

Faculty of Engineering and Information Technology

Pécs, Hungary

Dóra M. Szegő

e-mail: szego.dora@mik.pte.hu

University of Pécs

Faculty of Engineering and Information Technology

Pécs, Hungary

Abstract

At the University of Pécs (Hungary) mathematics courses are the basis for programs such as engineering and computer science. An online question bank was developed for university students to practice mathematical problem-solving and to use for exam assignments.

Computer-aided test and assessment is widely used to support the teaching and learning of mathematics.

In the research some aspects of question design were asked about the new possibilities of randomizing the question::

- 1. What type of randomization is useful to introduce, and what are the limits of randomization?*
- 2. Why is it sometimes so dangerous, what are the benefits, and what are the limits of it?*
- 3. What type of math problems can be solved using random variables?*
- 4. How can we ensure equal difficulty for the variation of questions?*

In our paper, some case studies of the task design are presented. The examples are from courses in mathematics at BSc and MSc levels, as well.

1. Introduction

During the pandemic lockdown, the teachers in schools and lecturers at the universities turned to formative and summative assessments [1], [2], [3]. Nowadays assessments are the focus of didactical research [4], [5]. The well-developed assessments (assessment with digital technology or assessment through digital technology) [6] are well-usable tools to get more accurate feedback about the student's mathematical knowledge, helping lecturers guide and monitor the students' progress [7], [8], [9]. At the Department of Mathematics, the University of Pécs (UP), Faculty of Engineering and Information Technology during the pandemic different types of questionnaires were introduced (first of all to avoid cheating), The MOODLE LMS can handle most digital technology-based assessment systems, but there are only few which manages the mathematical equivalences (STACK based on Maxima [10], MATHLAB Grader based on MATHLAB [11], GeoGebra assessment [12], MÖBIUS earlier MAPLE T.A. based on MAPLE, etc). Because we have had experience using Maple computer algebra system (CAS) during math courses for a long time [13], [14] we have chosen the Maple-based Möbius test and assessment system [15], [16]. Assessments with digital technology are used not only for online courses but conventional (face-to-face) courses as well.

The Möbius TA was introduced to practice mathematical problem solving (formative assessment) and to use for exam situations (summative assessment) as well.

In this paper, there is a discussion about the emerging problem during the development of question banks in online test and assessment system. Our didactical questions are about the ideas of randomization and evaluation.

There are so many ways to randomize in a test. In a conventional test system, there are

- randomly generated quizzes from pools of questions
- random orders in
 - blocks
 - questions
 - possible answers in multiple choice questions.

In a CAS-based system, the questions could be generated with random variables, and the students see different variants of a question.

In our research we are looking for answers to the following questions:

- What type of randomization is useful to introduce, and what are the limits of randomization?
- Why is it sometimes so dangerous, what are the benefits, and what are the limits of it?
- What type of math problems can be solved using random variables?
- How can we ensure equal difficulty for the variation of questions?

In the next chapters, some case studies of the task design and the evaluation changes are shown.

The examples are from courses in mathematics for STEM courses, at BSc and MSc levels, as well.

2. Simple randomization

The first example is for freshmen students. It is a simple problem, with six random values which are simple integers; (easy calculation is necessary and because from a didactical point of view, no calculator or computer algebra is allowed, the assessment system was used in proctored mode). Two cases (*maximum*, *minimum*) increase the variability of the two unknowns (Figure 1, Figure 2, Figure 3). There are two conditions, a and b are not equal to 0. a is not zero to have an absolute value function, and b is not zero for the questions to be of similar difficulty.

Find the values of the missing parameters if the form of the function is

$$f(x) = a|x| + b,$$

the 'minimum value' of the function is equal to -4, and

$$f(-5) = 21$$

The domain of the function is the real number set.

$a =$ $\quad b =$

Figure 1: Example 1. Simple random question, in the question's preview

Find the values of the missing parameters if the form of the function is

$$f(x) = a|x| + b,$$

the \$m of the function is equal to \$b, and

$$f($x0) = $c$$

The domain of the function is the real number set.

$a =$ $\quad b =$

Figure 2: Example 1. Simple random question, question's text

```

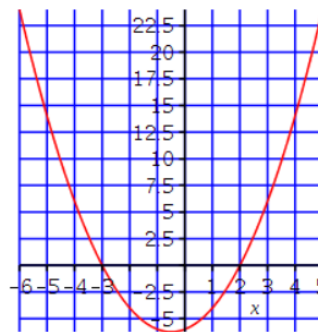
$a=range(-5,5);
condition: ne($a,0);
$b=range(-5,5);
condition: ne($b,0);
$x0=range(-5,-1);
condition: ne($x0,0);
$c=maple("$a*abs($x0)+($b)");
$m=maple("if $a>0 then `minimum value` else `maximum value` end if");
$m_szep=maple("MathML[ExportPresentation]($m)");

```

Figure 3: Example 1. Simple random question, question algorithm

3. Randomization of figure

Example 2. is about the random figure in a question. This question is for freshmen students, as well, they had to read the parameters from the figure. Conditions were: the whole square was to be avoided, the figure axes must be dynamic ones, and the intervals on the axes depend on the function's definition. Three answers are needed, so the points of the question could be partial (Figure 4). The commutativity is handled in the grading part. Remark: the disadvantage of the display is, if the answer is negative, there are no parentheses for it. Maybe it's not confusing because there's a relatively large space separating the answer from the text of the question. From a didactical point of you, the quality of the figure is very important, students have to understand the connection between the meaning of zero points and the existence of minimum or maximum and the asked values. Because of the dynamical visualization, the condition in the question is that $b < c$.



Find the formula for the above-plotted parabola in factorized form

y= ·(x+) ·(x+)

```

$m=range(-1,1);
$b=range(-3,-1);
$c=range(1,3);
condition: ne($m,0);
condition: ne($b,0);
condition: ne($c,0);
condition: ne($c,$b);
$f=maple("$m*(x-($b))*(x-($c))");
$f_szep=maple("MathML[ExportPresentation]($f)");
$hv1=maple("-( $b )");
$hv2=maple("-( $c )");
$x1=maple("( $b )-3");
$x2=maple("( $b )+3");
$y1=maple("if $m=1 then $c-4 else $c-($c)/2 end if");
$y2=maple("if $m=1 then ($c)+4 else 1 end if");
$wave1=plotmaple("plot($f,x=($b)-3..($c)+3,'color'=red,
axis = [thickness=1,gridlines = [10,colour = blue]]),
plotdevice='jpeg', plotoptions='width=250,height=250'");

```

Figure 4: Example 2. Random figure

4. Randomization of wrong answers in multiple choice and theoretical question

Example 3. shows, how the random variables are connected, and how wrong answers depend on the correct ones. The wrong answers are calculated from the correct ones, using the *ListTools* Maple package. The question is not about the solutions of the equation, but only the number of solutions on a closed or open or half-closed, half-open interval. From didactical points it is a complex question, it connects different knowledge backgrounds, the meaning of interval, and the number of the solution of the trigonometrical equation. The variables are reduced depending on whether k is odd or even, and the equations are $\sin(kx) = 0$ or $\cos(kx) = 0$ (Figure 5). Planning is not so easy: the designer must be an expert on math didactic, a perfect Maple user, and a Möbius script writer. That's why most of the teachers are using only easily programable questions or well-prepared questions from other question banks.

How many roots does the equation strigeq have on the interval Sint ?

\$correct
 \$wrong1
 \$wrong2
 \$wrong3
 \$wrong4

How many roots does the equation $\cos(3x) = 0$ have on the interval $\left[\frac{\pi}{2}, \frac{3\pi}{2}\right]$?

05 04 02 06 03

```

$K = range(2,3); # sin(k*x), oos(k*x)
$var1 = rint(2); # left side is open or closed
$var2 = rint(2); # right side is open or closed
$bo = switch($var1, "\biggl[", "\biggl[");
$jo = switch($var2, "\biggr]", "\biggr");
$ver = rint(2);
#interval J=[Pi/2;3Pi/2[, if k is odd, if k is even and k/2 is odd,
#then [Pi/4;5Pi/4[, if k/2 is even [Pi/(2k);Pi/(2k)+Pi[
$int = switch($ver, "0;\pi", if($k-2, "\frac{\pi}{2};\frac{3\pi}{2}",
"\frac{\pi}{4};\frac{5\pi}{4}");
$int = "\(" $bo $int $jo \)";
$trigeq = switch($ver, "\(\sin($k*x)=0 \)", "\(\cos($k*x)=0 \)");
$h = -1+$k+$var1+$var2; # correct answer
# 4 wrong answers
$T = min($h,rint(5)); # using Maple built in package
$s = maple("with(ListTools):
L:=seq($h-$T+i,i=0..4);
L:=Rotate(L,$T);
L[ ]");
$correct = switch(0,$s);
$wrong1 = switch(1,$s);
$wrong2 = switch(2,$s);
$wrong3 = switch(3,$s);
$wrong4 = switch(4,$s);
    
```

Figure 5: Example 3. Multiple choice question

If the question is a theoretical one from the differential equation (Example 4.), only the coefficients and exponent values manage the correct answer. The possible answers are on the lists, but they are not static, the random coefficient, exponent, and the function on the right-hand side manage them. The simple lists manage the answer, but the correct answer depends on the equation (Figure 6, Figure 7).

Let $2 \left(\frac{d^2}{dx^2} y(x) \right) + 3 \left(\frac{d}{dx} y(x) \right) + y(x)^2 = \cos(x)$

This ODE is

(Click for List)	(Click for List)	(Click for List)
(Click for List)	(Click for List)	(Click for List)
'second order'	'non-linear'	homogenous
'first order'	linear	inhomogenous

Figure 6: Example 4. Theoretical question

```

$a:=rint(3);
$b:=rint(4);
condition:=ne($a,$b);
$c:=range(1,2);
$f:=switch(rint(3),y*cos(x),cos(x),0);
$de:=maple("($a)*diff(y(x),x$2)+($b)*diff(y(x),x)+y(x)^(c)=$f");
$de_szep:=maple("MathML[ExportPresentation]($de)");
$hv1:=maple("if $a=0 then `first order` else `second order` end if");
$rv1:=maple("if $a=0 then `second order` else `first order` end if");
$hv2:=maple("if $c=1 then `linear` else `non-linear` end if");
$rv2:=maple("if $c=1 then `non-linear` else `linear` end if");
$hv3:=maple("if $f=cos(x) then `inhomogenous` else `homogenous` end if");
$rv3:=maple("if $c=cos(x) then `homogenous` else `inhomogenous` end if");

```

Figure 7: Example 4. Conditions in theoretical question

5. Randomization using a self-made Maple package

Sometimes developers have to create their own Maple package to design a question of equal difficulty for everyone. Example 5. is a linear algebra question, asking about the reduced row echelon form from a linear system and the number of solutions. In this situation, the correct answer to the multiple-choice question depends on the rank of the system. The developed *LinAlgTools* package [15] solve an everyday problem for teaching linear equation system. If there are arbitrary coefficients in the system, the result of the row operation process sometimes causes miscalculations because of the fractions, and the students can not focus on the meaning of the results (mainly the number of solutions and the explanation). Using this new Maple package the coefficients are integers, but the solution types could be different. To avoid mistyping there is some instruction for input written in red (Figure 8), this is the way how the users are helped to have the input correctly.

Find the solution using Gaussian elimination

$$\begin{aligned}
 2x - 10y - 14z &= 28 \\
 5x - 23y - 33z &= 70 \\
 -4x + 23y + 29z &= -48
 \end{aligned}$$

A) The augmented matrix of the LES is

The form of the matrix is $\text{Matrix}([[a_{11}, a_{12}, a_{13}, a_{14}], [a_{21}, a_{22}, a_{23}, a_{24}], [a_{31}, a_{32}, a_{33}, a_{34}]])$

B) The reduced row echelon form is

C) The LES has

'no solution'

'unique solution'

'infinite number of solutions'

Correct

Your Answer: $\text{Matrix}([[1, 0, 0, 6], [0, 1, 0, 4], [0, 0, 1, -4]])$

Correct Answer: $\begin{pmatrix} 1 & 0 & 0 & 6 \\ 0 & 1 & 0 & 4 \\ 0 & 0 & 1 & -4 \end{pmatrix}$

```

$x:=range(-5,5);
$y:=range(-5,5);
$z:=range(-5,5);
$r:=switch(rint(2),2,3);
$a:=range(1,2);
$Q:=maple(" M:=if $a=1 and $r=2 then LinAlgTools:-SpecialMatrix([3,3,$r],aug,nosol)
else LinAlgTools:-SpecialMatrix([3,3,$r],aug) end if:
S:=LinearAlgebra:-GenerateEquations(M,[x,y,z]):

R:=LinearAlgebra:-ReducedRowEchelonForm(M);
convert~([M,S[1],S[2],S[3],R],string),
libname=/web/Ptemik001/Public_Html/Packages/LinAlgTools.mla");
$M:=switch(0,$Q);
$M_szep:=maple("MathML:-ExportPresentation($M)");
$S1:=switch(1,$Q);
$S2:=switch(2,$Q);
$S3:=switch(3,$Q);
$R:=switch(4,$Q);
$R_szep:=maple("MathML:-ExportPresentation($R)");
$L:=maple("$R[3]");
$L_szep:=maple("MathML:-ExportPresentation($L)");
$R34:=maple("$R[3,4]");
$S1d:=maple("MathML:-ExportPresentation($S1)");
$S2d:=maple("MathML:-ExportPresentation($S2)");
$S3d:=maple("MathML:-ExportPresentation($S3)");
$hv:=maple("if $R[3,3]<>0 then `unique solution` elif $R[3,4]=0 then `infinite number of solutions`
else `no solution` end if");
$rv1:=maple("if $R[3,3]<>0 then `no solution` elif $R[3,4]=0 then `unique solution`
else `infinite number of solutions` end if");
$rv2:=maple("if $R[3,3]<>0 then `infinite number of solutions` elif $R[3,4]=0 then `no solution`
else `unique solution` end if");

```

(1) \$hv fixed

(2) \$rv1 fixed

(3) \$rv2 fixed

Figure 8: Example 5. Using self-made package

6. Backward thinking – Maple and precise mathematics

As tutors, we know from our earlier practice developing a good question, sometimes is useful to think backward. In Example 6. the question is about the indefinite integral of rational functions, using partial fractions. Inside the script, the improper fraction is given as a sum of a polynomial and a proper fraction but in factorized form. But in the question text, the function appears in expanded form. It is necessary to have the same number of factors, the same number of polynomial terms, and proper terms (Figure 9) to have equivalent difficulty in the answer.

Divide the numerator into the denominator to get a polynomial plus a proper fraction, and determine the antiderivative

$$f(x) = \frac{4x^3 + 15x^2 + 7x - 10}{(x+1)(x+3)}$$

Polynom part $\frac{4x^3 + 15x^2 + 7x - 10}{(x+1)(x+3)} =$

Proper fraction $\frac{4x^3 + 15x^2 + 7x - 10}{(x+1)(x+3)} =$

The indefinite integral $\int \frac{4x^3 + 15x^2 + 7x - 10}{(x+1)(x+3)} dx =$

```

condition: ne(%c,0);
condition: ne(%a,0);
condition: ne(%d,0);
condition: ne(%e,0);
condition: ne(%b,1);#because of ln(abs(x))
condition: ne(%b,0);
condition: ne(%e,($g));#two different quotients
$f:=maple("factor(%a*x+(%b)+(%c)/(x+(%e))+(%f)/(x+(%g)))"); #reverse thinking
$sol:=maple("convert($f,parfrac");#reverse thinking

$poli:=maple("op(1,$sol))+op(2,$sol)");#the polynomial has 2 terms
$proper:=maple("op(3,$sol))+op(4,$sol)");
    
```

Figure 9: Example 6. Backward thinking

Another possibility to define rational function is to use Maple *randpoly* command, but the result could be varying difficulties and forms (Figure 10), so it was neglected in the question.

<pre> Random polynomial -> > num := randpoly(x, coeffs = rand(-2..2), degree = 4) num := x^3 - 2x^2 - 2x - 2 > denom := randpoly(x, dense, coeffs = rand(-2..2), degree = 2) denom := -x^2 - x > g := num/denom g := (x^3 - 2x^2 - 2x - 2)/(-x^2 - x) > convert(g, parfrac) -x + 3 - 3/(x+1) + 2/x </pre>	<pre> Random polynomial -> > num := randpoly(x, coeffs = rand(-2..2), degree = 4) num := x^4 + 2x^3 - 2x^2 + x - 2 > denom := randpoly(x, dense, coeffs = rand(-2..2), degree = 2) denom := -x^2 - 2x + 2 > g := num/denom g := (x^4 + 2x^3 - 2x^2 + x - 2)/(-x^2 - 2x + 2) > convert(g, parfrac) -x^2 + (-x + 2)/(x^2 + 2x - 2) </pre>
--	--

Figure 10: Example 6. Different results using Maple *randpoly* command

In this situation, as strict teachers, we are not satisfied with the indefinite integral for $\frac{1}{x}$ as $\ln(x)$, which is given by Maple but we are waiting for $\ln|x| + C$. So it has to be realized which part of the integral has *ln* form to transform it into the correct answer form. (Figure 11.)

```

$intsol:=maple("int(($f),x)");#integral in Maple form not ln(abs) no C
$op21:=maple("op(2,op(1, $intsol))");
$op22:=maple("op(2,op(2, $intsol))");
$op23:=maple("op(2,op(3, $intsol))");
$op24:=maple("op(2,op(4, $intsol))");
$i1sol:=maple("if $op21 = ln(x+($e)) then ln(abs(x+($e)))
elif $op21 = ln(x+($g)) then ln(abs(x+($g)))
else $op21 end if"; # int(1/x,x)=ln(x) and not ln(abs(x))+C
$i2sol:=maple("if $op22 = ln(x+($e)) then ln(abs(x+($e)))
elif $op22 = ln(x+($g)) then ln(abs(x+($g)))
else $op22 end if");
$i3sol:=maple("if $op23 = ln(x+($e)) then ln(abs(x+($e)))
elif $op23 = ln(x+($g)) then ln(abs(x+($g)))
else $op23 end if");
$i4sol:=maple("if $op24 = ln(x+($e)) then ln(abs(x+($e)))
elif $op24 = ln(x+($g)) then ln(abs(x+($g)))
else $op24 end if"); #the order is not always appropriate
$isol:=maple("(op(1,op(1, $intsol)))*($i1sol)+(op(1,op(2, $intsol)))*($i2sol)+
(op(1,op(3, $intsol)))*($i3sol)+(op(1,op(4, $intsol)))*($i4sol)+C");
    
```

Incorrect	
Your	No answer
Answer:	
Correct	$2x^2 - x - 3 \ln(x + 1) + 2 \ln(x + 3) + C$
Answer:	

Figure 11: Example 6. Handling integral $1/x$

7. Using CAS to have the right answer

It is a question to MSc students, they are allowed to use CAS during the exam. The students are familiar with Maple commands, the well-prepared worksheets were introduced in the face-to-face classes, which were held in a computer lab. In the exam problem, there were randomized data, but they are defined in connection to each other (Figure 12). On the preview page, the correct answer is seen, but only on a figure, which helps to have the correct answer (Figure 13). Randomized data, randomized figures, and intervals were used.

The table below shows the relationship between the average speed of a car (km / h) and the stopping distance (m) for that speed

X	Y
5.4	5.6
9.6	11.8
14.9	22.4
19.8	39.9
25.6	53.9
29.4	71.9
35.3	90.3
39.7	122.3

Determine - using the least-squares method - whether a linear, quadratic or quadratic function relationship between the two quantities approximates the relationship between the data with the least error.

Use Maple or Excel for your calculation

```

$X:=maple("[5.4, 9.6, 14.9, 19.8, 25.6, 29.4, 35.3, 39.7]");
$Z:=maple("[5.6, 11.8, 22.4, 39.9, 53.9, 71.9, 90.3, 122.3]");
$Y:=maple("for 1 to 8 do
    R[1] := rand(-8 .. 8);
    YY[1] := $Z[1] + evalf(R[1]()/10, 3);
end do;
[seq(YY[j], j = 1 .. 8)]");
    
```

Figure 12: Example 7. Randomized data with condition

8. Evaluation

It is an interesting and important issue to investigate the result of exams with and without an online test system. We had an experiment during the Covid 19 when our students had remote exams. The course was Engineering Mathematics 2 (BSc, Semester 2). There were two groups, in the first group the students were from the Electrical and Civil Engineering (EE and CE) program, and in the second one the students were from Computer Science Engineering (CSE) program. The same classes were held for both groups, they had two parts, one part was the lecture, and the other is the practice. During the practice part, the students got an assignment with non-randomized questions. They had 45 minutes to solve the problems, it was allowed to collaborate. Every week they had an assignment with randomized questions to practice the discussed topics alone. During the semester there was two homework to be submitted on Möbius, with randomized questions. The difference was in the exam situation. The group CSE had the homework and exam on Möbius with

randomized questions, and the control group's (CE and EE) homework was on Möbius, but during the exam, the 'solve-it on paper-then-upload-it ' method was used.

Linear approximation: $y =$ $\cdot x +$

The sum of the squares of the differences:

Quadratic approximation: $y =$ $\cdot x^2 +$ $\cdot x +$

The sum of the squares of the differences:

Third ordered approximation: $y =$ $\cdot x^3 +$ $\cdot x^2 +$ $\cdot x +$

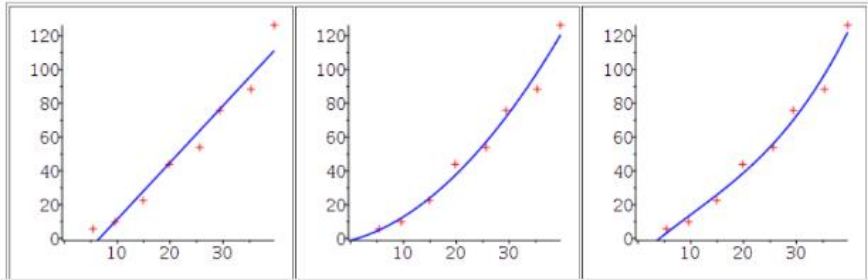
The sum of the squares of the differences:

The best approximation

second ordered

first ordered

third ordered



```
$hv=maple("if ($diff_lin<$diff_square) and ($diff_lin<$diff_cube) then 1 elif $diff_cube<$diff_square then 3 else 2 fi");
```

Figure 13: Example 7. Calculation in Möbius with help of CAS

The next example from the test highlights the difference between the two forms of the exam. For the paperwork, one question was:

Find the regions of integration and evaluate the double integral over the region bounded by $y = 4x, y = x, x = 2, x = 4$ lines, if $f(x, y) = x - 4y$.

A similar question on Möbius is seen in Figure 14.

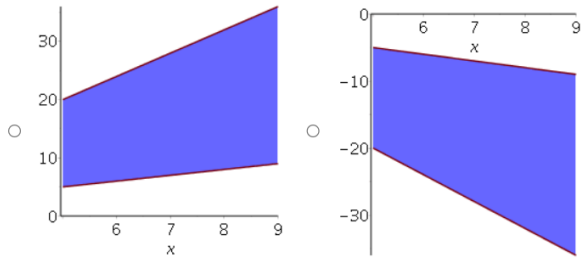
We expected that Möbius question helps the students to go through to the solution, but unfortunately, it was not true. Comparing the two groups we found that there is a much higher degree of correlation between the homework average and the exam average for CE and EE group than for CSE. Unsurprisingly, identical (identically flawed) solutions were prevalent among CE and EE group. One explanation of this phenomenon is that randomized questions prevent unwanted student collaboration (Figure 15, Table 1) the other (more benevolent) one is the unusual way of typing the degraded result. In the future, we have to have some new similar experiments when all students write their exams in the university building.

Find the regions of integration and evaluate the double integral over the region bounded by $y=4x$, $y=x$, $x=5$ and $x=9$, if

$$f(x,y) = x - 4y$$

The region is a normal region respect to
The shape of the region is:

(Click for List) ▾



The intervals of the integration are:

$$y_1 = \text{[input]} \leq y \leq \text{[input]} = y_2$$

$$x_1 = \text{[input]} \leq x \leq \text{[input]} = y_2$$

$$\int x - 4y \, dy = \text{[input]}$$

$$\int_{y_1}^{y_2} x - 4y \, dy = \text{[input]}$$

exact value please

$$\int_{x_1}^{x_2} \int_{y_1}^{y_2} x - 4y \, dy \, dx = \text{[input]}$$

Figure 14: One exam question with - and without TA

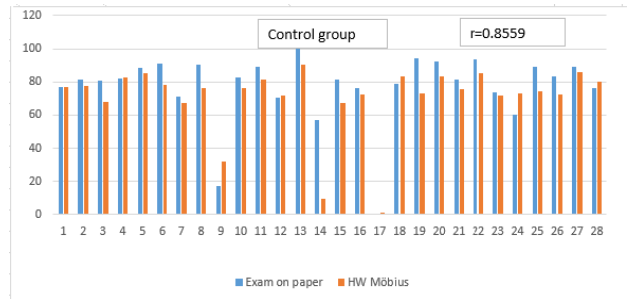
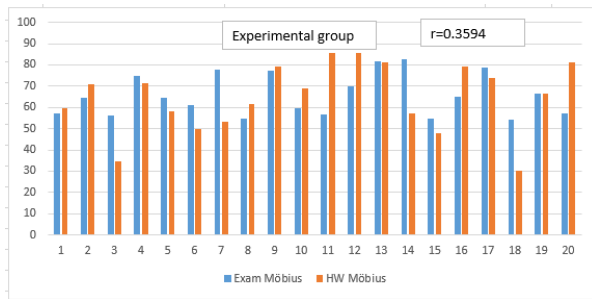


Figure 15: Exam results with - and without TA

	Civil-, Electrical Engineering	Computer Science Engineering
HW Möbius	70.48	64.79
Exam Paper	77	
Exam Möbius		66
correlation	0.8559	0.3594

Table 1: Result of experimental – and control group

A significant advantage of using the system from the professor's point of view is that it is much easier for lecturers to grade the tests and if there are a huge number of questions in the question banks, they can use them year-by-year. The system has many item statistics, which help the instructor correct the question hardness, form, and question types in the assignment.

9. Conclusion

After the above-mentioned examples, one possible answer to the question posed in the introduction is as follows.

What type of randomization is useful to introduce, and what are the limits of randomization?

Randomization in variables and figures is easy. For theoretical questions, the multiple-choice or list type is more usable. Sometimes self-made Maple packages are needed to avoid complicated calculations (e.g. Example 5.) Preparing the assignments, similar types of questions could be collected in a group, and the students get only one (or more) from each group. So not only the randomization of data but the randomization of questions increases the variability of assignments.

Why is it sometimes so dangerous, what are the benefits, and what are the limits of it?

Questions that can be easily divided into parts, but the response area can not handle if one answer is wrong and the user continues to calculate with this wrong value (e.g. Example 7).

Using randomized question banks is profitable for students because

- there is no transmitter language – in contrast to computer algebra systems
- it is based on cloud computing, for the user needs only a browser and a username
- it understands the mathematical equivalence
- they have prompt feedback
- they can practice without a time limit.
- visualization helps to understand the problem.

It is helpful for teachers because

- there are a lot of question types (open-ended and closed-ended questions)
- every student gets different questions
- there is flexible scoring, partial points
- they can create a different assessment for the same question bank easily
- it can follow up on the student's activity.
- there is no need to correct tests, and there is no photocopying.

Difficulties are liable to occur for students because

- there is no personal connection with the teacher
- mistype causes incorrect answer
- the software sometimes is not user friendly
- there is no cheating.

Some difficulties for teachers are that

- the process is time-consuming
- unconventional question definition is needed
- the developer has to get ready for all possible answer
- they need some knowledge not only in mathematics but in computer algebra and programming, as well
- the software sometimes is not user-friendly.

What type of math problems can be solved using random variables?

Asking definitions, conditions of theorems, and complex problem-solving problems can be randomized (naturally proof is not easy to randomize) (e.g. Example 3).

How can we ensure equal difficulty for the variation of questions?

Because similar difficulty is needed, the design sometimes does not allow using Maple randomization possibilities the backward thinking ensures a similar type and hardness (e. g. Example 6.).

Concluding a CAS-based assessment needs very careful planning, programming, and checking phases. In the planning period, it must be defined clearly, what part of the curriculum is important to ask, who are the target groups, and what is their background. Construct different assessments for different purposes (practicing, self-regulation, exam). Data acquisition is necessary, mainly the selection of the type of questions, splitting the exercises into parts, weighting, defining the questions clearly, and limiting randomization. We have to be careful that everyone gets a question of equal difficulty. In this part, the main guiding principle is the didactic of mathematics (naturally together with the correct mathematics).

During the programming section, close teamwork is necessary between the curriculum developer and IT expert (the best situation is if the members of the group are those math teachers, who are good in programming).

The check can take a long time. It must be teamwork to realize all possible sources of error.

Firstly the developers have to answer the questions in a different situation. Using the grading options in Möbius TA (class grades and item statistics) the developers could see which questions are easy and which are hard.

It seems to be a time-consuming process, but the work pays off. The same question bank could be used year by year, the teacher gets rid of boring test corrections. Using a well-prepared questionnaire (with detailed feedback) and after oral explanation, the role of the teacher is only to guide students, they can learn alone.

In the next future, our didactical research will focus on how these new techniques change the topics of mathematics curriculum in engineering education, and how will it help to focus better on deeper understanding instead of problem-solving schematically.

References

- [1] Barlovits, S., Jablonski, S., Lázaro, S., Ludwig, S. Recio, T., *Teaching from a distance— Math lessons during COVID-19 in Germany and Spain* Education Sciences 11 (8), 406. 2021. <https://doi.org/10.3390/educsci11080406>
- [2] Iannone, P., *Assessing Mathematics at University: Covid-19 and beyond* 2020. https://www.researchgate.net/publication/342765751_Assessing_Mathematics_at_University_Covid-19_and_beyond
- [3] Henley, M., Grove, M., Hilliam, R., *University Mathematics Assessment Practices During the Covid-19 Pandemic*. MSOR Connections, 20(3) pp. 5–17. 2022. <https://journals.gre.ac.uk/index.php/msor/article/view/1325>
- [4] Winkler, S., Körner, A., Breiteneker, F., *A New Approach Teaching Mathematics, Modelling and Simulation* Proceedings of the 9th EUROSIM Congress on Modelling and Simulation, 416–421. 2016. DOI: [10.3384/ecp17142416](https://doi.org/10.3384/ecp17142416)
- [5] Beumann, S., Wegner, S. A., *An outlook on self-assessment of homework assignments in higher mathematics education* International Journal of STEM Education, 5, 55, 2018. DOI: [10.1186/s40594-018-0146-z](https://doi.org/10.1186/s40594-018-0146-z)
- [6] Drijvers, P., *Digital assessment of mathematics: Opportunities, issues and criteria* Mesure et évaluation en éducation Vol. 41, No 1, 41-66 2018. <https://doi.org/10.7202/1055896ar>
- [7] Hoogland, K., Tout, D., *Computer-based assessment of mathematics into the twenty-first century: pressures and tensions* Zentralblatt für Didaktik der Mathematik 50, 675–686. 2018. DOI: [10.1007/s11858-018-0944-2](https://doi.org/10.1007/s11858-018-0944-2)
- [8] Barana, A., Marchisio, M., Sacchet, M., *Interactive Feedback for Learning Mathematics in a Digital Learning Environment* Education Sciences, 11(6), 279, 2021. DOI: [10.3390/educsci11060279](https://doi.org/10.3390/educsci11060279)
- [9] Tuluk, A., 1, Yurdugul, H., *Design and Development of a Web-Based Dynamic Assessment System to Increase Students' Learning Effectiveness* International Journal of Assessment Tools in Education 7(4), 631–656. 2020. DOI: [10.21449/ijate.730454](https://doi.org/10.21449/ijate.730454).
- [10] Lopes, A.P., Soares, F., *Online Assessment Using Different Tools and Techniques in Higher Education* 14th International Conference on Education and New Learning Technologies, Palma, Spain, 510-517, 2022 DOI: [10.21125/edulearn.2022.0157](https://doi.org/10.21125/edulearn.2022.0157)
- [11] Gregg, A. WT, O'Dell, N., Farnworth, T., Renton, C., *Automatic assignment marking using MATLAB grader and offline unit testing code* 31st Annual Conference of the Australasian Association for Engineering Education (AAEE 2020): Disrupting Business as Usual in Engineering Education, Barton, ACT, 430-438, 2020. <https://search.informit.org/doi/10.3316/informit.727282152310853>
- [12] Radović, S., Radojičić, M., Veljković, K., Marić, M., *Examining the effects of Geogebra applets on mathematics learning using interactive mathematics textbook*, Interactive Learning Environments, 28:1, 32-49, 2020. DOI: [10.1080/10494820.2018.1512001](https://doi.org/10.1080/10494820.2018.1512001)

- [13] Perjési- Hámori, I., *Teaching numerical methods using CAS*, The Electronic Journal of Mathematics and Technology Vol. 9. No 2. 229-238, 2015.
- [14] Perjési- Hámori, I., *Principcle of Spirality and Gradation in the Usage of Technology in the Courses of Engineering Mathematics* Proceesings SEFI 2021 49th Annual Conference, Berlin, 1113-1122, 2021. <https://www.sefi.be/wp-content/uploads/2021/12/SEFI49th-Proceedings-final.pdf>
- [15] Szegő, D., Perjési-Hámori, I. and Maróti, Gy., *Maths in the Time of Corona: Experiences in Remote Education* Electronic Proceedings of the 25th Asian Technology Conference in Mathematics 1940. 2021. <https://atcm.mathandtech.org/EP2020/abstracts.html>
- [16] Szegő M. D., *How Blended Learning Techniques can be Applied in Teaching Mathematics to Engineering Students* The International Journal for Technology in Mathematics Education Vol. 30. 1 under publication 2022.

Inversion of Equiangular Spirals

Elias Abboud*

Faculty of Education, Beit Berl College, Doar Beit Berl 44905, Israel
eabboud@beitberl.ac.il

Abstract

In this article we focus on properties of equiangular spirals and their inversion in a circle. Our aim is to emphasize the use of polar coordinates and describe how to draw the inversion of equiangular spirals to get two-pole spirals. In particular, we provide a connection to the art of Escher through the use of GeoGebra software. This allows to create exploring activities that enrich the teaching process and expose both students and instructors to the beauty of mathematics.

1 Introduction

A *spiral* is a curve in the plane that winds continuously about a fixed point called a *pole*. *Equiangular* spirals or the *Logarithmic* spirals, are plane curves with polar equation $r = e^{a\theta+b}$, where a and b are real numbers. The main property of equiangular spirals is that the tangent at any point on the curve makes a constant angle with the radial line that issues from the pole and passes through the point. The spiral of Archimedes with polar equation $r = a\theta$, and Fermat's spiral with polar equation $r = a\sqrt{\theta}$, where $a \neq 0$ is a fixed real number, are not equiangular. To see this for the spiral of Archimedes, we draw with GeoGebra the polar equation of the spiral of Archimedes for the value $a = 1$. In the input bar of GeoGebra we insert the equation $r = \theta$, the software will recognize that we are working with polar coordinates. The obtained curve is shown in Fig. 1. We mark two points B and C and draw the radial lines, using the ray tool, between the pole A and each one of the points B and C . Then using the tangent tool we draw the tangents of the curve at the points B and C . Finally, we use the angle tool to measure the angle between these tangents and the radial lines. We see that the angle is not preserved, see Fig. 1.

On the other hand, the spiral $r = e^\theta$ is equiangular as shown in Fig. 2, the tangent at any point on the curve makes a constant angle with the radial lines, see also the animated Figure [10].

*This topic was presented at CADGME 2022 conference

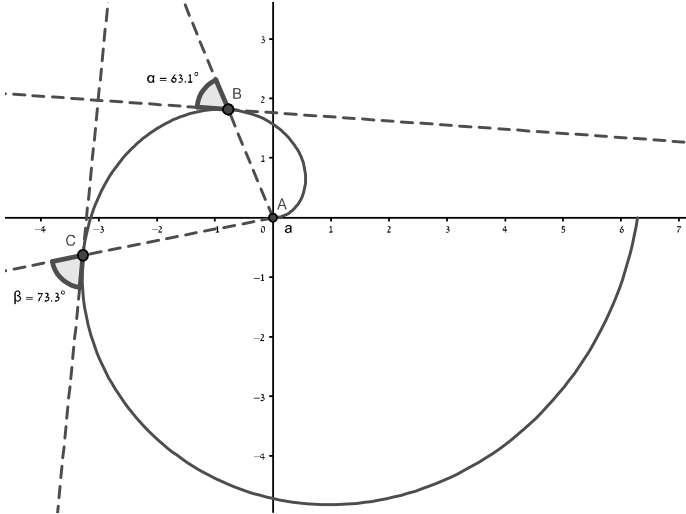


Figure 1: The spiral of Archimedes with polar equation $r = \theta$ is not equiangular

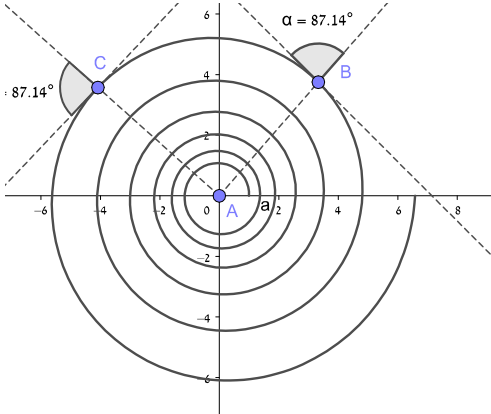


Figure 2: Equiangular spiral

The equiangular spiral was first considered in 1638 by Descartes. His discussion was based upon the consideration of a curve cutting radii vectors from a fixed point O under a constant angle, ϕ . From this he inferred the polar equation $r = ke^{c\theta}$ where $c = \cot \phi$. When $c = 1$, then the ratio of two radii vectors corresponds to a number and the angle between them to its logarithm; whence the name of the curve, see [1].

Torricelli, who died in 1647, worked on it independently and found the length of the curve. He used for a definition the fact that the radii are in geometric progression if the angles increase uniformly, i.e., for each angle θ_0 the radial line $\theta = \theta_0$ meets the spiral at infinitely many discrete points. The radii vectors from the center of the spiral to these points form a geometric progression.

Jacob Bernoulli, some fifty years later, found all the “reproductive” properties of the curve; and these almost mystic properties of the “wonderful” spiral made him wish to have the curve incised on his tomb: *Eadem mutata resurgo: “Though changed I rise unchanged”*, see [1] and [6].

In this article, we focus on inversion of equiangular spirals in a circle. We bring a discussion of Coxeter on the whirlpool of Escher, and through the use of GeoGebra software we experiment in drawing two-pole spirals. Teachers and instructors at schools and colleges often use the Cartesian coordinates in the graphic window of GeoGebra. Our aim is to emphasize the use of polar coordinates with equiangular spiral curves. This allows to create exploring activities that may enrich the teaching process and expose both students and instructors to the beauty of mathematics.

2 Inversion of equiangular spirals

Inversion in a circle with center O and radius R is a transformation of the plane that maps each point P to a radial point P' (a point that lies on the line issuing from O) such that $OP \cdot OP' = R^2$. In reference to the unit circle, inversion is defined in the extended complex plane by rule:

$$I : C^* \rightarrow C^*$$

$$I(z) = \frac{1}{\bar{z}}.$$

Indeed, let $z = re^{i\theta}$ be any point in extended complex plane, then $\frac{1}{\bar{z}} = \frac{1}{r}e^{i\theta}$ lies on the same ray issuing from the origin through z and $|z| \cdot \left|\frac{1}{\bar{z}}\right| = \frac{1}{r} \cdot r = 1$. Therefore, in polar coordinates (r, θ) inversion in the unit circle is given by

$$(r, \theta) \rightarrow \left(\frac{1}{r}, \theta\right).$$

Inversion in a circle reverses direction: if the point approaches infinity then its inverse approaches the center of the circle and if the point winds in clockwise

direction around the pole on the curve then its inversion winds in anti clockwise direction around the image of the pole.

Points on the circle of inversion are preserved and points inside the circle are mapped one-to-one to points outside the circle and vice versa. In particular, inversions map equiangular spirals to equiangular spirals. To see this fact using GeoGebra, we apply the following steps: In fact, GeoGebra provides inversion by using a simple tool “reflection about a circle”.

- Draw the unit circle with center $O(0,0)$ and radius 1.
- In the input bar insert the polar equation $r = e^{(\frac{0.7\theta}{2\pi} + 0.1)}$ of an equiangular spiral.
- In the input bar insert the equation of the spiral $r = e^{(-\frac{0.7\theta}{2\pi} - 0.1)}$.
- By drawing the tangent lines, measuring the angles between the radial lines and the tangents and dragging points A and D , we can validate that both curves are equiangular (see Fig. 3).

Measuring angles with GeoGebra is done by using the angle tool and clicking on the two rays that define the angle. In Fig. 3, when animation is on point A along the original spiral we see that the angle, the radial lines and the tangents is preserved. Likewise, when animation is on point D along the inversion spiral the angle the radial lines and the tangents is preserved, see the animated Figure [11].

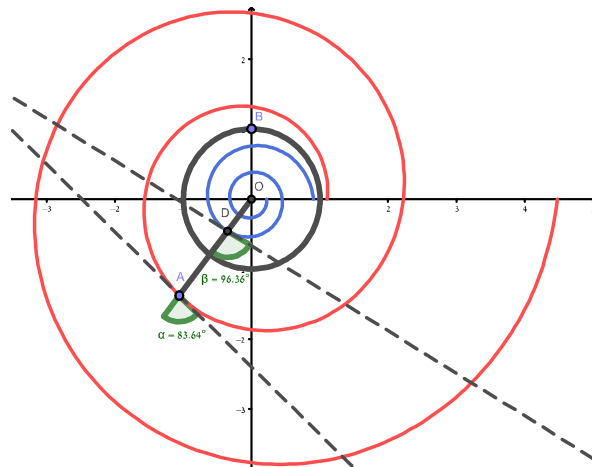


Figure 3: Both spiral and its inversion are equiangular

Another important feature of equiangular spirals and their inversion is that when θ increases arithmetically then r will increase geometrically. We can check this property in GeoGebra, by drawing one radial line and find the intersection points with the spiral or its inversion. Measuring the distance of these points from O yields a geometric progression. Indeed, if (r_1, θ_1) and $(r_2, \theta_1 + 2\pi)$ are

two consecutive intersection points of the radial line with the spiral $r = e^{a\theta+b}$ then $r_1 = e^{a\theta_1+b}$ and $r_2 = e^{a(\theta_1+2\pi)+b} = e^{2\pi a}r_1$.

2.1 Two-pole spirals

Two-pole spirals can be obtained by inverting a spiral, the pole of which lies outside the inversion circle. In fact, a spiral has one finite pole in the plane and a second pole at infinity. Inversion in this case creates a spiral inside the circle with two poles: one pole at the center of the inversion circle and another pole at the image of the pole in the original curve.

The following procedure illustrates how to get two-pole spirals with GeoGebra.

1. In the input bar insert the equation of the family of equiangular spirals $r = e^{\frac{a}{2\pi}\theta+b}$.
2. Define sliders for a and b , $0 < a < 1$ with increment 0.01 and $0 \leq b \leq 1$ with increment 0.1.
3. Enlarge the domain of θ to 20π .
4. Draw a circle with center A and radius AB such that the circle does not contain the pole nor intersect the curve as shown in Fig. 4.
5. Mark a tracing point C on the curve and reflect C about the circle with center A and radius AB .
7. Finally, trace the inversion point C' of C and turn animation on for point C .

Fig. 4, shows a two-pole spiral which is the image by an inversion of the curve $r = e^{\frac{a}{2\pi}\theta+b}$ for the values $a = 0.68$ and $b = 1$, see also the animated Figure [12] with other values for a and b .

2.2 Connection to the art of Escher

Coxeter discussed Escher's *whirlpool* (see [8] (minute 41), and [9]). He first explains what is inversion in a circle:

“One way to bring infinity to finite terms is by the transformation called inversion in a circle, whereby a point outside the circle is transformed into a point inside the circle so that it is on the same diameter but the distance from the center is reciprocal of the distance to the original point. In this way, if a point moves outside the circle, the inverse point moves inside and even if the point moves infinitely far away its image is still inside the circle. As the point moves farther and farther away, the image point gets closer and closer to the center”.

Then Coxeter describes the inversion of equiangular curve:

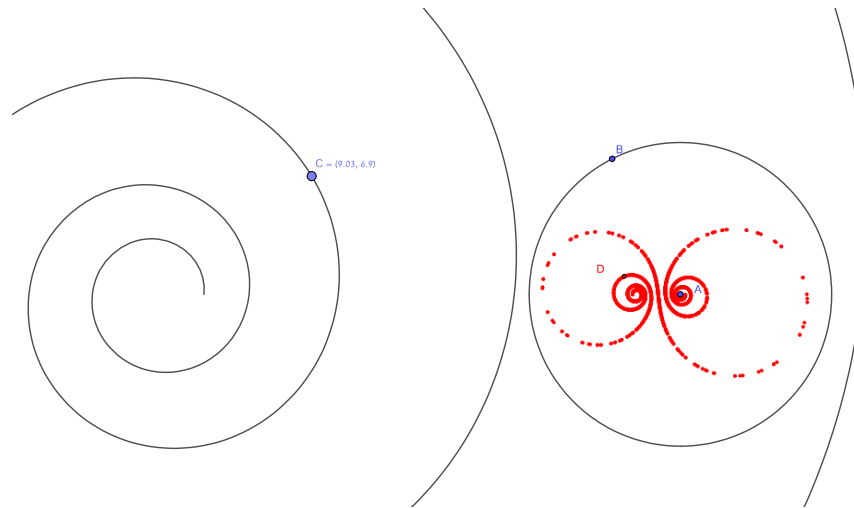


Figure 4: A two-pole spiral for the values $a = 0.68$ and $b = 1$

“If one considers the important curve called an equiangular spiral, which is a curve that goes round and round one point, that curve is inverted in a circle (Coxeter draws a circle between two rounds of the curve), we get a kind of spiral with one pole at the inverse of the original pole, going the opposite way round. But, the part that goes to infinity makes a second pole at the center. So, you have the curious effect of a curve that has two poles and that is the curve which Escher used in his work”.

This short discussion of Coxeter on Escher’s whirlpool is found also in the book [3, p. 290]. In fact, Coxeter asserts that Escher used equiangular spirals in this discussion, although in [2] he emphasizes that Escher’s work was based on his intuition rather than computations. So, the main question is why Escher used inversion of equiangular spirals? The answer could be hidden in the main feature of these spirals: If θ increases arithmetically then r will increase geometrically by a constant ratio q and the painter can easily resize his pattern by this constant ratio q .

In 1957 Escher finished his woodcut and wood engraving Whirlpools [9]. He used two inversions of equiangular spirals by drawing two curves on which the fish swim in opposite directions. In fact, Escher used a new printing technique for it, cutting one block which he printed on the same piece of paper in two colours. Two rows of fish swimming head to tail fill the space. The red row has exactly the same shape as the grey one, but has been turned 180 degrees. It seems that Escher painted a row of red fish swimming on the inversion of an equiangular spiral on a rectangular piece of paper and finished the wood engraving, then he turned around the piece of paper in 180 degrees and finished the wood engraving to get another row of grey fish swimming head to tail and

filling the space.

In GeoGebra, see Fig. 5, we can draw directly the inversions of two equiangular spirals: $r = e^{\frac{0.89\theta}{2\pi}+2}$ and $r = e^{\frac{0.83\theta}{2\pi}+1}$, $0 < \theta < 20\pi$. The reader is encouraged to change slightly the coefficients of θ to see how the view of the curves is resized inside the circle.

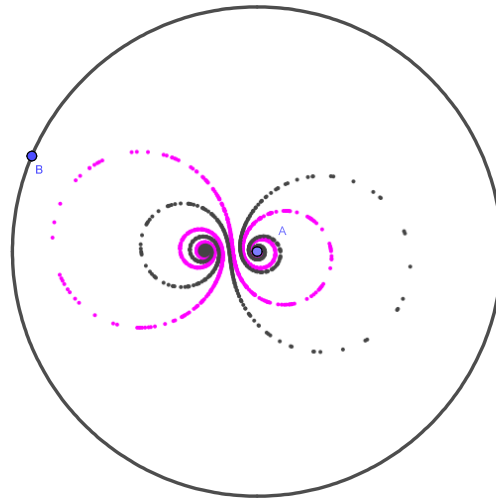


Figure 5: Inversions of two equiangular spirals

3 Concluding remarks

Many other researchers were fascinated with equiangular spirals. The authors of [7] used both hand-drawn and computer-drawn graphics with conformal mappings to generate advanced Escher-like spiral tessellations. In [1], the author reviews the history of discovering the logarithmic (equiangular) spirals and their properties between the seventeen to nineteen centuries. The author of [4], describes and illustrates two conformal mappings, inversion and anti-Mercator, and the symmetry implications of their combined use. The author of [5], investigated the logarithmic spirals in nature by means of dynamic geometry and computer algebra systems and discussed how we can combine the pupil's knowledge with the computational and graphical power to model some real-world phenomena.

The implication for teaching is that instructors can use GeoGebra to create exploring activities such as: drawing different kinds of spirals, checking whether a spiral is equiangular or not, drawing the inversion of a spiral, checking whether the inverted spiral is equiangular or not, and drawing two-pole spirals.

Finally, concerning the two-pole spirals, the use of the family of equiangular spirals $r = e^{\frac{a}{2\pi}\theta+b}$ with sliders for a and b in GeoGebra allows us to create

different kinds of inverted curves. We recommend the reader to try executing the inversion of these curves for different values of a and b and compare the result with other families of spirals not necessarily equiangular.

Acknowledgement. The author is indebted to the reviewers for their comments and valuable suggestions that improved the exposition of the paper. Special thanks are due to Csaba Sárvári for communicating and handling the manuscript.

References

- [1] Archibald, R. C. (1918). "The Logarithmic Spiral." *Amer. Math. Monthly* 25, 189-193.
- [2] Coxeter, H. S. M. (1979). The Non-Euclidean Symmetry of Escher's Picture 'Circle Limit III', *Leonardo*, 12(1), 19–25.
- [3] Coxeter, H. S. M., Davis, C., & Ellers, E. W. (Eds.). (2006). *The Coxeter Legacy: Reflections and Projections*. American Mathematical Soc.
- [4] Dixon, R., (1992). Two Conformal Mappings, *Leonardo* 25 (3/4), 263-266.
- [5] Hasek, R. (2012). Investigation of logarithmic spirals in nature by means of dynamic geometry and computer algebra systems. *Electronic Journal of Mathematics and Technology*, 6(3), 216-230.
- [6] Lockwood, E. H. (1961). *A Book of Curves*, Cambridge: Cambridge University Press.
- [7] Ouyang, P., Chung, K.W., Bailey, D. et al. (2021), Generation of advanced Escher-like spiral tessellations. *The Visual Computer*. <https://doi.org/10.1007/s00371-021-02232-0>
- [8] <https://www.youtube.com/watch?v=zCbS6D-y0do>
- [9] <https://www.nga.gov/collection/art-object-page.47970.html>
- [10] <https://www.geogebra.org/m/ee8fx3sh>
- [11] <https://www.geogebra.org/m/k6g3fppk>
- [12] <https://www.geogebra.org/m/nzq4s6gw>

Easy (but exact) study of caustics of conics

Zoltán Kovács

zoltan@geogebra.org

The Priv. Univ. Coll. of Educ. of the Diocese of Linz

Salesianumweg 3

4020 Linz, Austria

Abstract

We give a concise summary on the technical history of visualizing implicit locus equations in the widely used dynamic geometry system GeoGebra. We mainly focus on the “draggable locus” equation, introduced in GeoGebra 5 (2014), and the dynamic envelopes. We discuss how user interface improvements (the LocusEquation and Envelope tools in GeoGebra Discovery), backend updates (the Giac subsystem) and algebraic experiments (to automatically exclude degeneracy) lead to easy study of caustics of a circle or a parabola in the classroom.

1 Introduction

At CADGME 2014 (Halle, Germany), Francisco Botana and the author presented a novel way of visualizing locus and envelope curves. The “draggable locus” feature was introduced in GeoGebra 5 – the authors showed how the **LocusEquation** and **Envelope** commands can be used to bring algebraic curves closer to the students.

As a closing remark in that past presentation, Sander Wildeman’s remark was cited: “Once you have written an article about caustics you start to see them everywhere.” Indeed – and this fact encouraged us to do further developments on the topic! Since 2014 we continuously enhance our approaches to support the study of locus and envelope equations for classroom situations as easily as possible. Our work consisted of

- user interface improvements (like the availability of the above commands as toolbar icons),
- backend updates (to speed up the underlying elimination process in the background)
- and algebraic experiments (to find the best suitable formula to express the tangents of conics in general, to obtain fast computational results).

Our research led finally to make it possible to obtain non-trivial results in a user friendly way. As an example of these improvements, we are going to study the caustics of a circle or a parabola in the second part of this paper. Despite our results are not new from the mathematical point of view, they are novel from the educational approach.

2 A brief history of “draggable loci”

We recall some of the milestones of the long road to achieve difficult algebro-geometric results in a simple way. The very beginnings include Reinhard Oldenburg’s *Feli-X* and *FeliX* systems [15, 16]. Their first version was available in March 2004. It provided a simple user interface to work with planar geometric constructions. They could be expressed by direct algebraic inputs like the command `addEquation[yC[A]==0]` or geometric declarations like `B=addObject["point",0,4]`. The output as an algebraic equation was provided algebraically and also graphically. *Feli-X* used *Mathematica* as its backend but Oldenburg stated clearly that several schools could not afford *Mathematica* licenses – therefore a free alternative computer algebra system (CAS) should be considered for the long term.

In fact, an earlier work [5] (January 2003) published by Francisco Botana and José Luis Valcarce already described a similar system. The software tool *Lugares* was able to use a free CAS as its main backend: *CoCoA*. A later publication [6] by these authors (July 2004) described the software tool *GDI* which could compute and plot the envelope equation of a family of lines parametrized by the positions of a point on a geometric object, by providing a simple user interface.

Botana continued to work on making these concepts available for a wider audience. As of 2010 it turned out that the freely available *GeoGebra* system becomes very popular among end users in educational communities. Hence he published the *LADucation* system at CADGME 2010 (Hluboká nad Vltavou, Czech Republic¹) – it was able to import *GeoGebra* files and manipulate them via a web service. *LADucation* internally used a *CoCoA* installation on the server.

A collaboration between a research group in algebraic geometry, led by Tomás Recio, and the *GeoGebra* Team, led by Markus Hohenwarter, seemed to be a fruitful cooperation at this point. Botana’s concept on outsourcing the heavy computations to an external system remained an important part of the project. The first publicly available version was implemented by a student Sergio Arbo in the frame of the Google Summer of Code (GSoC) 2010, advised by Miguel Á. Abánades, by using Heinz Kredel’s Java Algebra System (*JAS*) on the top of *GeoGebra* 4.0. This first version already provided the **LocusEquation** command. It heavily relied on another GSoC project that aimed at contour and implicit plotting, programmed by Philipp Birklbauer and advised by Darko Drakulic, in the same year.

The first implementation had some difficulties with speed. It turned out that the implementation of Gröbner basis computations is the main bottleneck. Finally, several changes in *GeoGebra*’s CAS backend (Reduce in 4.2, 2011; SingularWS [3] and Giac in 4.4, 2013; Giac in 5.0 [10], 2014) and some substantial speedups of Giac’s internal command `eliminate` led to major visual improvements that made fast animations possible when the inputs were changed via a dragging move [9].

Meanwhile the **Envelope** command was added to *GeoGebra* 5.0 by Botana and the author [4]. It heavily exploited Giac’s fast elimination algorithm. Also, a general geometric prover subsystem was developed by Simon Weitzhofer and the author in 2011, and supported by some other researchers in the following years [2]. To avoid implementing similar ideas multiple times, the commands **LocusEquation**, **Envelope** and **Prove** were unified in 2017 by the author. As a result, *GeoGebra* was extended with a general geometric prover subsystem called *GeoGebra Automated Reasoning Tools* [12]. This subsystem was thoroughly tested, documented and further improved by additional re-

¹The slides for Botana’s talk are available at http://home.pf.jcu.cz/~cadgme2010/proceedings/botana/Francisco_Botana_talk.pdf.

searchers, among others: M. Pilar Vélez, Pavel Pech, Roman Hašek and Thierry Dana-Picard. This fruitful collaboration among several researchers yielded to further improvements like

- automated removal of some degenerated components ([11], 2019),
- toolbar access of the **LocusEquation** and **Envelope** commands (2020),
- attaching points to arbitrary algebraic curves that are defined by the user via a polynomial equation ([7], 2020).

In fact, some of the latest improvements are not yet official parts of GeoGebra. Instead, an experimental version called *GeoGebra Discovery*² is launched to make it possible for the researchers to try out these novel techniques in a preliminary version that can be considered “unstable” for the every day use. After being stable enough and confirmed by the GeoGebra Team, some of these new features may be supported officially by the mainstream version of GeoGebra as well.

Now in 2022, the locus equation and envelope algorithms are ready to play a substantial role in helping students to experiment with algebraic curves, up to eventually a degree of 20 for the studied polynomials. In the second part of the paper some simple ways will be presented on how to get the caustics of a circle or a parabola. This can be fruitful not just for mathematics classes but for STEAM projects (for example, with optical applications in physics). Also, the underlying mathematical and technological details will be explained at some extent. Finally, as future plan, the easy study of caustics of an ellipse or hyperbola will be mentioned – even if these tasks are too difficult yet for the current stage of the project.

3 Locus and its equation

The “draggable locus” feature appeared in certain software systems after the millicentenary. It is based on locus *equations*, and it therefore has a *symbolic* property. On the other hand, the appearance of geometric locus in computer programs is an older feature, and it has a *numerical* property from the computational view.

The first exhaustive work on presenting the benefits of geometric loci is perhaps the doctoral dissertation [8] by Ulrich Kortenkamp. Its chapter 10.4 “Exploring Geometry with Loci” lists several applications of drawing a geometric locus. In a later work [18] by Kortenkamp and Jürgen Richter-Gebert we find the following *definition of a locus*:

A locus is the trace of a point under the movement of another point. A locus is defined by three objects:

- The *mover*, a free element whose movement drives the generation of the locus.
- The *road*, an element incident to the mover. The mover will be moved along the road.
- The *tracer*, the element whose trace is calculated and presented as a geometric locus.

²Available at <https://github.com/kovzol/geogebra-discovery>

In some software systems (like GeoGebra) the road is called *path*.

When computing the equation of a locus, GeoGebra uses computational algebraic geometry to manipulate the equations that describe the coordinates of the points in the figure. The obtained output is always an algebraic curve (or the union of discrete points) which is computed by—roughly speaking—eliminating some variables in the algebraic translation of the geometric construction.

The process to get the locus equation is performed by denoting the locus point by (x, y) , and the other points of the construction by (v_i, v_{i+1}) for some i , and the relationships among the points are described by polynomial equations $f_j(v_1, v_2, \dots, v_n, x, y) = 0$. Now the goal is to eliminate all variables but x and y from the ideal $\langle f_j \rangle$.

In fact, similar steps can be used to compute an envelope of a family of curves. We start with the same procedure, but we define the locus point virtually by putting it on the object which is tangent to the envelope. Now by computing the determinant of the Jacobian matrix

$$D = \begin{vmatrix} \frac{\partial f_1}{\partial v_1} & \frac{\partial f_2}{\partial v_1} & \dots & \frac{\partial f_n}{\partial v_1} \\ \frac{\partial f_1}{\partial v_2} & \frac{\partial f_2}{\partial v_2} & \dots & \frac{\partial f_n}{\partial v_2} \\ \vdots & \vdots & \ddots & \vdots \\ \frac{\partial f_1}{\partial v_n} & \frac{\partial f_2}{\partial v_n} & \dots & \frac{\partial f_n}{\partial v_n} \end{vmatrix}$$

an extra polynomial $f_{n+1} = D$ will be obtained. As a final step, we eliminate all variables but x and y from the ideal $\langle f_j \rangle$.

GeoGebra (since 2016) also supports the computation of *implicit locus* curves [1]. This means the algebraic discovery of the path curve which is prescribed by some expected geometric property of the figure. In this case the sought mover point is denoted by (x, y) , and the other points of the construction by $(v_i, v_i + 1)$. The relationships among the points are described by the polynomial equations $f_j = 0$: they are the *hypotheses*. The algebraic translation of the assumed implicit condition (the *thesis*) is also added to the polynomials. Now by eliminating all variables but x and y from the ideal $\langle f_j \rangle$ the implicit locus will be obtained.

In GeoGebra, technically, dynamic plotting of a locus or envelope equation is performed as a mixture of symbolic and numerical computations that are shown in Figure 1. The computationally heavy part is to eliminate the variables from the ideal obtained during the algebraization process. If the user drags one of the free points during the use of a dynamic applet, a number of consecutive eliminations must be performed. When using an efficient algorithm, it is possible to achieve a high number of symbolic computations within a second. This leads to a continuous movement on the screen – unless the input construction is too complicated and it results in a heavy computation. We recall that elimination can be in worst case doubly exponential in the number of variables [14] because the underlying algorithm uses Gröbner bases in the background.

Finally, here we refer to the paper [13] by Peter Leeb and Richter-Gebert that proposes a different way to compute the locus equation. This approach starts with a collection of sample points that are graphically constructed when moving the mover point. The algorithm then looks for a curve, that goes through the sample points, of bounded degree, to establish a rigorous bound on the degree of the locus equation. This sophisticated method, however, does not seem to be widespread in practice.

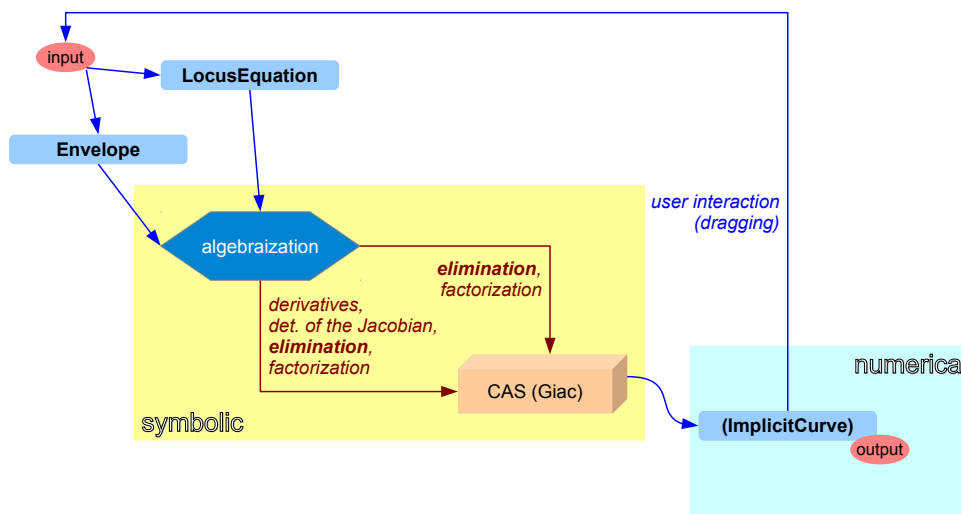


Figure 1: Workflow of plotting a locus or envelope equation in GeoGebra

4 Caustics of a conic

4.1 The case of the circle

According to mathcurve.com, the caustics by reflection of circles are the envelopes of the reflection of rays, emitted by a light source placed at finite or infinite distance, by a circle. It is well known how to classify these curves:

- in the finite cases we usually get a sextic curve,
 - if the light source is outside the circle, then it is a nephroid curve, and
 - inside a circle it is still a sextic but it looks differently (Fig. 2).
 - If the light source is on the circle, we get a cardioid of degree 4 (Fig. 3).
- Otherwise, if the light source is placed at infinite distance, we get a nephroid again (Fig. 4).

We emphasize that the method we use in GeoGebra differs from the usual parametric way. We use just elimination to get the algebraic output before the plotting step. This explains why the case of the cardioid results in an extra degenerate linear component that is tangent to the circle and the cardioid at the point of light source (Fig. 3).

Figures 2, 3 and 4 use similar notations which will be summarized here quickly. The circle is denoted by c and defined with midpoint M and circumpoint C . The light source S is explicitly given in Figures 2 and 3, but it is created dynamically in Figure 4 by setting up the direction of the light first via a vector $\vec{v} = \overrightarrow{OV}$. In each figure we use a tangent point T that is attached to circle c and designates the mirror m accordingly. In Figure 4 we create point S to have $\overrightarrow{ST} = \vec{v}$. Now we can get point S' as the reflection of S about m in all three setups. By reflecting S' about T we get the technical point S'' so that it is possible to graphically present the segment ST and then the ray TS'' which together show the beam of the light.

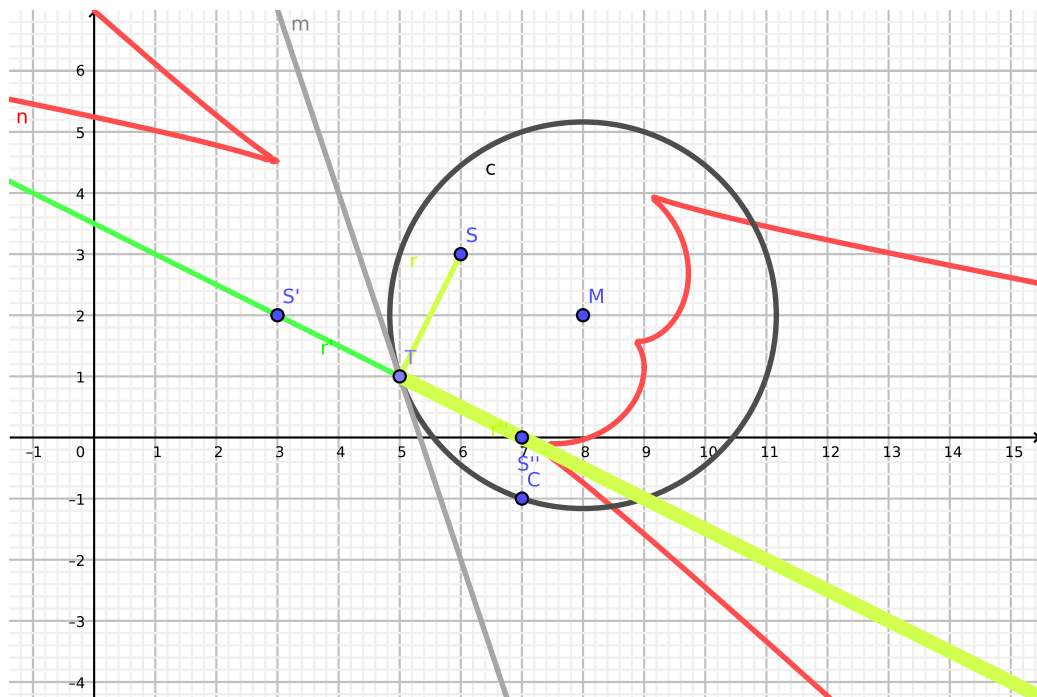


Figure 2: A caustic of a circle, the light source is placed inside

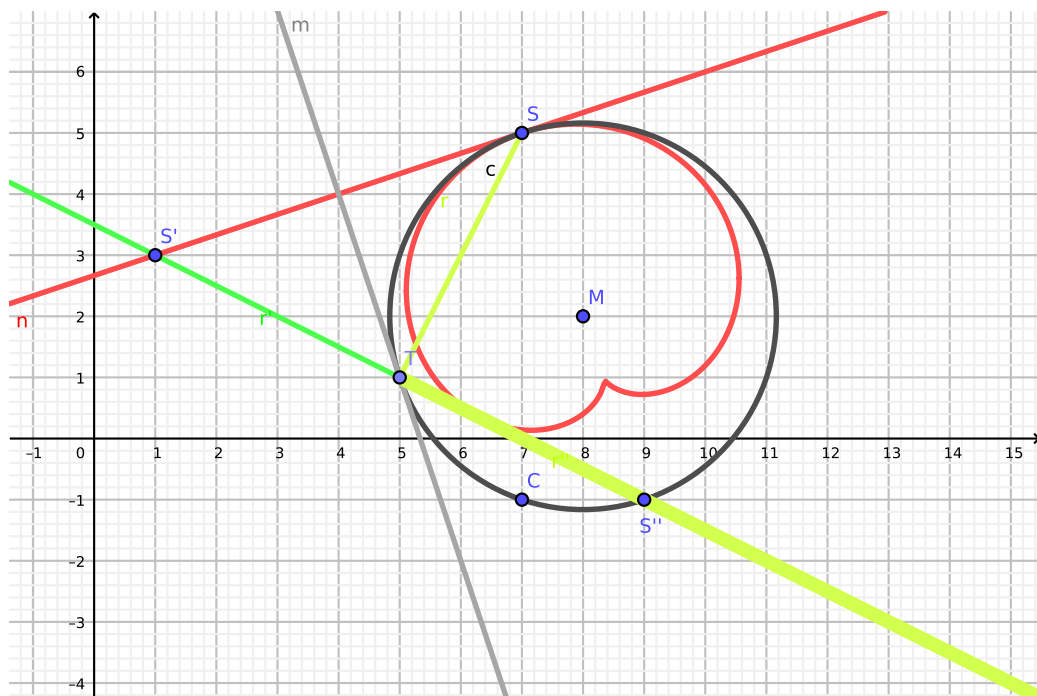


Figure 3: A caustic of a circle, the light source is placed on the circle

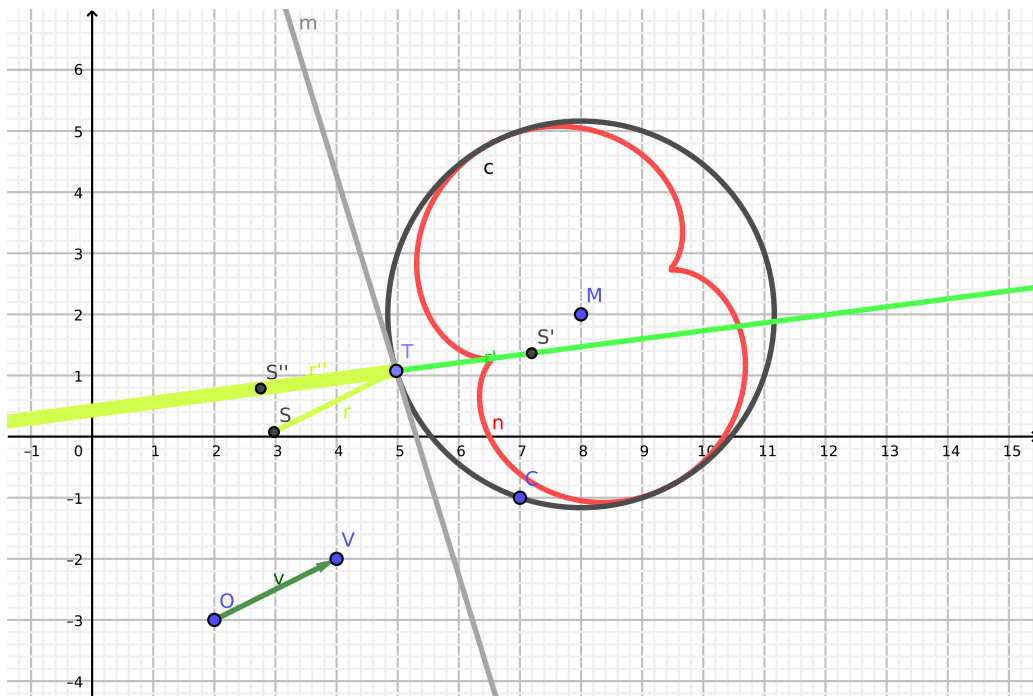


Figure 4: A caustic of a circle, the light source is placed at infinite distance

In the mathematical sense we simply use the family of lines (or rays³) TS' (which is the same as the family of lines $S''T$) and compute the envelope n tangent to these lines. This makes us to compute and plot the caustics of a circle in a very simple way in GeoGebra, see Table 2. In fact, only steps 1–9 are required to plot the caustic, the remaining steps are just explaining the optical details. Step 9 as a toolbar icon is supported only in GeoGebra Discovery – the corresponding *command* must be used in the mainstream version of GeoGebra. We highlight that the whole construction can be built by using only the mouse – no keyboard input is required!

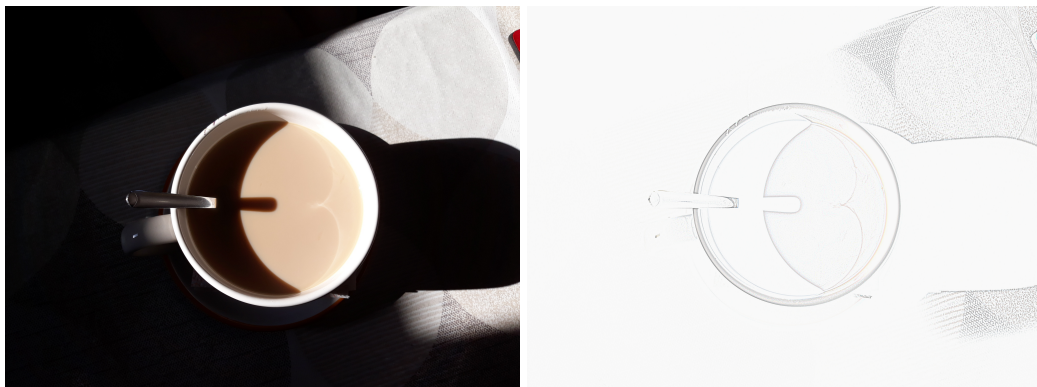


Figure 5: A caustic of a circle in a cup of coffee – the right figure emphasizes the appearing curves after an automatic edge-detection

No.	Name	Toolbar Icon	Description
1	Point M		
2	Point C		
3	Circle c		Circle through C with center M
4	Point S		
5	Point T		Point on c
6	Line m		Tangent to c through T
7	Point S'		S mirrored at m
8	Ray r'		Ray through T, S'
9	Implicit Curve n		Envelope(r', T)
10	Segment r		Segment S, T
11	Point S''		S' mirrored at T
12	Ray r''		Ray through T, S''

Table 2: Easy construction of caustics of a circle, the light source is at finite point



Figure 6: An outdoor activity in Dubrovnik, Croatia, demonstrating sound transmission via two parabolic mirrors: the mirrors are made of yellow metal disks and their foci are highlighted with blue circular rings

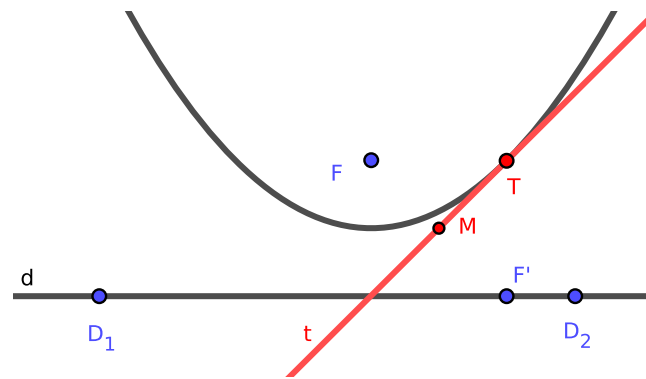


Figure 7: Geometric setup for the tangent of a parabola

Application of the obtained results is very common in every day life. Objects that have a circular cross-section can usually be observed that they behave as mirroring surfaces. Inside them, eventually on the bottom of a cup or a bucket, or in a liquid material (maybe in the water that fills the bucket), the caustic can be seen, sometimes very sharply. Figure 5 shows one photo taken recently by the author – the half of a nephroid curve can be detected easily.

We omit the equation system that was used to create the envelope curves. We emphasize, on the other hand, that a smooth animation of the curves can be achieved on a recent PC: on an Intel(R) Core(TM) i7-4770 CPU @ 3.40GHz (Ubuntu Linux 22.04) we managed to get 14.3 frames per second (FPS) for the finite point case and 11.5 FPS for the infinite one.

4.2 The case of the parabola

It is well known that in the case of the parabola we can have a unique behavior of reflection when the light source is put in the focus. In this case the reflected rays are all parallel lines. An important application of this fact is data transmission (or broadcasting) via parabolic mirrors: the sender (and/or the receiver) needs to be in the focus of a parabola so that the direction of transmission will be orthogonal to the directrix (Fig. 6).

Now we continue with a general position of the light source (Fig. 7). We assume that the parabola is given with focus F and directrix d (which is defined with line points D_1 and D_2). Let T be a tangent point of the parabola. We are searching for a point M such that MT is the tangent line of the parabola.

We give a list of geometric properties that should be fulfilled to describe the setup geometrically:

1. D_1, D_2 and F' are collinear.
2. $F'T$ and D_1D_2 are orthogonal.
3. $FT = F'T$.
4. M is the midpoint of FF' .

³Lines are *algebraic closures* of rays. In *algebraic geometry* we deal with polynomial equations, so we cannot distinguish between a line or its infinite subsets. Similarly, when removing a point from a conic, we cannot distinguish between the full conic and the object we obtain after removing that point.

5. F , F' and T should not be collinear.

After several attempts, the following equations seem to be a fruitful list to describe the setup algebraically:

$$\det \begin{pmatrix} d_{1x} & d_{1y} & 1 \\ d_{2x} & d_{2y} & 1 \\ f'_x & f'_y & 1 \end{pmatrix} = 0, \quad (1)$$

$$(f'_x - t_x)(d_{1x} - d_{2x}) + (f'_y - t_y)(d_{1y} - d_{2y}) = 0, \quad (2)$$

$$(f_x - t_x)^2 + (f_y - t_y)^2 = (f'_x - t_x)^2 + (f'_y - t_y)^2, \quad (3)$$

$$m_x = \frac{f_x + f'_x}{2}, m_y = \frac{f_y + f'_y}{2}, \quad (4)$$

$$t \cdot \det \begin{pmatrix} f_x & f_y & 1 \\ f'_x & f'_y & 1 \\ t_x & t_y & 1 \end{pmatrix} = 1. \quad (5)$$

Here (4) consists of two equations for the two coordinates of M . Also, in (5) we deny the equality by introducing a new variable: this technique is well-known in algebraic geometry to express certain inequalities (it is also known as *Rabinowitsch's trick* [17]).

We highlight that this set of equations is not the only way to describe the setup geometrically or algebraically. But this seems to be a useful way, because it allows us to obtain the envelope curve when the tangent line MT is changing dynamically. In fact, the most important equation to explain is (5): if we omit it, we allow T to be the vertex of the parabola, and this is to be avoided, because this would imply $M = T$ and no line MT would be exactly defined: each line going through the vertex would be allowed. Therefore, when (5) is not explicitly stated, an infinite amount of lines would be introduced and this would prevent us from getting the correct envelope equation! On the other hand, even if we exclude the presence of the vertex in the study, we still get the correct envelope, because it corresponds to an algebraically closed set. In other words: by considering the input without the vertex, we get a geometric output that may lack of some points, but the algebraic closure of that output is still the correct, full envelope.

Figures 8, 9 and 10 show the rich geometry of different cases when the light source is

- inside the parabola,
- on it, or
- outside it.

In the first and third cases we get a sextic curve, while in the second one a quartic curve will be obtained (together with an extra degenerate linear component that is tangent to the parabola and the quartic).

In the case of infinite distance we get that the output is cubic – unless the direction of parallel lines is orthogonal to the directrix (in this case we obtain the focus F as a single point of the envelope, as expected). See Figures 11 and 12. In fact, we obtain a Tschirnhausen cubic in the general case [19].

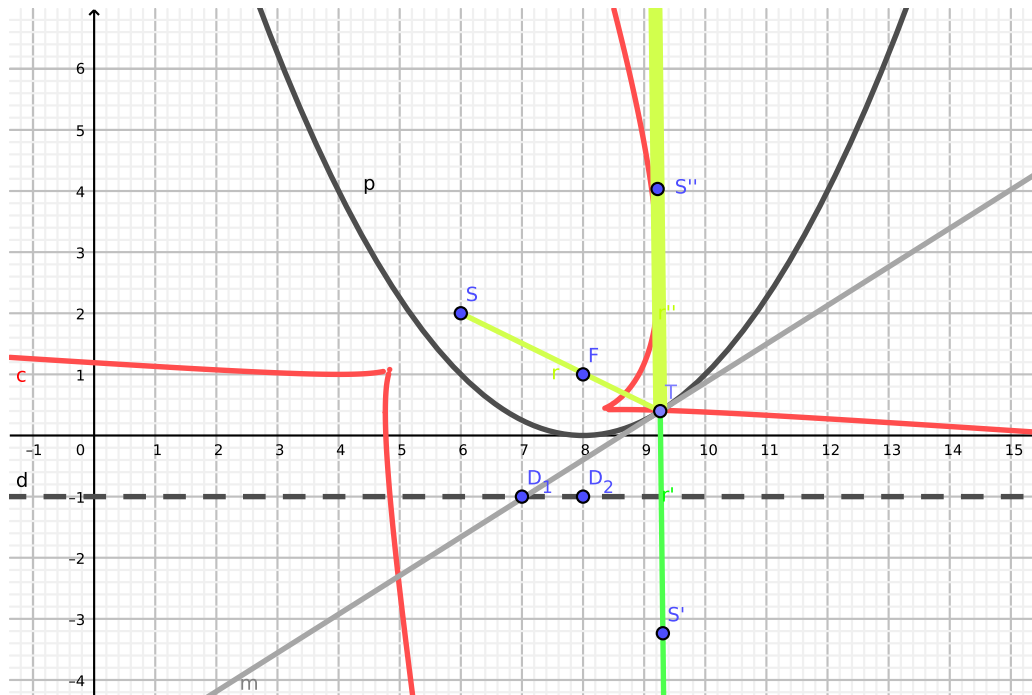


Figure 8: A caustic of a parabola, the light source is placed inside

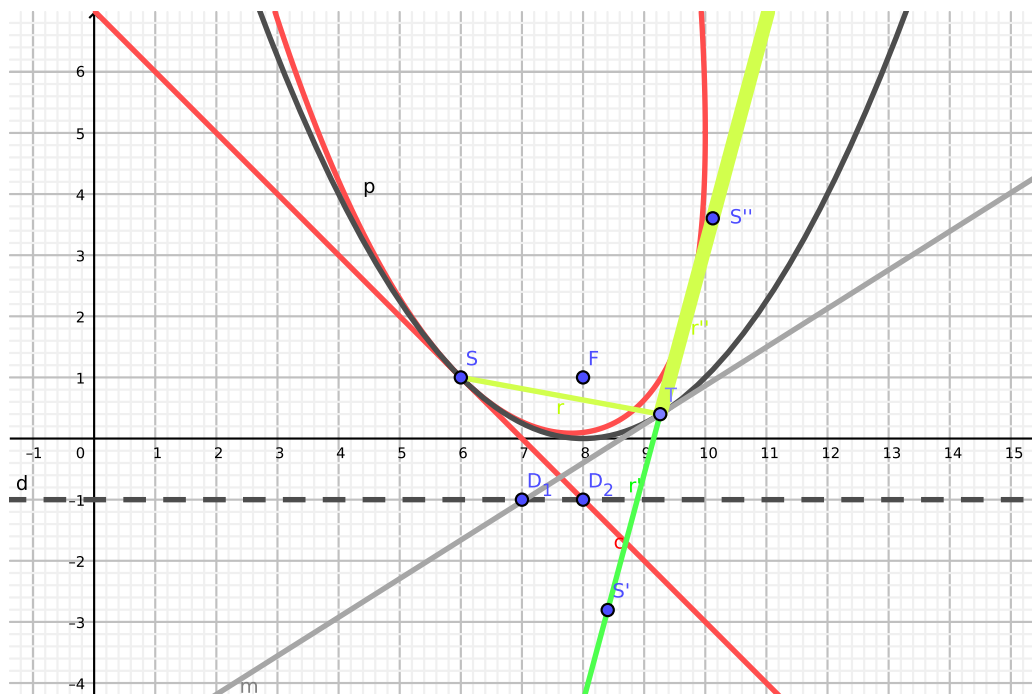


Figure 9: A caustic of a parabola, the light source is placed on the parabola

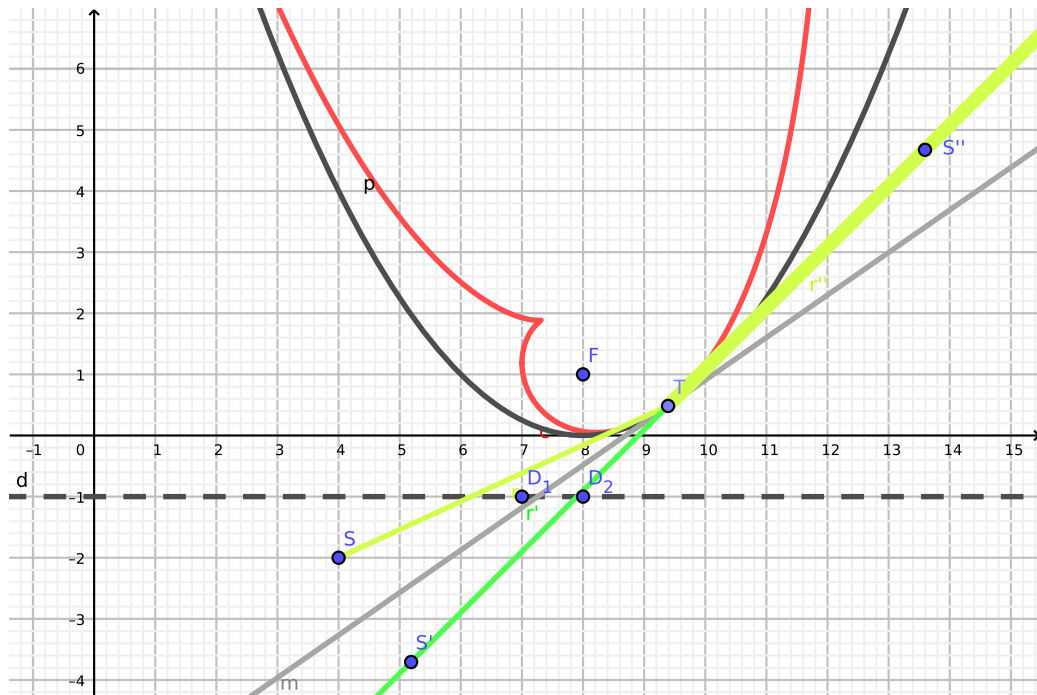


Figure 10: A caustic of a parabola, the light source is placed outside

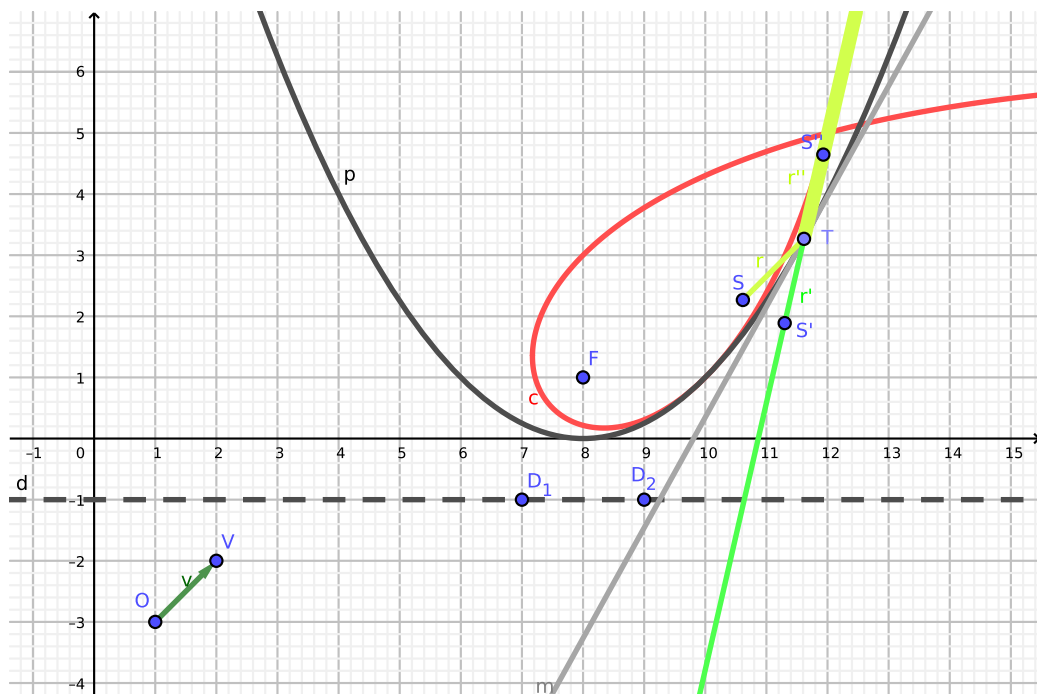


Figure 11: A caustic of a parabola, the light source is at infinite distance, general case

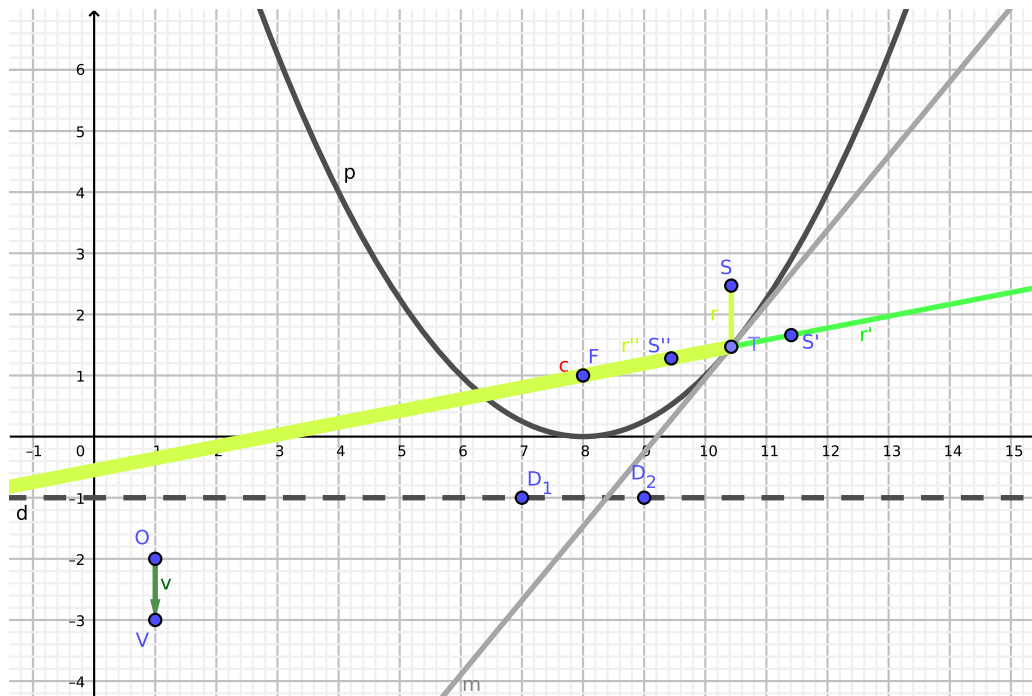


Figure 12: A caustic of a parabola, the light source is at infinite distance, “orthogonal” case

Finally we provide here the construction steps how the last two cases were built by using GeoGebra Discovery. In Table 4 a list of 17 steps are given (in fact, the last three steps are just explaining the optical details). Only one of them (step 10) requires the use of the keyboard. This only step can be worked around by using a line o (given with free points O_1 and O_2) and attaching the point S to it, then projecting S orthogonally to the parabola to get the tangent point T (see Figure 13) – in this case, however, the output contains *two* degenerate linear components and the animation is somewhat slower (see Table 5 for a speed comparison).

4.3 The case of the ellipse and the hyperbola

Table 5 already prognosed the bad news about the case of ellipses and hyperbolas. Indeed, an algebraic geometry approach was in our research work not yet possible because of the too high amount of computations.

We give a brief overview about how we tried to handle the difficulties. First of all, ellipses and hyperbolas have the same equations if they are defined by their foci A and B and a circumpoint C . We assume this setup because GeoGebra’s user interface supports this kind of synthetic construction of conics (Fig. 14).

No.	Name	Toolbar Icon	Description
1	Point O		
2	Point V		
3	Vector v		$\text{Vector}(O, V)$
4	Point D_1		
5	Point D_2		
6	Line d		Line D_1, D_2
7	Point F		
8	Parabola p		Parabola with focus F and directrix d
9	Point T		Point on p
10	Point S		$T - v$
11	Line m		Tangent to p through T
12	Point S'		S mirrored at m
13	Ray r'		Ray through T, S'
14	Implicit Curve c		Envelope(r', T)
15	Segment r		Segment S, T
16	Point S''		S' mirrored at T
17	Ray r''		Ray through T, S''

Table 4: Easy construction of caustics of a parabola, the light source is at infinite point

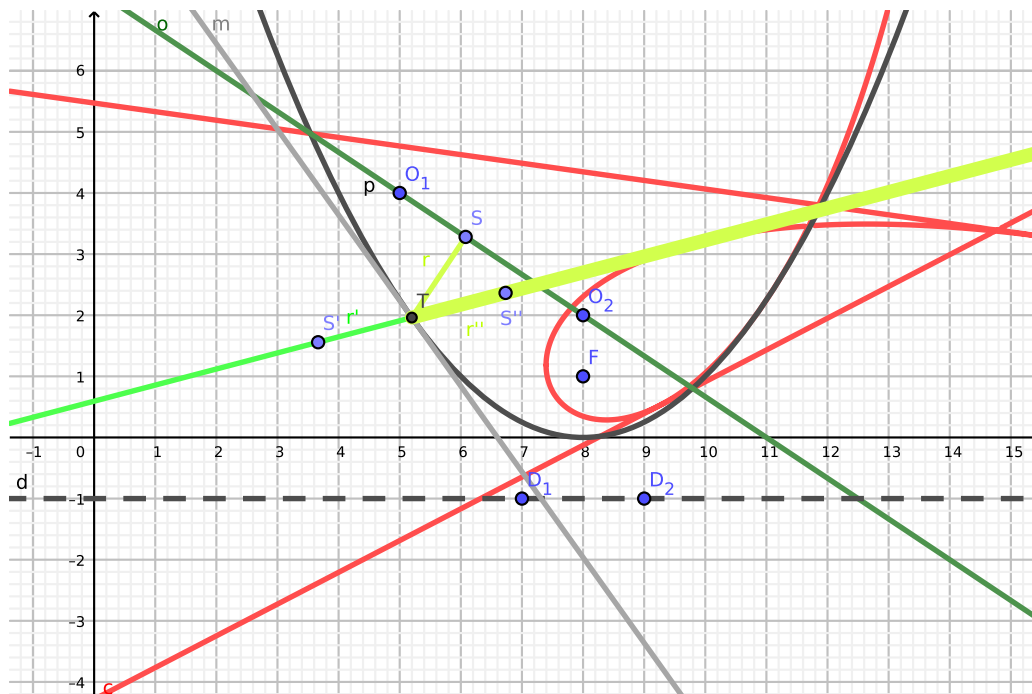


Figure 13: A caustic of a parabola, the light source is at infinite distance (“mouse only” version)

Conic	<i>Finite</i>	<i>Infinite</i> ("mouse only")	<i>Infinite</i> (via vector)
Circle	14.3	4.0	11.5
Parabola	11.6	1.6	7.2
Hyperbola/Ellipse	–	–	–

Table 5: Benchmarking animation speed (FPS) of caustics of conics, according to the distance of light source

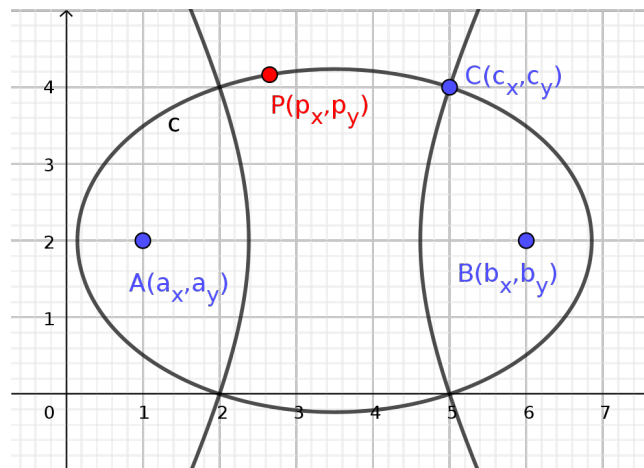


Figure 14: Ellipses and hyperbolas may be indistinguishable in the algebraic geometry approach

We would like to algebraically express the coordinates of P . We tried two strategies to describe the coordinates p_x and p_y :

1. Set up an equation system that contains all required constraints. Use these equations in the complete equation system also, when additional constraints are added (for example, the ones that describe the tangents and mirror images).
2. Set up the same system, but use elimination to obtain *one* equation (a union of the two conics, that is, a *quartic*). Remove the other constraints, and keep only the quartic one which is obtained after elimination. Use only the quartic, and add eventually additional constraints for the “rest” of construction (for example, the ones that describe the tangents and mirror images).

These methods are mathematically equivalent, but in the further computation steps, they may be of different complexity.

In fact, the geometric setup can be expressed by using the following equations:

$$\begin{aligned} AC^2 &= (a_x - c_x)^2 + (a_y - c_y)^2, \\ BC^2 &= (b_x - c_x)^2 + (b_y - c_y)^2, \\ AP^2 &= (a_x - p_x)^2 + (a_y - p_y)^2, \\ BP^2 &= (b_x - p_x)^2 + (b_y - p_y)^2, \\ AP \pm BP &= AC \pm BC, \end{aligned}$$

where the last operations decide if an ellipse (+) or a hyperbola (−) is observed. But, as stated above, these operations will have no effect on the obtained output. So we will use “+” from now on.

After several attempts with the first strategy, it can be learned that the number of variables may be too high for the underlying CAS. So we tried to use the second strategy by writing a short program in Giac that obtains the quartic in parameters of a_x, a_y, b_x, b_y, c_x and c_y . We needed to eliminate all helper variables from the equation system by using this code:

```
>> poly:=eliminate([ac^2=(a_x-c_x)^2+(a_y-c_y)^2,
    bc^2=(b_x-c_x)^2+(b_y-c_y)^2,
    ap^2=(a_x-p_x)^2+(a_y-p_y)^2,
    bp^2=(b_x-p_x)^2+(b_y-p_y)^2,
    ap+bp=ac+bc],
    [ac, bc, ap, bp])
>> print(poly)
```

Giac gave the following answer (reasonably quickly):

```
poly:[c_x^4*a_y^4
-4*a_x*c_x^3*a_y^3*c_y
+6*a_x^2*c_x^2*a_y^2*c_y^2
-4*a_x^3*c_x*a_y*c_y^3
+a_x^4*c_y^4
...
-4*c_y*b_x^2*b_y*p_y^4
-4*a_x^2*b_y^2*p_y^4
+8*a_x*c_x*b_y^2*p_y^4
-4*c_x^2*b_y^2*p_y^4]
```

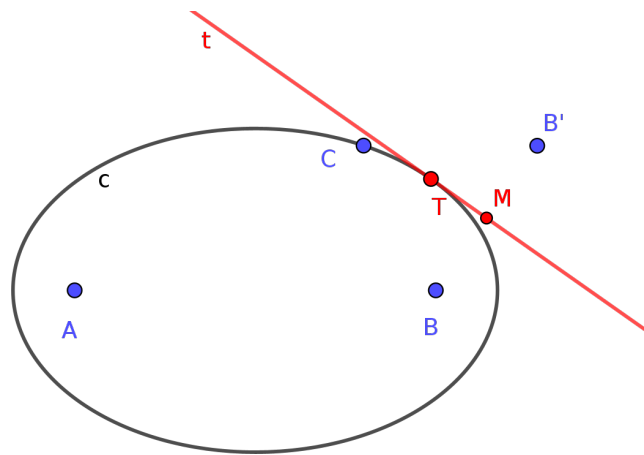


Figure 15: Geometric setup for the tangent of an ellipse/hyperbola

The answer consisted of 1171 terms and more than 20000 characters, so we omit showing the output here.⁴ We translated Giac’s output into Java and added it explicitly in GeoGebra’s source code.

Now we are ready to formalize the tangent of an ellipse (or hyperbola) in a similar way as shown in equations (1)–(5) for the case of a parabola, that is, the “rest”. See Figure 15.

The following properties need to be set up:

1. A, T and B' are collinear.
2. M is the midpoint of BB' .
3. $BT = B'T$.
4. A, B and T should not be collinear.

Similarly, we can set up 5 equations (*two* for the midpoint), similarly to (1)–(5). Here we emphasize again that the last property is required to avoid the degenerate case $M = T$.

As mentioned above, the equation system is still too heavy for elimination, if we add some other equations that describe the reflection. So we need to give up studying the caustics of an ellipse/hyperbola by using algebraic equations at this point.

Nevertheless, at least, we are able to obtain some beautiful curves that are created by an arbitrary free point E and its mirror image E' about the family of tangents t of a given ellipse/hyperbola.

Figure 16 shows a union of two curves that are algebraically one curve, a degree 8 curve. This consist of a larger red geometric component (according to the ellipse) and a smaller yellow one (according to the hyperbola). In fact, GeoGebra Discovery computes an additional algebraic component as well, a degree 12 curve (see Figure 17). Despite the high degrees, the relatively fast computa-

⁴The full output can be found in <https://github.com/kovzol/geogebra/commit/8654b0e17446c53c3fc2f51aba606d1f87eb7174>, in the file `common/src/main/java/org/geogebra/common/kernel/algos/AlgoEllipseHyperbolaFociPoint.java`.

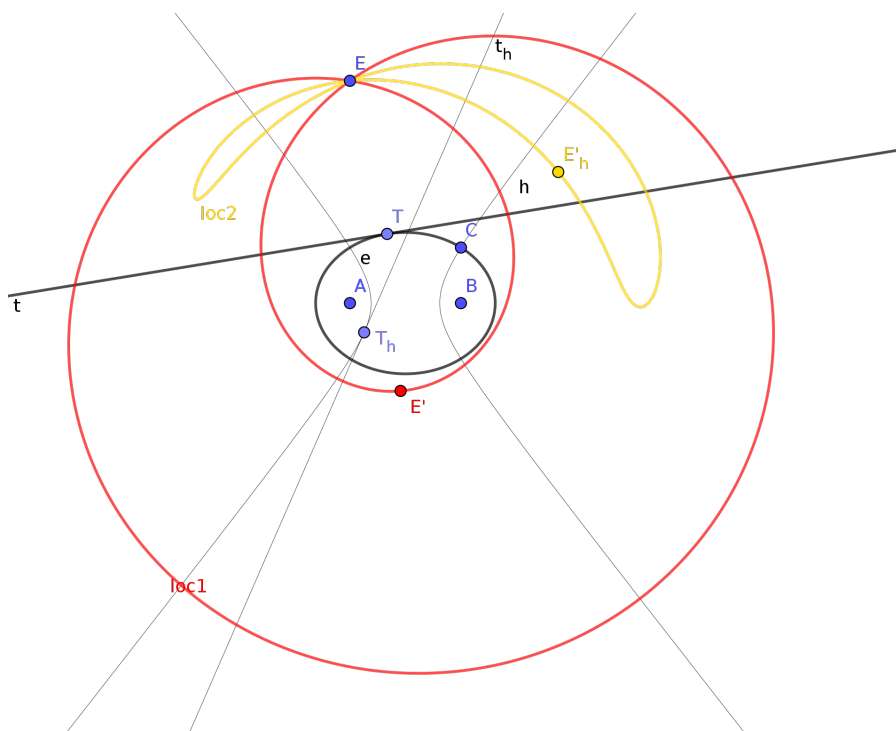


Figure 16: A union of two curves

tion time (animation is between 3.43 and 4.38 FPS⁵) may give some hope that this method has not yet found its extents and some further improvement could allow us to visualize the caustics of an ellipse/hyperbola in a similar way.

5 Conclusions

First, we give some technical remarks. We learned that fast computations may require suitable geometric definitions and a “lucky” way of algebraization. Maybe it is surprising, but avoiding degeneracy can be crucial in certain envelope computations. Since elimination is slow in general (double exponential in the number of variables), a simplification of the figure may play an important role. Finally, exploiting important properties from elementary geometry may also be helpful.

From the educational point of view, we strongly believe that visualization of optics can be a fruitful direction in STEAM projects. Unfortunately, algebraic curves of higher degrees are sometimes completely ignored or underrated in schools. It is clear that several polynomial curves of higher degrees “live among us”, and their computer based visualization strengthens the validity to find them a place in the school curriculum as well. Even more so, if the visualization process consists of just a couple of mouse clicks in a popular free software tool!

Higher degree curves have a rich geometry. The same definition with different parameters may re-

⁵See https://prover-test.geogebra.org/job/GeoGebra_Discovery-art-plottertest/105/artifact/fork/geogebra/test/scripts/benchmark/art-plotter/html/all.html for a recent benchmark on a set of test cases – our latest example is called `ellipse-point-mirror-tangent*.ggb`.

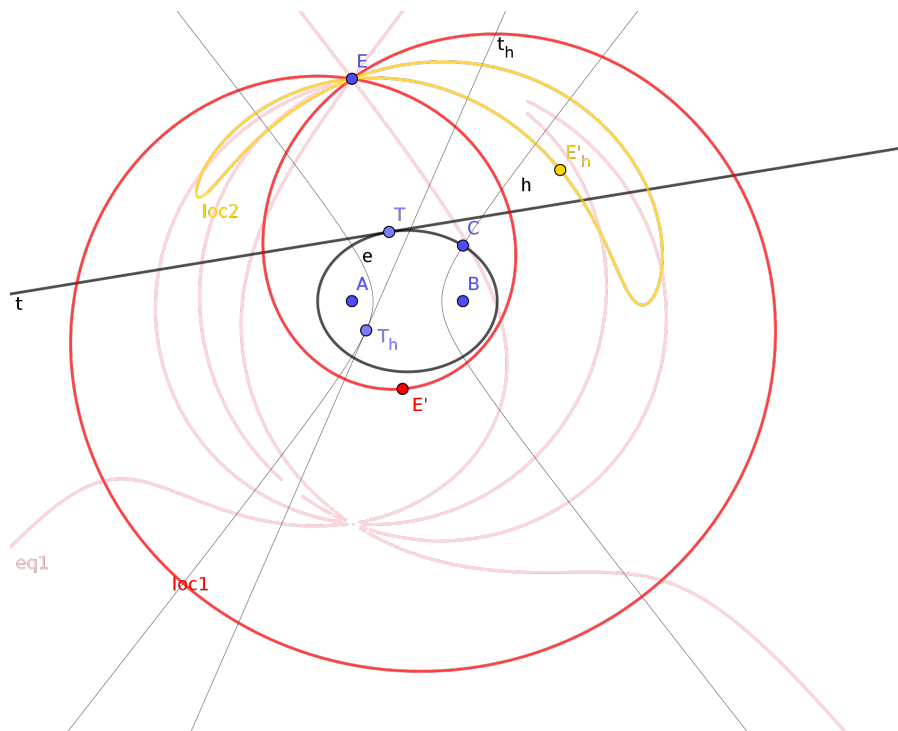


Figure 17: A union of two curves with the extra component

sult in completely different curves. This may encourage young learners to perform self-explorations, on the one hand, because of seeking for beauty, and on the other hand, to discover the challenging (and non-trivial) world of algebraic geometry. Here further steps could be, for example, factorization of the obtained polynomials, removing degenerate components, or self-studying geometric properties.

At CADGME 2010 Botana closed his plenary talk with the rhetorical question after showing the huge and exotic coefficients of a mechanically obtained algebraic curve:

“Should we hide this (kind of) result to students?”

An appropriate answer today in 2022 may be the following: “We cannot.” Science is proving more complicated than we ever thought. But is not complexity beautiful and fascinating?

6 Acknowledgment

The author was supported by the grant PID2020-113192GB-I00 from the Spanish MICINN.

Gerda and Domonkos Kovács kindly helped in the preparation of Figure 6.

Thanks to Csaba Sárvári for his motivation in writing this paper.

References

- [1] Miguel Abánades, Francisco Botana, Zoltán Kovács, Tomás Recio, and Csilla Sólyom-Gecse. Development of automatic reasoning tools in GeoGebra. *ACM Commun. Comput. Algebra*, 50(3):85–88, 11 2016.
- [2] Francisco Botana, Markus Hohenwarter, Predrag Janičić, Zoltán Kovács, Ivan Petrović, Tomás Recio, and Simon Weitzhofer. Automated theorem proving in GeoGebra: Current achievements. *Journal of Automated Reasoning*, 55(1):39–59, 2015.
- [3] Francisco Botana and Zoltán Kovács. A Singular web service for geometric computations. *Annals of Mathematics and Artificial Intelligence*, pages 1–12, November 2014.
- [4] Francisco Botana and Zoltán Kovács. New tools in GeoGebra offering novel opportunities to teach loci and envelopes. *CoRR*, abs/1605.09153, 2016.
- [5] Francisco Botana and José Luis Valcarce. A software tool for the investigation of plane loci. *Mathematics and Computers in Simulation*, 61(2):139–152, January 2003.
- [6] Francisco Botana and José Luis Valcarce. Automatic determination of envelopes and other derived curves within a graphic environment. *Mathematics and Computers in Simulation*, 67:3–13, July 2004.
- [7] Thierry Dana-Picard and Zoltán Kovács. Offsets of a regular trifolium (curvas paralelas a un trifolium regular). *Boletín de la Soc. Puig Adam*, 112:63–81, 2021.
- [8] Ulrich Kortenkamp. *Foundations of Dynamic Geometry*. PhD thesis, ETH Zürich, 1999.
- [9] Zoltán Kovács. Real-time animated dynamic geometry in the classrooms by using fast Gröbner basis computations. *Mathematics in Computer Science*, 11(3-4):351–361, 3 2017.
- [10] Zoltán Kovács and Bernard Parisse. Giac and GeoGebra – improved Gröbner basis computations. In Jaime Gutierrez, Josef Schicho, and Martin Weimann, editors, *Computer Algebra and Polynomials*, Lecture Notes in Computer Science, pages 126–138. Springer, 2015.
- [11] Zoltán Kovács and Pavel Pech. Experiments on automatic inclusion of some non-degeneracy conditions among the hypotheses in locus equation computations. In Cezary Kaliszyk, Edwin Brady, Andrea Kohlhasse, and Claudio Sacerdoti Coen, editors, *Intelligent Computer Mathematics*, volume 11617 of *Lecture Notes in Artificial Intelligence*, pages 140–154. Springer International Publishing, July 2019.
- [12] Zoltán Kovács, Tomás Recio, and M. Pilar Vélez. Using automated reasoning tools in GeoGebra in the teaching and learning of proving in geometry. *International Journal of Technology in Mathematics Education*, 25(2):33–50, 2018.
- [13] Peter Lebmeir and Jürgen Richter-Gebert. Recognition of computationally constructed loci. In Francisco Botana and Tomas Recio, editors, *Automated Deduction in Geometry*, pages 52–67, Berlin, Heidelberg, 2007. Springer Berlin Heidelberg.

- [14] Ernst W. Mayr and Albert R. Meyer. The complexity of the word problem for commutative semigroups and polynomial ideals. *Advances in Mathematics*, 46:305–329, 1982.
- [15] Reinhard Oldenburg. Feli-X – ein Computeralgebra-gestütztes dynamisches Geometrieprogramm. *Computeralgebra Rundbrief*, March 2004.
- [16] Reinhard Oldenburg. FeliX – mit Algebra Geometrie machen. *Computeralgebra Rundbrief, Sonderheft zum Jahr der Mathematik*, April 2008.
- [17] J.L. Rabinowitsch. Zum Hilbertschen Nullstellensatz. *Math. Ann.*, 102(1):520, 1929.
- [18] Jürgen Richter-Gebert and Ulrich H. Kortenkamp. *The Cinderella.2 Manual. Working with The Interactive Geometry Software*. Springer Berlin, Heidelberg, 2012.
- [19] Eric W. Weisstein. “Tschirnhausen cubic.” from MathWorld—a Wolfram web resource, 2022. <http://mathworld.wolfram.com/TschirnhausenCubic.html>.

A STEAM approach to canal surfaces

Thierry Dana-Picard

ndp@jct.ac.il

Department of Mathematics
Jerusalem College of Technology
Havaad Haleumi Street 21
9116011 Jerusalem, Israel

Abstract

Canal surfaces are a special occurrence of envelopes of parameterized families of surfaces in 3D space, namely envelopes of families of spheres centered on a given space curve. When the radius of the sphere is constant, they are called tubular surfaces, or simply tubes. In every country, numerous examples can be found all around (water pipes, canals for traffic of merchandises, etc. All these can incite to study such objects or models in mathematics. Dynamic Geometry Systems are an efficient tool to model such concrete objects, as they enable both a geometric construction and an exploration of the corresponding algebraic data (equations, parametric presentation). In order to have a more powerful tool for the algebraic computations, a Computer Algebra System can be used, whence a new need to communicate between DGS and CAS. In the past, a concrete construction of such canal surfaces was viewed as an artistic creation, whose abstract basis was quite complicated to grasp. For the beginner, understanding the switch from a concrete occurrence towards abstraction (equations, etc.) was a non-trivial issue. Neither was the reverse direction. We start from a geometric description of a spinal curve and of spheres centered on it, from there we derive equations whose solutions describe the desired surface. Nowadays, these paths can be completed by a new step, from an abstract presentation with equations towards a concrete realization using 3D printing. This approach, from real world to mathematical presentation, and then back to concretization, is typical of STEAM education.

1 Introduction

In the past, mathematical domains used to be considered separately, both in research and in teaching. Along the generations, more and more connections between domains emerged, producing richer domains of knowledge. Bridges have been built between mathematics and other domains of knowledge; a modern approach is called STEAM, an acrostic for Science, Technology, Engineering, Arts and Mathematics. This approach involves exploration, inquiry, discovery, critical thinking and creativity.

Envelopes of parametric families of plane curves and of surfaces in 3D space are a live domain of study. They have numerous applications in industry, such as robotics, zones of safety [13], depollution of soils [22]. Despite their importance, they almost disappeared from the syllabus already in the sixties of the 20th century, and Thom complained about that situation [32]. New technologies enabled to revive the topic, and to propose it to both pre-service and in-service teachers. The first software used in [17] was Derive to explore 1-parameter families of plane curves. In subsequent papers, another Computer Algebra System (CAS) and a Dynamic Geometry System (DGS) have been used. In [13, 18, 19], these are Maple and GeoGebra. They are used in the present paper too.

A central feature of a DGS is the possibility to visualize and to manipulate directly on the screen all the objects of plane geometry. The main tools are point dragging and slider bars. Both are commanded by the mouse, and are central for the man-and-machine relationship. In GeoGebra a slider bar can run an automatic animation also. The most basic object in GeoGebra are points; for example a line is defined by 2 points, and a circle can be defined with a center and a point on the circle. Some of the points are free, and further constructs depend on them. Dragging a free point using the mouse induces automatically changes in all the constructs dependent on this point. Similar features characterize slider bars, and multiple sliders can be defined for a family of objects. In order to understand an object in 3D shown on a screen, the possibility to turn around using the mouse is a must, in order to discover the object from different points of view. This grants the possibility to explore, analyze, discover, and then to conjecture results which have to be proven later. Proofs can be written in a "traditional" way, we mean by pen-and-paper, but a DGS offers also tools for automated exploration and automated proofs. We refer especially to the algorithms developed by Wu [33, 34, 35] and to new algorithms which are continuously developed since then, these developments being applied in classrooms and labs, and receiving feedback from them [29, 5, 4, 9, 10, 24, 28]. Recio and Vélez analyze the different work areas allowed by a DGS: "While automatic proving deals with verifying geometric statements, automatic discovery tries to find complementary hypotheses for statements to become true or to find the missing hypotheses so that a given conclusion follows from a given incomplete set of hypotheses".

Computer Algebra Systems have been initially developed around symbolic computations, whence their name, *to do mathematics*. Quickly other features have been implemented. We use the possibilities of symbolic computations together with the graphical affordances, to *teach/learn mathematics*. We mean to explore, conjecture, develop a more profound understanding and, if possible, prove. DGS contribute strongly to this trend.

In contradiction to other scientific domains where the objects under study are graspable physically, and are often "on the table", a mathematical object is an abstract one and can be grasped only via different representations, symbolic, numerical, graphical, etc. [21]. Switching between registers of representation enables to consider the same object from different points of view. Generally, a CAS offers the switching from either symbolic or numerical representation to graphical representation. A DGS offers this switch, but also a switch in reversed direction, and knows how to translate the changes made when dragging points or using a slider directly in the algebraic representation. In GeoGebra, the algebraic window and the graphical windows are fully synchronized. This too is important for R & D and classroom work.

The graphical affordances of the two kinds of software are sometimes different. In our study, animations are important. GeoGebra enables continuous animations using the **Animation on** of a slider, and also animation driven by the user's hand on the mouse. A CAS requires writing a specific

command such as Maple’s **animate** and then to press a button to run the animation. Several options are available, such as speed, number of frames, parameter increment, etc. Both kinds of software, DGS and CAS, allow to save the animation as an animated GIF. In [24], Kovács writes that ”animations can be performed quickly enough by using today’s computers with implicit computer algebra use. In the background, without notifying the user on the fact that thousands of symbolic computations are performed, a pure dynamic geometry experience can be relived, making geometry more geometrical than before.” More advanced features, described in [28], are available as a companion package called *GeoGebra discovery*, new versions being published at a frequent pace¹.

We must mention that among other commands for automated exploration and discovery, GeoGebra has a command **Envelope** for the automated determination of envelopes in a 2D setting. The current version of **Envelope** requests the tracer to be a variable point and not a slider for variations of a real parameter; see [6, 7, 8]. This has an influence on our choices: here we use a parametric representation of a space curve, and not a pure geometric construction. This has been already the case for the study of a Maltese Cross as an envelope in [13].

Finally, we add here an old-new way of representing mathematical objects: 3D construction. The evolution of teaching passed from the concrete representation in wood or metal towards more abstract drawing on a sheet of paper or plots on a screen. We are now back to a genuine 3D represen

2 Enhancing motivation via concrete occurrences

2.1 Canals in real life

Canals are almost ubiquitous in the world:

- Small canals to bring water from the source to the consumers. Figure 1(a) shows an ancient canal in Peru² - pay attention that the shape of the section varies, to ease the fluidity of the flow. Note that most of these canals are open above, but not always, and pipes can be found. Figure 1(b) shows an underground part of the aqueduct from Solomon Pools in Judea mountains to Jerusalem. Figure 2 shows an exit to an open-air part of the same system, dating hundreds of



(a) Precolombian water canal



(b) Aqueduct in Judea

Figure 1: Ancient canals

¹The package is freely downloadable from <https://github.com/kovzol/geogebra-discovery>

²Source: <https://www.audleytravel.com/ca/peru/country-guides/inca-sites-to-visit>

years earlier, and an early 20th century replacement by a pipe³. Note that the pipe seems to have variable radius, despite the fact that the inner part may be quite different, the larger radius corresponding to connections of different sections (needed in particular to connect straight and curved parts).

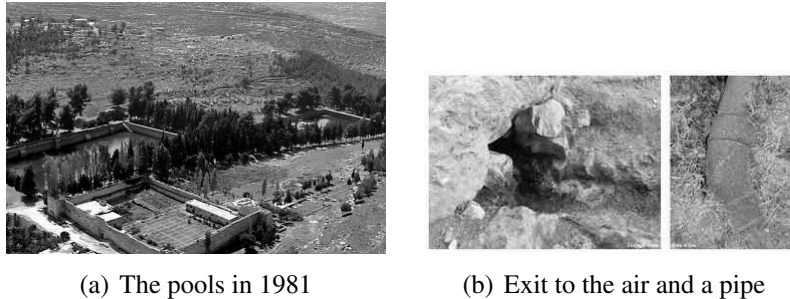


Figure 2: Solomon's Pools

- Larger canals for the circulation of goods. In Europe, heavy loads used to be transported by waterways, nowadays these canals are often used for tourism and cruises (Figure 3).

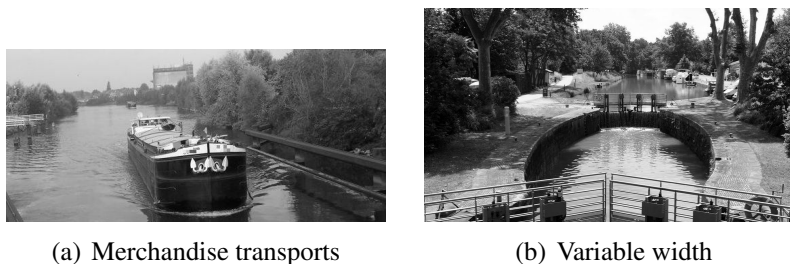


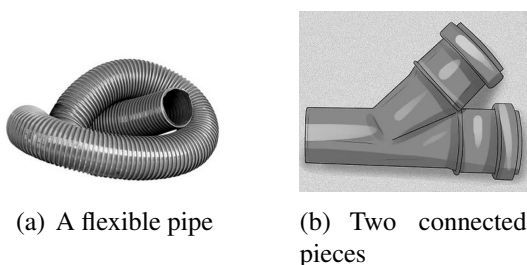
Figure 3: Circulation of goods and tourism

- Entertainment parks yield nice examples. Figure 4 shows an open water slide and a tubular one.
- At a smaller scale, Figure 5 show pipes which can be found in any household, for a washing machine or a dish washing machine. One example has variable radius (periodic when the pipe is straight); as by nature it is very flexible, it can help to visualize several mathematical objects. It is quite clear that for the second example, two different mathematical surfaces have to be defined and "glued" together.
- Washers are shown in Advanced Calculus as examples of surfaces of revolution. They can be viewed also as canal surfaces.

³Sources: (a) https://commons.wikimedia.org/wiki/File:Solomon%27s_pools2.jpg; (b) <https://www.jpost.com/travel/around-israel/solomon-pools-fit-for-a-king>.



Figure 4: two kinds of water slides



(a) A flexible pipe

(b) Two connected pieces

Figure 5: Home water pipes

These different examples may be an incentive for students for the mathematical study that we propose. As discussed in [14, 16], the usage of items from the cultural background of the students encourage them to study of various more theoretical topics, and then to discover applications. Moreover, visits on the field (mathematical trails) can contribute to enhancing motivation. The configurations may be very different, but the presence of such canals in the vicinity of the students may be such an incentive to study mathematical models, a part of a mathematical trail. The variety itself, or the the changes along the canals will be a good reason to study canal surfaces with variable radius.

2.2 Mathematics and Art

The “Institut Henri Poincaré” in Paris has a large collection of models of surfaces in 3-dimensional space, established in the 19th century. Some of them are models of canal surfaces. Apéry wrote recently a description accompanied by photos [1]. Figure 6 shows two examples, both from the Brill-Schilling collection: (a) a ruled surface⁴, and (b) a canal surface, which is the envelope of spheres with variable radius⁵. This is the topic of next section. Note that explicit equations are not always available, and that even then, it is understood that the endeavor to construct these objects was quite hard.

Figure 7(a) shows a piece of string art⁶, and Figure 7(b) presents a GeoGebra model⁷. This model

⁴<https://patrimoine.ihp.fr/item/3490>

⁵<https://patrimoine.ihp.fr/item/3392>

⁶It illustrates activities in France, by EchoSciences-Occitanie - <https://www.echosciences-sud.fr/communautes/diffusion-de-la-culture-mathematique-en-occitanie/articles/mathematiques-des-fils-tendus-vers-le-reve>

⁷<https://www.geogebra.org/m/nkxrwmxd>



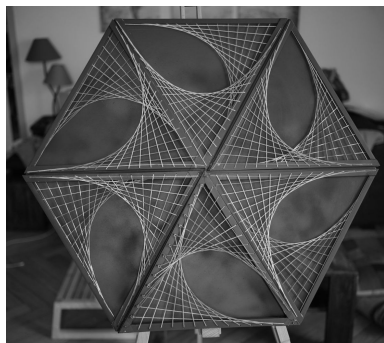
(a) Ruled surface of degree 3



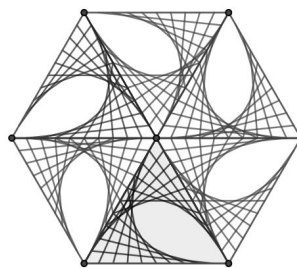
(b) Canal surface

Figure 6: Physical models of surfaces

is 2-dimensional, but the threads create a ruled surface, because of their thickness. This topic may be explored in a course in Linear Algebra or elsewhere, and the visualization is important. Moreover, the animation helps to visualize the envelopes of the various segments in motion.



(a)



(b)

Figure 7: A piece of string art and a computerized model

The empty zones, shaped as leaves, are bounded by something which can be modeled as an envelope of segments. The description using equations may be unilluminating, thus we will not describe it here, and we address simpler examples in the next sections.

3 Envelopes and canal surfaces

There exist 4 different definitions of envelopes of 1-parameter families of plane curves, given in [11]; all of them can be adapted to 1-parameter families of surfaces in 3-dimensional space. A version for 1-parameter families of surfaces of Definition 5.8 in [11] (page 80) is the following:

Definition 1 Let \mathcal{S}_k denote a family of 1-parameter surfaces in 3D space.

1. The characteristic curves of the family are the limit curves, when ϵ goes to 0, of the intersection of nearby surfaces \mathcal{S}_k and $\mathcal{S}_{k+\epsilon}$.

2. *The envelope of this family, if it exists, is the union of the characteristic curves.*

Following a 3D version of [11] (5.12 page 81), it can be shown that \mathcal{E} is a surface tangent to every \mathcal{S}_k .

Suppose that the surfaces \mathcal{S}_k are given by an equation of the form $F(x, y, z, k) = 0$, where k is a real parameter. The intersection $\mathcal{S}_k \cap \mathcal{S}_{k+\epsilon}$ is determined by the following system of equations:

$$\begin{cases} F(x, y, z, k) = 0 \\ F(x, y, z, k + \epsilon) = 0 \end{cases} \quad (1)$$

After sidewise subtraction and computation of a limit for ϵ going to 0, we obtain the following result:

Proposition 2 *If it exists, an envelope of this family is the solution set of the system of equations:*

$$\begin{cases} F(x, y, z, k) = 0 \\ \frac{\partial}{\partial k} F(x, y, z, k) = 0 \end{cases} \quad (2)$$

Note that this is the only definition of an envelope given by Berger [3]. For elementary situations (such as [18] III, example 2), the system (2) of (generally) non-linear equations can be solved by hand. In heavier situations, a Computer Algebra System can be used (the user has already some understanding of what happens and the usage is not purely as a black box. The **solve** command may use different algorithms, according to whether the equations are polynomial or not. The interested reader can refer also to [17, 19]. As we will see in the next subsection, for canal surfaces we consider families of spheres, and the characteristic curves are circles.

3.1 Canal surfaces

Definition 3 *Let \mathcal{C} be a curve in the 3-dimensional space given by a parametrization $M(t)$ and let r be a function which associates a positive real number $r(M)$ to every point on \mathcal{C} . For a point M on \mathcal{C} , we denote by S_M the sphere centered at M with radius $r(M)$. If it exists, the envelope of the family of spheres S_M is called a canal surface. The curve \mathcal{C} is called the spinal curve of the canal surface. If the function r is constant, we call the envelope a pipe surface or a tubular surface, or simply a tube.*

With the emergence of various technologies, at the beginning plotters, later CAS and Dynamic Geometry Systems, it became possible to model envelopes in general, and canal surfaces in particular, on a screen. As these plots are projections of 3D objects on a 2D screen, they have some drawbacks. For example, Figure 8 illustrates the envelope of spheres of radius $3/2$ centered on the parabola in the x, y -plane whose equation is $y = x^2$. We use here the synchronisation between the 2D window and the xy -plane in the 3D window. The dotted curves in the 3D window are the circles of the 2D window. From Figure 8(a) it can be understood that the envelope is self-intersecting, which is not clear from Figure 8(b). We have here a typical situation of the difficulty to visualize 3D objects on a 2D screen. Figure 8(c) is nicer and shows the envelope, but the self-intersection is hidden. Conviction (not a proof) can be obtained when revolving the plot on the screen. Creating the model with a 3D printer allows the learner to turn the surface with his/her fingers; see Section 5. Conviction becomes stronger.

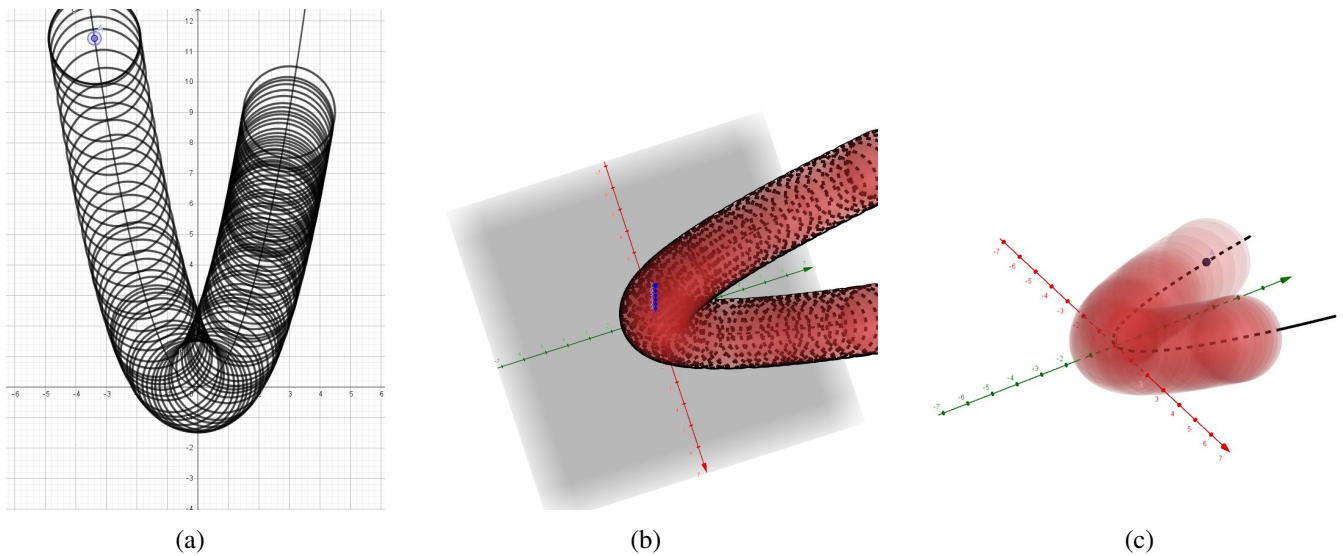


Figure 8: A self-intersecting envelope

3.2 Example: a torus

We consider the family of spheres of radius $1/2$ centered on the circle in the xy -plane whose center is at the origin and with radius equal to 2 (the spinal curve). A general equation of these spheres is

$$(x - 2 \cos t)^2 + (y - 2 \sin t)^2 + z^2 - \frac{1}{4} = 0. \quad (3)$$

We denote by $F(x, y, z, t)$ the right-hand side of Equation (3). Then we have:

$$\frac{\partial F}{\partial t} = 4(x - 2 \cos t) \sin t - 4(y - 2 \sin t) \cos t.$$

Solving System (2) for this case, we obtain the two following parametric presentations:

$$\begin{cases} x = v \cot t \\ y = v \\ z = \frac{\sqrt{-15 \sin^2 t + 16v \sin t - 4v^2}}{2 \sin t} \end{cases} \quad \text{and} \quad \begin{cases} x = v \cot t \\ y = v \\ z = -\frac{\sqrt{-15 \sin^2 t + 16v \sin t - 4v^2}}{2 \sin t} \end{cases} \quad (4)$$

Note that we obtained the envelope as the union of two components, who are symmetric about the xy -plane.

Using the method described in [13, 15], we transform these parametrizations into rational parametrizations, then into a system of polynomial equations. These polynomials generate an ideal in $\mathbb{R}[x, y, z, t]$. By elimination we obtain a single polynomial in $F_1(x, y, z)$ whose vanishing locus is the desired envelope, i.e. we found an implicit equation of the envelope. In the present case, it is easy to identify this equation as an equation of a torus. Figure 9 has been obtained with GeoGebra, moving the sphere with the Trace On option. The spinal curve appears by transparency (the dotted circle)⁸.

⁸The full synchronisation between the 2D window and the xy -plane in then 3D window is very helpful for moving teh center of the sphere along the spinal curve.

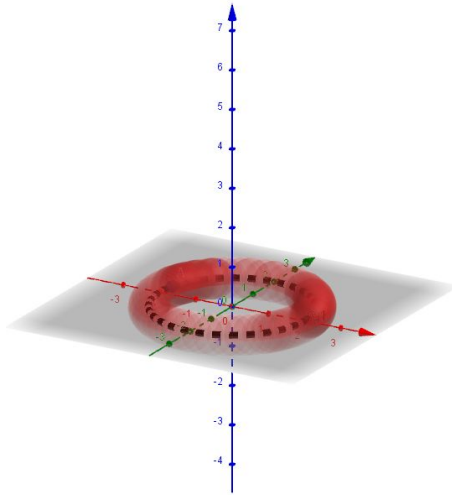


Figure 9: A torus as an envelope of spheres

3.3 Example: a necklace

Consider every point $P(r, 0, 0)$ on the x -axis as the center of a sphere of radius $|\sin r|$. They are defined in GeoGebra using the command $Sphere(A, abs(sin(r)))$. The envelope of this family of spheres, is displayed in Figure 10; it looks like a necklace.

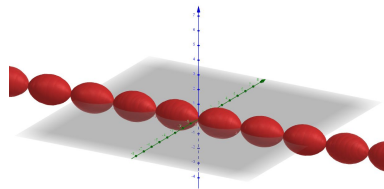


Figure 10: A necklace

The general equation of the spheres is

$$(x - r)^2 + y^2 + z^2 - \sin^2 r = 0. \quad (5)$$

Solving System (2), we obtain the two following parametric presentations:

$$\begin{cases} x = x = r - \sin r \cos r \\ y = \sqrt{\sin^4 r - t^2} \\ z = t \end{cases} \quad \text{and} \quad \begin{cases} x = x = r - \sin r \cos r \\ y = -\sqrt{\sin^4 r - t^2} \\ z = t \end{cases} \quad (6)$$

Consider now the family of circles centered on the same segment as above, with the same variable radius. Figure 11 has been obtained using the command $Circle(A, abs(sin(r)), i)$ and **Trace On**, where i denotes a unit vector on the x -axis. The figure on the left has been obtained after one run of the

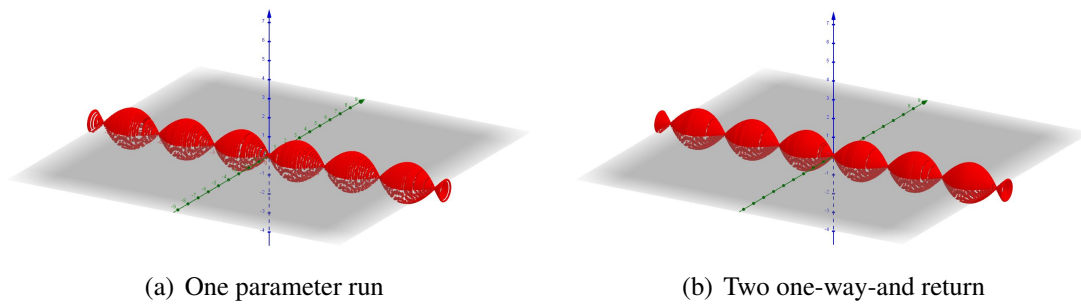


Figure 11: Another construction of the necklace

parameter, the figure on the right after 2 returns. Note the accuracy differences between them and between them and Figure 10: in Figure 11, white spots appear, which are not present in Figure 10.

Definition 2 is not applicable here, as we have a 1-parameter family of space curves and not 1-parameter family of surfaces. The space curves are defined by a parametric representation and not by an implicit equation, which is requested by Definition 2. Kock relates shortly to this case in [23] but without computational expressions. Here we can use the definition and its translation into a theorem given by the Mathcurve site⁹.

Definition 4 *The envelope of a 1-parameter family of space curves C_k is the geometric locus \mathcal{E} of the characteristic points of the curves C_k , which are the limit points of the intersection points between C_k and $C_{k'}$ when k' tends to k . These points only exist if the curve C_k is secant with the infinitely close curves C_{k+dk} . \mathcal{E} is then tangent at each of its points to a curve C_k and, in general, any curve C_k is tangent at least at one point to \mathcal{E} .*

Theorem 5 *Suppose that the curve C_k is given by*

$$\begin{cases} F(x, y, z, k) = 0 \\ G(x, y, z, k) = 0 \end{cases} \quad (7)$$

Then the envelope exists if and only if the following system of 4 equations

$$\begin{cases} F(x, y, z, k) = 0 \\ G(x, y, z, k) = 0 \\ \frac{\partial}{\partial k} F(x, y, z, k) = 0 \\ \frac{\partial}{\partial k} G(x, y, z, k) = 0 \end{cases} \quad (8)$$

has a solution for (x, y, z) for all values of k . This solution gives the parametrization of the envelope.

Note that it is rather exceptional that a family of space curves has an envelope. It is generally a curve, but may degenerate to a set of isolated points (see [17] 4.2, for an example in 2D).

Here we have $F(x, y, z, k) = (x - r)^2 + y^2 + z^2 - \sin^2 r$ and $G(x, y, z, r) = x - r$. System (8) has no real solution, therefore no envelope exists in the sense of Theorem 5. An extension of the theory would be welcome; it is discussed, for example, in [31] but is beyond the scope of the present paper.

⁹<https://mathcurve.com/courbes3d.gb/enveloppe/enveloppe.shtml>

Nevertheless, we provide the source code for an animation with Maple, showing successive positions of the circles. The animation with **Trace On** creates a surface, generated by the circles with variable radius. The number of plotted circles is determined either by the slider or by the speed of moves with the mouse; the less circles are plotted, the more discrete is the plot. In order to have a feeling of continuity, it is necessary to increase the number of frames and the number of circles which have to remain on the screen.

```
F := (x - r)^2 + y^2 + z^2 - sin(r)^2;
G := x - r;
solve({F = 0, G = 0}, {x, y, z});
circ := allvalues(%):
a1 := animate(spacecurve, [[rhs(circ[1][1]), rhs(circ[1][2]),
    rhs(circ[1][3])], z = -3 .. 3], r = -10 .. 10,
    scaling = constrained, thickness = 2, trace = 100,
    frames = 100):
a2 := animate(spacecurve, [[rhs(circ[2][1]), rhs(circ[2][2]),
    rhs(circ[2][3])], z = -3 .. 3], r = -10 .. 10,
    scaling = constrained, thickness = 2, trace = 100,
    frames = 100):
display(a1, a2);
```

Figure 12 shows a partial plot in the middle of the animation and the final plot.

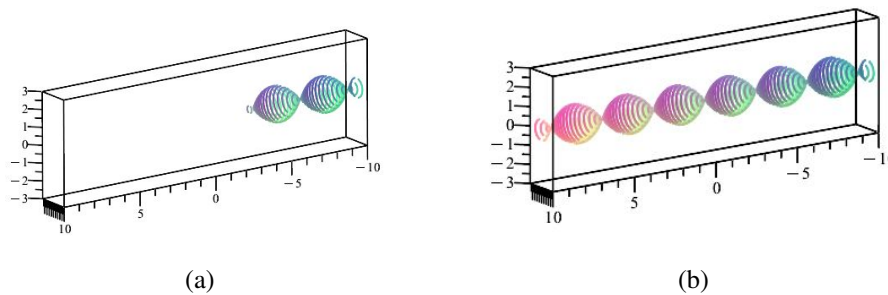


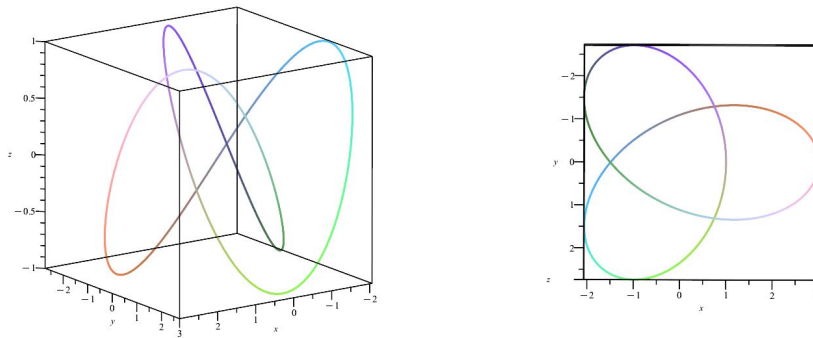
Figure 12: The necklace with a Maple animation

4 A trefoil knot as a canal surface

Consider the space curve \mathcal{C} defined by the parametric presentation

$$\begin{cases} x = \cos t + 2 \cos 2t \\ y = \sin t - 2 \sin 2t \\ z = \sin 3t \end{cases} \quad (9)$$

Two views are displayed in Figure 13, obtained with Maple. We will take this curve as a spinal curve



(a) The trefoil curve \mathcal{C}

(b) Its projection on the xy -plane

Figure 13: A trefoil space curve

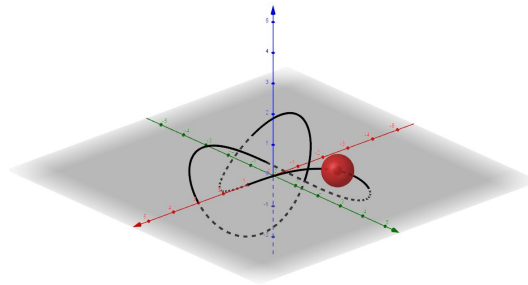


Figure 14: A trefoil space curve

for a family of spheres, namely the family of spheres centered on this curve, with radius $1/2$. Figure 14 shows the space curve \mathcal{C} and one of the spheres of the family. Figure 15 shows two views of the envelope of the family, which is a canal surface. Actually it is a tubular surface, as the radius of the spheres is constant. Both figures have been obtained with GeoGebra; for Figure 15, a point A has been attached to the curve \mathcal{C} and a sphere of center A and radius $1/2$ plotted, then A has been dragged along the curve while the **Trace On** property has been chosen for the sphere.

A general equation for spheres centered on \mathcal{C} with radius $1/2$ is

$$(x - (\cos t + 2 \cos 2t))^2 + (y - (\sin t - 2 \sin 2t))^2 + (z - \sin 3t)^2 - \frac{1}{4} = 0. \quad (10)$$

As usual, we denote by $F(x, y, z, t)$ the left-hand side in Equation (10) and solve the System of Equations (2) in this case. The output is too heavy to be displayed here, and has to be studied using the software. For the reader's convenience, we give here the source code with Maple:

```
c := spacecurve([cos(t) + 2*cos(2*t), sin(t) - 2*sin(2*t), -sin(3*t)],
               t = 0 .. 2*Pi, labels = [x, y, z]);
F := (x + (-cos(t) - 2*cos(2*t)))^2 + (y + (-sin(t) + 2*sin(2*t)))^2
```

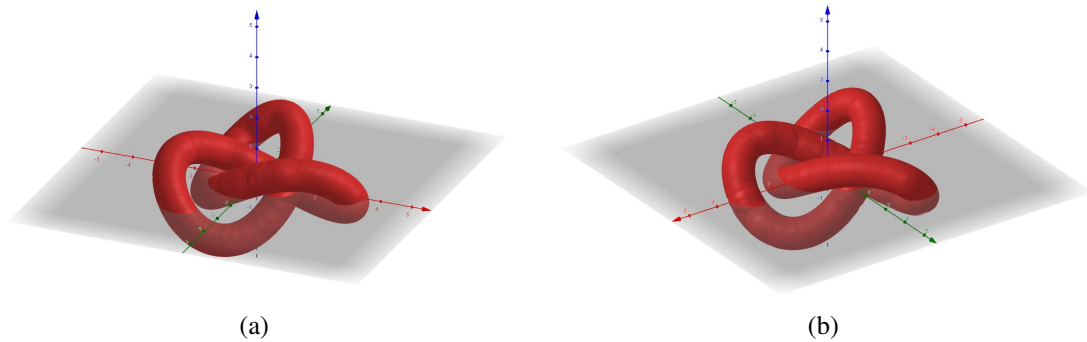


Figure 15: The concrete knot

```

+ (z + sin(3*t))^2 - 1/4;
derF := diff(F, t);
env := solve({F = 0, derF = 0}, {x, y, z});
env := allvalues(%);
x1 := simplify(rhs(env[1][1]));
y1 := simplify(rhs(env[1][2]));
z1 := simplify(rhs(env[1][3]));
s1 := plot3d([x1, y1, z1], t = 0 .. 2*Pi, y = -3.5 .. 3.5,
  numpoints = 25000, labels = [x, y, z], axes = none);
x2 := simplify(rhs(env[2][1]));
y2 := simplify(rhs(env[2][2]));
z2 := simplify(rhs(env[2][3]));
s2 := plot3d([x2, y2, z2], t = 0 .. 2*Pi, y = -3.5 .. 3.5,
  numpoints = 40000, labels = [x, y, z],
  style = patchnogrid, axes = none);
display(s1, s2);

```

Figure 16 shows the output of the **display** command. We used the *style=patchnogrid* option for one of the components only, in order to show how the mesh has been chosen by the software .

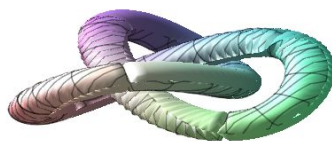


Figure 16: The trefoil knot

The output of the computation described with the source code above is really heavy (therefore we did not display it here). It cannot be reasonably used to 3D print the trefoil. Other parametrizations may be used. For example, see the method proposed on the dedicated [wikipedia page](#). There a substitution $u = \cos t$ and $v = \sin t$ is used. In order to take into account that $u^2 + v^2 = 1$, the computations have to be performed according to $v = \pm\sqrt{1 - u^2}$. Each case provides two components,

and the envelope is the union of 4 components. Here too, our computations yielded a heavy answer. A more applicable way for 3D printing has been developed with GeoGebra by Diego Lieban¹⁰.

As a final remark in this section, we should note that when plotting a curve with a DGS, the user has the choice of the plot thickness. Figure 17 shows the same trefoil knot as Figure 14, but with the maximal thickness offered by GeoGebra. Actually, this can be viewed as a view of a pipe surface, and a beginner cannot be aware of this fact.

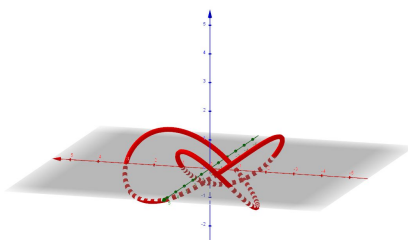


Figure 17: A pipe surface obtained by thickening the plot of a space curve

5 Discussion

5.1 New registers of representation

As mentioned previously, Duval [21] noted that a mathematical object is an abstract object, which cannot be grasped in our hands, contrary to objects of other scientific domains. It can be studied only via different registers of representation. Traditionally, these are numerical, symbolic, and graphical, and the possibility to switch between different registers is of the utmost importance. Different kinds of software provide different possibilities to switch. Generally, a CAS offers switching from symbolic representation to graphical representation. Actually it uses in between a numerical representation, but does not display it if not requested. And if requested, the numerical and graphical representations are obtained with two distinct commands. Working with a DGS (here GeoGebra), both switching directions are offered: from symbolic/numerical to graphical and from graphical to symbolic/numerical. Moreover, the dragging in a DGS enables to explore interactively, and, in the case of Figure 15, it enabled to have a very smooth display.

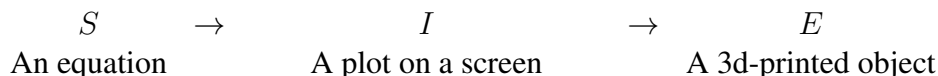
The evolution of teaching passed from the concrete representation in wood or metal (we refer here to Subsection 2.2) towards more abstract drawing on a sheet of paper or plots on a screen. In a more general framework than Mathematics Education, Jerome Bruner [12] proposed three modes of representation: Enactive representation (action-based), Iconic representation (image-based) and Symbolic representation (language-based). He described the first years of children development as

$$E \rightarrow I \rightarrow S.$$

Of course, the topic of the present paper does not belong to these first years, but we can describe

¹⁰<http://www.geogebra.org/3d/kvzcezcp>.

it in Bruner’s terminology. In our case we may have the following sequence:



The last step (marked by E) can be made concrete with 3D printing. Figure 18 shows: (a) a graphical presentation with GeoGebra, using point dragging of the center of the spheres along the curve, and (b) the result of 3D printing for the canal surfaces obtained by spheres centered on a non planar curve, given by the parametrization $(x, y, z) = (\cos 2t, \sin 2t, 3 \sin t)$.



Figure 18: A 3D printed tubular surface

This new kind of representation is sometimes feasible directly from the DGS, but in the present case it requested an extra step. Either point dragging (or using the slider bar) with **Trace On** for the spheres, or using the **Locus** command shows something which is not recognized by the software as a 3D object (a surface). Therefore some algebraic work had to be performed before the GeoGebra file could be translated into the language of the 3D printer. The 3D printer requires a specific input, mostly a triangulated mesh of the object to be printed. This has to be generated either from the equations or from the parametrization. We have here a new example of the necessity of a dialog between different kinds of mathematical software, as discussed in [20]. Here we have 3 kinds of technology involved: a CAS, a DGS and a 3D printer.

Note that we do not have much information on how the handcrafted objects presented in Subsection 2.2 (Figure 6) have been constructed.

5.2 The role of technology

Using a Computer Algebra System (CAS), it is generally possible to compute parametric presentations of these surfaces. If the original parametrization of the spinal curve is rational, the equations describing the envelope are transformed into polynomials; this has been done, for example, in [20]. Then a package for computations of Gröbner bases enables to derive an implicit equation. This is not always possible. Even when possible, it may be possible to plot with Maple, but not with GeoGebra. In both cases, there are limitations: with Maple, the plot options have to be chosen in order to avoid a strange plot (a problem analyzed in [37]), and with GeoGebra the limitation is sometimes on the degree of the polynomial.

In early 2000's a great mathematician published an interview in a French scientific magazine aimed at a general audience, where he regretted that math educators work with their students in a way too different from the way researchers work¹¹. His concern is met in the papers quoted in Section 1: working in a technology rich environment provides experimental approaches, similar for researchers and their students. Moreover, such an environment enables a revival of classical, and sometimes almost forgotten domains. In the previous studies we obtained another byproduct: a unifying framework for a family of plane curves, which had been generally viewed as different objects without any connection between them [13]. We have also an opportunity to re-express the wish to see in the near future more advances towards automated networking CAS and DGS. The history of such a wish goes back to the early 2000's and knew continuous advances, both in programming and in applications (e.g. [29, 25, 28, 20, 30]).

Three years later, Papadopoulos and Dagdilelis wrote in [26] that a "DGS allows students to generate assumptions that later can be verified or rejected through formal proof", adding that "this verification of assumptions takes place much more easily in the DGS environment than in other computational environment or in the more traditional setting of paper and pencil". We hope that the different parts of our study will contribute to an incentive to develop skills for exploration, discovery, conjecture. An accurate verification may be out of reach from the DGS alone (even when a CAS is implemented in it), and the derivation of accurate results is obtained by the networking of a DGS and a powerful CAS together, thus answering both the educators' requirements and Bourguignon's wish. This networking exists already since the implementation of the Giac CAS into GeoGebra [25]. Other important developments can be found in GeoGebra-discovery.

Combining in class mathematical software together with the concrete realizations and applications in real world is a genuine STEAM approach to canal surfaces.

Acknowledgement: The author wishes to thank Eva Ulbrich, from Johannes Kepler University, Linz, Austria, for 3D printing for him various objects. In particular Figure 18 shows her work. He wishes to thank also the anonymous reviewers for their fruitful remarks.

References

- [1] Apéry, F. *The Cabinet de mathématiques of the Henri Poincaré Institute in Paris*, Kwartalnik Historii Nauki I Tech 65 (3) (2020), 97-108. Available: <https://www.ejournals.eu/pliki/art/17658/> (accessed July 2022)
- [2] Balka, D. *Estándares de práctica matemática y STEM*, Boletín informativo del conector Math-science (2011), 6-8.
- [3] Berger, M.: *Geometry*, Springer Verlag, 1994.
- [4] Blazek, J. and Pech, P.: *Locus Computation in Dynamic Geometry Environment*, Mathematics in Computer Science 13 (1-2) (2019), 31-40
- [5] Botana, F. and Abánades, M.A. *Automatic deduction in (dynamic) geometry: Loci computation*, Computational Geometry 47(1) (2014), 75-89.

¹¹The issue of the magazine is not available anymore, therefore we did not mention the name of this mathematician

- [6] Botana, F. and Recio, T. *Some issues on the automatic computation of plane envelopes in interactive environments*, Mathematics and Computers in Simulation **125** (2016), 115-125.
- [7] Botana, F. and Recio, T. *Computing envelopes in dynamic geometry environments*, AMAI (Annals of Mathematics and Artificial Intelligence) **80**(1) (2017), 3-20.
- [8] Botana, F. and Recio, T. *A proposal for the automatic computation of envelopes of families of plane curves*, Journal of Systems Science and Complexity **32**(1) (2019), 150-157.
- [9] Botana, F., Valcarce, J.: *A dynamic-symbolic interface for geometric theorem discovery*, Computers & Education **38**, 21-35 (2002).
- [10] Botana, F. and Valcarce, J.L.: *Automatic determination of envelopes and other derived curves within a graphic environment*, Mathematics and Computers in Simulation **67** (2004), 3-13.
- [11] Bruce, J.W. and Giblin, P.J.: *Curves and Singularities*, Cambridge University Press, 1992. Online <https://doi.org/10.1017/CBO9781139172615> (2012).
- [12] Bruner, J. S. *Toward a Theory of Instruction*. Cambridge: Harvard University Press, 1966.
- [13] Dana-Picard, Th. *Safety zone in an entertainment park: Envelopes, offsets and a new construction of a Maltese Cross*, Electronic Proceedings of the Asian Conference on Technology in Mathematics ACTM 2020; Mathematics and Technology, 2020, ISSN 1940-4204 (online version).
- [14] Dana-Picard, Th., and Hershkovitz, S. *STEAM Education: technological skills, students' cultural background and Covid-19 crisis*, Open Education Studies **2**(1) (2020), 171-179.
- [15] Dana-Picard, Th. *Envelopes and offsets of two algebraic plane curves: exploration of their similarities and differences*, Mathematics in Computer Science **15**, Springer (2021).
- [16] Dana-Picard, Th., Hershkovitz, S., Lavicza, Z. and Fenyvesi, K.: *Introducing Golden Section in the Mathematics Class to Develop Critical Thinking from the STEAM perspective*, the South-East Asia Journal of STEM Education **2**(1) (2021), 151-169.
- [17] Dana-Picard, Th., and Zehavi, N. *Revival of a classical topic in Differential Geometry: the exploration of envelopes in a computerized environment*, International Journal of Mathematical Education in Science and Technology **47**(6) (2016), 938-959.
- [18] Dana-Picard, Th. and Zehavi, N. *Automated Study of Envelopes transition from 1-parameter to 2-parameter families of surfaces*, The Electronic Journal of Mathematics and Technology **11**(3) (2017), 147-160. Printed version in the Journal of Research of Mathematics and Technology **6**(2), (2017), 11-2.
- [19] Dana-Picard, Th. and Zehavi, N. *Automated study of envelopes: The transition from 2D to 3D*, The Electronic Journal of Mathematics and Technology **13**(2) (2019), 121-135.
- [20] Dana-Picard, Th. and Kovács, Z. *Networking of technologies: a dialog between CAS and DGS*, The Electronic Journal of Mathematics and Technology **14**(1) (2021), 43-59.

- [21] Duval, R. *Understanding the Mathematical Way of Thinking – The Registers of Semiotic Representations*, Springer Cham, 2017. DOI: <https://doi.org/10.1007/978-3-319-56910-9>
- [22] Zeitoun, D. and Dana-Picard, Th. *Delineation of the Zone of Influence of Pumping Wells using CAS and DGS*, the Electronic Proceedings of the Asian Conference on Technology in Mathematics ACTM 2021, Mathematics and Technology, 2022.
- [23] Kock, A. *Envelopes – Notion and Definiteness*, Beiträge zur Algebra und Geometrie (Contributions to Algebra and Geometry) **48**(2) (2007), 345-350.
- [24] Kovács, Z. *Achievements and Challenges in Automatic Locus and Envelope Animations in Dynamic Geometry*, Mathematics in Computer Science **13** (2019), 131-141.
- [25] Kovács, Z., Parisse, B. *Giac and GeoGebra – improved Gröbner basis computations*. In Gutierrez, J., Schicho, J., Weimann, M. (eds.), Computer Algebra and Polynomials, Lecture Notes in Computer Science 8942. Springer, 2015, 126-138.
- [26] Papadopoulos, I. and Dagdilelis, V. *Computer as a Tool of Verification in a Geometry Problem-Solving Context*, in (Novotná, J. ed) Proceedings of the International Symposium on Elementary Mathematics Teaching (SEMT), Prague 2005, 260-268. <https://www.semt.cz/proceedings/proceedings.html>
- [27] Recio, T. and Vélez, M.P. *Automatic discovery of theorems in elementary geometry*, Journal of Automated Reasoning **23** (1999), 63-82.
- [28] Kovács, Z., Recio, T., Richard, P., Van Vaerenbergh, S. and Pilar Vélez, M. *Towards an ecosystem for computer-supported geometric reasoning*, International Journal of Mathematical Education in Science and Technology **53**(7) (2022), 1701-1710, DOI: [10.1080/0020739X.2020.1837400](https://doi.org/10.1080/0020739X.2020.1837400)
- [29] Roanes-Lozano, E., Roanes-Macías, E. and Vilar-Mena, M. *A Bridge Between Dynamic Geometry and Computer Algebra*, Mathematical and Computer Modelling **37** (2003), 1005-1028.
- [30] Roanes-Lozano, E. *Boosting the Geometrical Possibilities of Dynamic Geometry Systems and Computer Algebra Systems through Cooperation*, In: M. Borovcnik, H. Kautschitsch (Eds.) Technology in Mathematics Teaching. Proceedings of ICTMT-5, Schriftenreihe Didaktik der Mathematik **25**. öbv & hpt, Vienna (2002), 335-348.
- [31] Shin, H. and Cho, S.K. *Directional offset of a 3D curve*, SMA '02: Proceedings of the 7th ACM symposium on Solid modelling and applications, 329-335. DOI: <https://doi.org/10.1145/566282.566.329>
- [32] Thom, R. *Sur la théorie des enveloppes*. Journal de Mathématiques Pures et Appliquées **XLI**(2) (1962), 177-192.
- [33] Wu, W.T. *Some recent advances in mechanical theorem proving of geometries*, in: W.W. Bledsoe, D.W. Loveland (Eds.), *Automated Theorem Proving: After 25 Years*, in: Contemporary Mathematics **29**, AMS (1984), 235-241.

- [34] Wu, W.T. *Basic principles of mechanical theorem proving in geometries*, Journal of Automated Reasoning **2** (1986), 221-252.
- [35] Wu, W.T. *Mechanical Theorem Proving in Geometries*, Springer, 1994.
- [36] MacTutor History of Mathematics Archive: *Interactive Curves: Talbot's Curve*, retrieved January 2021 from <https://mathshistory.st-andrews.ac.uk/Curves/Talbots/curvesapplet/>
- [37] Zeitoun, D. and Dana-Picard, Th.: *Accurate visualization of graphs of functions of two real variables*, International Journal of Computational and Mathematical Sciences **4**(1), 1-11, 2010..